Dipesh Nepal

Master's thesis

2019

Dipesh Nepal

Master's thesis

NTNU
Norwegian University of
Science and Technology
Faculty of Engineering
Department of Civil and Environmental Engineering

NTNU
Norwegian University of
Science and Technology

3D CFD Simulation of flow structures and bed load movement at Binga HPP

June 2019

NTNU
Norwegian University of
Science and Technology

NTNU
Norwegian University of
Science and Technology

3D CFD Simulation of flow structures and bed load movement at Binga HPP

Dipesh Nepal

Hydropower Development
Submission date: June 2019
Supervisor: Nils Ruther
Co-supervisor: Diwash Lal Maskey

Norwegian University of Science and Technology
Department of Civil and Environmental Engineering

Preface

The present report is a master’s thesis on 3D CFD simulation of flow structures and bed load movement at Binga HPP. The hydropower plant is located in Philippines. This report is submitted to the Department of Civil and Environmental Engineering of the Norwegian University of Science and Technology, Trondheim.

As a fulfillment of one of the requirements for Master of Science in Hydropower Development, this report was started in January 2019 and completed in June 2019. The assignment includes the use of CFD program named SSIIM 2 to simulate the hydraulics and sediment transport in Binga reservoir.

It is a genuine pleasure to express my gratitude to supervisor Associate Professor Nils Ruther for his timely advice and scientific approach. His valuable support has helped me to complete my thesis. I am indebted to my Co-supervisor Diwash Lal Maskey, Ph.D. candidate at Department of Civil and Environmental Engineering for his continuous support throughout my study period. His valuable suggestions with kindness and co-operation have helped me to accomplish the task to a great extent. I am thankful to Adjunct Associate Professor Siri Stokseth for providing necessary documents and data during my study period.

Regards,

Dipesh Nepal

June 2019

Abstract

The present study aims to perform three-dimensional numerical modeling of a water reservoir called Binga situated in Philippines. The hydraulic and sediment simulation should be performed. A working hypothesis on how to transport the bed load should be made and its modeling should be done.

The numerical modeling program used for simulation is SSIIM 2, developed at NTNU by Professor Nils Reidar B. Olsen. This program is capable of modeling sediment transport with a movable bed and varying water level. Due to this reason, it is a powerful tool to simulate both sediment deposition and reservoir flushing.

The Binga HPP was commissioned in 1960 with an original storage capacity of 95 mill. m^3. By the survey of 2015, it is found that the volume dropped to 21 million m^3 resulting in only 22% volume left in the reservoir. The storage capacity is still decreasing and the sediment delta that is deposited is advancing towards the intake. Therefore, there is a high risk of intake being clogged. Because of this heavy sedimentation problem, the project is aimed to be converted into the run- of- river scheme. By doing this the reservoir is allowed to be filled up or the volume is kept as it is as much as possible and it is made sure that intake is not clogged by the sediments.

Both the hydraulic and sediment simulations (bed load) were carried for different discharge conditions and different operational rule of the reservoir. Necessary algorithms and parameter settings were finalized from hydraulic simulations which were used in the simulation of sediments. From the sediment simulation, it was proved that the risk of intake being clogged increases if proper sediment handling measure is not considered. A hypothesis was made that sediment routing approach (guide wall installation) can stop bed load transportation towards the intake. Based on this hypothesis, the geometry of the reservoir was changed by making a guide wall such that incoming sediment load is passed through the spillway and simulation was performed. The result of the simulation showed that by adopting this approach the bed load can be stopped from approaching the intake and the risk of intake being clogged will be reduced.

During the simulations, challenges were faced due to poor convergence of the solution. In many cases, changes in parameters of algorithms helped to improve the convergence. Assumptions on sediment concentration and granulometry have been made during the simulation of sediments due to lack of data. So, there are still many uncertainties related to input data and algorithms used. Further work on the model and result verification are therefore recommended. With more testing and development, the model can be used to predict future scenarios with more accuracy.

Table of Contents

List of Figures

List of Tables

List of Abbreviations

3D	Three dimensional
CFD	Computational Fluid Dynamics
HPP	Hydropower Plant
SSIIM	Sediment Simulation In Intakes with Multiblock option
R-O-R	Run- of- River
SIMPLE	Semi-Implicit Method for Pressure-Linked Equations
SIMPLEC	Semi-Implicit Method for Pressure-Linked Equations-Consistent
HRWL	Highest Regulated Water Level
LRWL	Lowest Regulated Water Level
D/S	Downstream
U/S	Upstream
POW	Power- Law Scheme
SOU	Second Order Upwind Scheme
NPC	National Power Corporation
Q	Discharge

List Symbols

k	Turbulence kinetic energy
e	Epsilon
x	X direction
y	Y direction
z	Z direction
mm	Millimetre
cm	Centimetre
m	Meter
km	Kilometer
m/s	Meter per second
m^2	Squared meter
m^3	Cubic meter
m^3/s	Cubic meter per second
masl	Meter above sea level
MW	Mega Watt
Kg	Kilogram
s	second
Mm^3	Million cubic meter
cumecs	Cubic meter per second

Chapter 1

Introduction

In this present world of globalization and improving standard of living, the demand for energy is escalating to new heights. The question is how to handle this rapidly growing demand for energy with the measure that is environment-friendly and meets the present need without compromising the ability of future generation to meet their own needs. This gives rise to the development of a clean energy source without impacting the environment and without the exhaustion of natural resources.

Solar energy, Wind energy, Thermal energy, Biomass, and Hydropower energy are examples of major renewable energy sources in the present century. Among these, the hydropower is of great interest among the market players and developers. The reasons behind it are the generation of energy from abundantly available water resource, highest energy payback ratio and ability to respond quickly during peak demands. So, when it comes to a renewable and sustainable source of energy, hydropower has taken a remarkable position in the energy market.

Having said that, the hydropower industry is facing many challenges among which the problem of sediments is the one. The artificial structures like dams trap the sediments behind them instead of flowing them downstream. Due to this reason, the storage capacity of the dams is reduced, ultimately affecting the plant’s output. In addition to this, the sediments are responsible for the erosion of the turbine, thus increasing operation and maintenance costs and start-stop losses.

At present, sedimentation is causing an annual decrease of 0.5%~1% in the world’s reservoirs (Schellenberg, Donnelly et al. 2017). This storage loss can lead to reduced operational flexibility. Furthermore, sediments that may get transported through the conveyance system can get deposited at the tailrace and reduce generation capacity. Sedimentation can also lead to reduced spillway capacity and compromise dam stability in a flood event (Hauer, Wagner et al. 2018).

1.1 Purpose and Project Background

With increased attention on sedimentation and its effects on Binga Hydropower Plant, Department of Civil and Environmental Engineering of Norwegian University of Science and Technology has started a project on physical modeling of sediment transport in Binga reservoir. This thesis aims to develop a three-dimensional numerical model that can simulate sediment transport in the reservoir and also provide a possible way to manage the incoming sediments.

There are several measures that can be adapted for sediment management like, sediment bypass, sluicing, dredging, flushing, etc. It’s really hard to state suitability and economical feasibility of sediment handling approaches in high sedimentation zones like Binga. Therefore, a careful case study has to be done before applying the sediment handling measures. To do this, prototypes/ physical models are built in lab that resemble the actual river and its flow characteristics. In the modern age of digitalization, numerical models are being very popular. They are basically the mathematical models in which the governing equations are discretized and solved using a computer. By means of numerical models, we can handle big data and save a lot of time, cost and effort and check the output of the physical model.

Binga Hydropower Plant, owned and operated by SNAP since 2008 is suffering a heavy sediment transport and deposition problem from early years of project commencement. Started in 1960, the reservoir was rapidly filled with sediments and by the year 1986, the reservoir had already lost approximately 35% of its original volume. Due to this considerable sedimentation, urgent sediment management measures must be applied to prevent clogging of intake and shut down of powerplant. It is also important to maintain the existing active volume of the reservoir and for this, the inflow and outflow of sediments should be stabilized to operate it as R-O-R project. (IHA 2017) The numerical modeling (CFD) is a study of this large project with an objective to achieve reliable and long-term operation of the Binga Hydropower Plant.

The CFD model can be a useful tool to determine the extent of physical model in the beginning and while running the physical model also, the CFD model can be used to simulate additional scenarios by easily changing geometry and flow structures.

1.2 Master’s Thesis Work

The present thesis work will study the flow pattern and bed load transport in the Binga reservoir using a three-dimensional numerical model. A 3D CFD simulation is used due to the possibility of three-dimensional effect of flow in the reservoir.
The objective is to model the bed load transport and deposition during floods in existing geometry and different reservoir levels. The present study also aims to find out possible sediment handling approach to stop bed load transport towards intake and test its performance in a numerical model. The modeling will be performed using a CFD program called SSIIM 2.

Chapter 2

Theory

2.1 Sediment Problems in Reservoirs

Sediments are the fragments of rock and minerals formed by disintegration or erosion and transported by different mediums like water, ice, and wind. In rivers, sediments are picked up and transported either as bed loads or in suspension. Stream sediments classified on the basis of relative size and mode of transport are bed load, suspended load and wash load. *Bed loads* describe the particles that are transported along the bed by rolling, sliding and saltation. They may be in continuous or in intermittent contact with the bed. *Suspended loads* are the fine particles carried in a stream and sustained in the water column by turbulence or colloidal suspension. *Wash loads* are part of sediment load with grain size of smallest 10% of the bed load by weight. They are normally carried in suspension without significant contact with the bed materials. (Morris and Fan 1998)

The sediment transport process depends on river discharge. In case of high velocity, more sediments are transported out of than into the considered reach and in case of low velocity like in the reservoirs, fewer sediments are transported out of than into the considered reach. The classification by mode of transport is dependent on both turbulence and grain size. For example, sand may be stable on bed or may be carried in suspension depending on the turbulent energy. Bed load constitutes less than 15% of the total load in many streams. (Morris and Fan 1998)

Reservoirs act as a trapping pool for the inflowing sediments. They reduce the velocity of the inflowing water carrying sediments and cause their deposition. In the course of time, the infill of the sediments will displace the storage capacity of the reservoir. Replacing the sedimented reservoir is very difficult because of high costs, resources scarcity and unavailability of suitable dam sites. Therefore, it is very important to consider the management of the reservoir to maximize the long-term storage capacity and minimize the trap efficiency. (Fan and Morris 1992)

A successive sediments deposition has many effects on the reservoir. Due to sedimentation, there’s loss of storage volume so a decreased amount of water to produce electricity. There will be a loss of flood control benefits as well due to reduced retention volume in the reservoir. Sediments are also responsible to block the bottom outlets and can enter inside the intake which causes abrasion of turbines. These all affect the financial aspect of the project and therefore it’s necessary to know about the sedimentation processes.

2.1.1 Sediment Deposition in Reservoirs

Sediment deposition is a major problem that affects the life of a reservoir. When a river reaches the reservoir the velocity of water decreases, and deposition of sediments begins. The coarser suspended sediments start to deposit immediately forming a delta, whereas the fine sediments are transported further downstream into the reservoir due to their lower settling velocities as shown in Figure 2. 1. In deep reservoirs, operated at different levels, distinct deltas can be seen at different water levels, whereas in long and narrow reservoirs, the delta deposit profile may be absent but an area with a rapid change in grain size can be present. (Morris and Fan 1998)

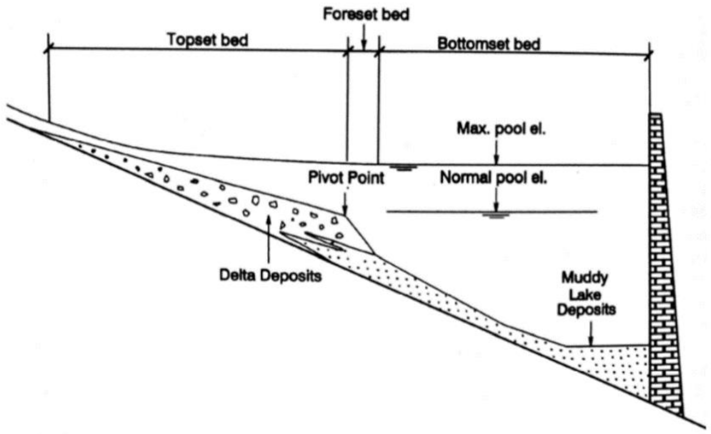

Figure 2. 1 Sediment deposition zones in the reservoir (Morris and Fan 1998)

As per the bathymetric survey of 2010, the delta is 280 meters away from the spillway and the advance rate is 50 m/year. (MulticonsultAS 2017) Because of the advancement of the pivot point of delta, it is posing a threat to the spillway as well as intake because an underwater slide may transport the debris and mud to the intake in case of flood and earthquake.

2.2 Sediment Management in Reservoirs

There are three strategies to manage reservoir sedimentation. First, the sediments can be reduced by sediment traps and erosion control upstream. The challenge associated with this approach is that adequate sediment storage capacity is required within the reservoir pool along with watershed management strategies. However, it is not a complete solution of sediment problem, but just postpones it and sediments will accumulate in a slower rate.

Second, dredging can be done to restore the volume of the reservoir but in large scale, it involves high cost and negative environmental consequences due to spoiling disposals.

Third, possibilities to route the sediment-laden water through or around the reservoir without allowing it to deposit and remobilize and flush out previously deposited sediments. (Fan and Morris 1992)

2.2.1 Sediment Routing

Sediment Routing is an approach to manipulate the geometry and/or hydraulics of a reservoir in-order to pass sediments through or around the pool or intake area to minimize the deposition. Sediment load in a river varies as per time and even within a cross-section. Only a fraction of inflow is sediment-laden water. Hence clear water and sediment-laden water should be treated separately. Sediment routing seeks to find out sediment-laden water and manage them to prevent/ minimize deposition. (Morris and Fan 1998) This measure will be taken into consideration in the present study of Binga HPP in order to divert the incoming sediments away from the intake.

2.3 Numerical Modelling

It is not easy to predict future deposition pattern of sediments in reservoirs since sediment transport is a complex process. Therefore, a model has to be made which resembles the prototype and studies can be conducted to understand the process. Such a model can either be a physical model or a numerical model. Due to possibility of scaling problems and high cost and time to build large physical models, an alternative approach of numerical modeling has evolved with increased speed of computers. The disadvantage of using numerical models is that the solution is complicated and it takes years to create the computer program. (Olsen 2010).

2.3.1 CFD Models

There are three governing principles that describe the physical aspects of fluid flow namely, conservation of energy, conservation of mass and Newton's second law (F=m*a). These three principles are generally expressed as partial differential equations. So, computational fluid dynamics is the approach of replacing these equations by numbers and advancing them in space and/or time to get a complete description of the flow field. (Anderson and Wendt 1995)

The numerical models of sediment transport can simulate flow in one, two or three dimensions. Among these, 1D models are popular because they are more robust and unlike 2D and 3D models they require less amount of computer time and calibration data. In addition, the river profiles and reservoirs are highly elongated and the flow can be assumed one dimensional to evaluate sediment problems. (Morris and Fan 1998) However, 3D modeling has become important because in many cases 1D and 2D models do not satisfy complex flow situations. (Mouris, Beckers et al. 2018) The software used in the present study is SSIIM, a 3D numerical model used for the simulation of water and sediment flow in rivers and reservoirs. (Olsen, Haastrup et al. 1985). Further information about the model and its application in the present case study is described in chapter 4.

2.3.2 Errors and Uncertainties

It is not a difficult task to obtain results using CFD models but the question is if the obtained results are relevant for practical engineering purposes. An organization named European Research Community On Flow, Turbulence And Combustion (ERCOFTAC) has highlighted some errors and uncertainties related to CFD models.

1. Errors in numerical approximations: This is an error of false diffusion that arises due to discretization of the equations and/or coarse grid. This can be solved by using different discretization method or changing the size of the grid.

2. Modeling errors: While doing time-dependent computations the iterative solvers are used and the computational time can be too long. Sometimes, the iterations are not performed until complete convergence.

3. Errors due to not complete convergence: The iterative solver is used many times and sometimes the results are used even if the solution is not converged fully. This can be an issue in case of time-dependent computations when convergence is not reached for each time step.

4. Round- off errors: Due to the limitation in the accuracy of the microprocessors of the computers, these errors occur. Nowadays, 64 bits floating point numbers with 12 digits accuracy is used by numerical programs. But, the rounding- off errors are significant with 32 bits programs that use numbers with only 6 digits accuracy.

5. Errors in input data: The needed input data for CFD like DTM, time series of sediment inflow and spatial variation in bed grain size distribution are not available in many cases. So, there are uncertainties while deciding these input data.

6. Human errors: The inexperience of user on CFD modeling can cause errors. There are many parameters and algorithms and the experience can be limited.

7. Programming errors: A 3D CFD program has thousands of code lines and it is likely to have bugs in the software. (Olsen 2010)

Chapter 3

Project Description

Most of the information in this chapter is based on the Concept Report for Binga by Multiconsult dated 31.08.2017.

3.1 Background

Binga Hydropower Project is a 140 MW storage scheme hydropower project located on the island of Luzon, in Agno river, in the northern part of Philippines. It is approximately 13.5 kms downstream of Ambuklao Dam. The tailrace outlet of Ambuklao is about 2.4 kms downstream of the dam and that of Binga is 8.8 kms downstream of the Binga Dam. The Ambuklao Hydropower Project is one of the oldest and first large powerplant in Philippines. The Binga Hydropower Plant was commissioned in 1960 and the Ambuklao Hydropower Plant was commissioned in 1958, both serving purposes of energy generation and flood control.

Figure 3. 1 Location of Ambuklao and Binga dams and tailrace outlets

Figure 3. 2 Binga intake and spillway

Source: Google Earth

Philippines is exposed to tropical storms and suffers from high magnitude earthquakes. Cyclones and typhoons hit the country which is responsible for problems like floods and landslides. Because of this, the inflow of sediments in the rivers are high. The Binga reservoir was designed based on the traditional approach without any sediment management strategy. Moreover, due to limited sediment data available the rate of sedimentation was underestimated. During the period of commissioning (1960), the reservoir volume was 95 Mm^3. The survey of 2015 shows that the volume dropped to 21 Mm^3. So, during a period of 55 years, the storage capacity has decreased drastically by 74 Mm^3 and only 22% of the original storage capacity is left. In other words, Binga has lost 78% of its storage capacity in 55 years, see Figure 3. 3 and Figure 3. 4. (MulticonsultAS 2017) If the same trend continues then the intake may be clogged and eventually, the whole reservoir may be filled with sediments. Therefore, a sustainable sediment management strategy has to be adopted.

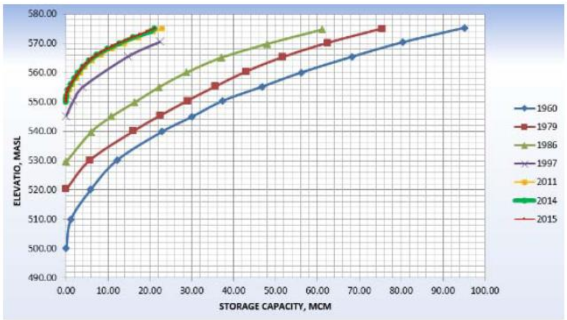

Figure 3. 3 Decrease in reservoir capacity

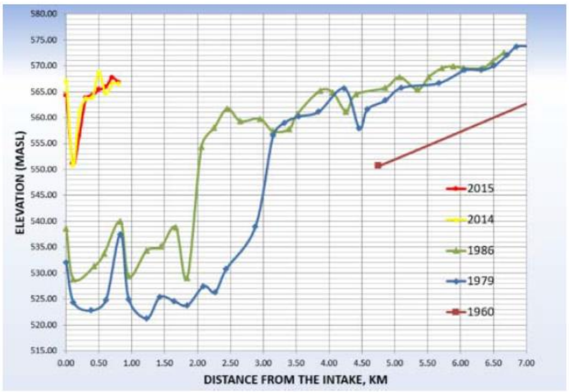

Figure 3. 4 Reservoir sedimentation over time (longitudinal profile)

Source: (MulticonsultAS 2017)

3.2 Project Salient Features

Table 3. 1 Key parameters for Binga Hydropower Project

Parameters- Binga reservoir		**Reservoir capacity (2015/1960)**
Installed Capacity	140 MW- 4 Francis units	
$Q_{turbine}$	76 m^3/s	
Head (H)	144 m	
HRWL	575 masl	21.2/ 95.1 mill m^3
LRWL	565 masl (flood operational rule)	6.3/ 68.3 mill. m^3
Maximum flood level	579.5 masl	
Spillway crest	563 masl (flood operational rule) (T&T use 563.5 masl)	
Spillway length	6*12m= 72m	
Spillway gates	12.5 m high, operational speed: 0.3m/min	
Intake invert level	555 masl	
Intake gate, H*W	7m*5.8m= 40.6 m^2	
Intake protective bund *not confirmed	564.5 masl	
Peak design flood	10300 m^3/s	
Flow when NPC takes over	500 m^3/s	
Agno River tolerable flow Agno River bank full flow	1600 m^3/s 2800 m^3/s	

Source: (MulticonsultAS 2017)

3.3 Major Concerns

Major challenges for the future operation of the Binga and Ambuklao HPP are:

1. Loss of remaining reservoir capacity resulting in loss of ability to regulate the future production
2. Clogging of the intake and full stoppage in production
3. Buildup of the river bed upstream burying the Ambuklao outlet.
4. Dam breach due to sediment load on dam
5. Reduction in the ability to dampen flood

3.4 Hydrology

The catchment area of Binga dam is 936 km^2 out of which 72% is regulated by upstream Ambuklao dam. The catchment area has dry period from November to April and wet rest of the year. The country being exposed to tropical storms is hit by approximately 20 cyclones each year mostly from June to September and is also prone to high magnitude earthquakes. (IHA 2017)

Table 3. 2 Flood estimates

Flood event, return period	Estimated inflow (m^3/s)	Reservoir elevation with existing operational rule (masl)
High discharge- several times a year	250	575.35
NPC takes over control	500	575.52
Q_2	1000	575.71
Q_5	2000	576.10
Q_{10}	3000	576.46
Q_{100}	5500	577.35

Source: (MulticonsultAS 2017)

3.4.1 Test Discharges

The test discharges used for the simulation are: flood with 2 years and 10 years return period, 1000 and 3000 m^3/s respectively. The working criteria were to simulate both the scenarios with existing operational rule and with fully open gates.

The days of occurrence of the floods above 500 m^3/s is 3.7 days based on the report V4 on Binga Sediment Challenges Study by Sediment Systems dated 28/02/2018.

Table 3. 3 Days of occurrence of discharges

Band of discharges (m^3/s)	Duration (days/year)
100-120	14.6
120-250	18.3
250-500	11.0
>500	3.7

Source: (StøleAS 2018)

3.5 Sediments

After recommissioning in 2010, reservoir curves and longitudinal profile of the reservoir is taken annually to access the sediment deposition. The long-term average from the year 1960 to

2007 has been 1.4 mill. m^3/year and this includes the effect of the 1990 Baguio earthquake. The long-term average excluding this earthquake effect is 1.1 mill. m^3/year, see Table 3. 4.

Table 3. 4 Observed and predicted sedimentation in Binga reservoir

Year	Sedimentation Observed/ Predicted (million m^3/ year)
Long term average (1960 – 2007)*[1]	1.4
Long term average excluding 1990 Baguio earthquake	1.1
Most recent period 2003 – 2007*[1]	1
Norconsult prediction 2010 – 2020*[2]	0.7
Norconsult prediction 2020 – 2030*[2]	0.5
Norconsult prediction 2030 – 2040*[2]	0.25

*[1] Norconsult (2009) Section 2.3

*[2] Interpreted from Norconsult (2009) figure 3.

Source: (MulticonsultAS 2017)

Based on the recent bathymetric surveys, mean annual sediment deposition from the year 2011 to 2014 has been 0.55 mill. m^3/year and 0.05 mill. m^3/year from the year 2014 to 2015. This deposition rate is lower than the long-term average because no recent earthquake has occurred, and the retention capacity has decreased due to a decrease in the volume of the reservoir.

The mean annual advance rate of the delta is found out to be 50 m/year from the year 1997 to 2010. A bathymetric survey in 2010 has shown that the delta is 280 m away from the spillway. In the downstream part of the reservoir, the bottom deposit is mainly of fine particles.

3.5.1 Grain Size Distribution

According to sampling done by Norconsult and SediCon (2009), the following grain size distribution was obtained:

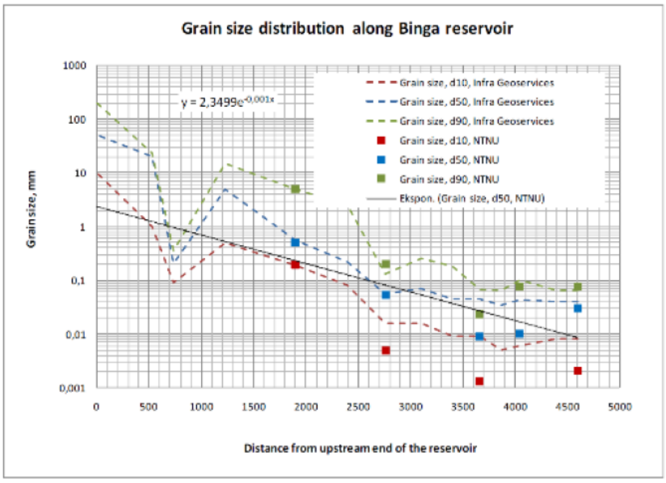

Figure 3. 5 Grain size distribution along Binga reservoir

Source: (MulticonsultAS 2017)

According to d_{90} in the upstream, the roughness of the model is decided to set to 0.1 m. Assumptions were made for the size fraction in reservoir sediment deposition based on the grain size distribution and are summarized as follows:

Table 3. 5 Grain size distribution in reservoir

Sediment source	**Cobble small (63.5-127 mm)**	**Gravel medium (7.62-15.24mm)**	**Coarse sands (0.508-1.016mm)**	**Coarse silts (0.05-0.076mm)**
Size fraction	10%	35%	35%	20%

According to the study of bed load deposits upstream of the reservoir, coarser sediments were found beneath the finer sediments. The bottom layer of coarser sediments is up to 0.05-0.1 m. The tributaries contributing sediments to the Agno river have coarser bed load in stock for Binga. The finer sediments are dominated by sand and were deposited by smaller floods. The finer deposits are expected to be transported in suspension during the next flood event when the water level is maintained at a low level. The transported suspended load will be transported further downstream to the intake and spillway. Therefore, the major concern here is the underlying layer of coarser sediments which are likely to be transported by the next flood towards the intake. (MulticonsultAS 2017)

Figure 3. 6 Two main tributaries of Agno river (Source: Google Earth)

Hence, the model will study the bed changes in different flood events and try to prove the situation that the bed load will approach the intake, thereby increasing the risk of clogging. The model under the present study will also find the arrangement to pass the bed load through the reservoir away from the intake that is likely to be transported in the near future.

3.6 Operational Rule

The existing operational rule aims to pass the flood safely and minimize flood damages downstream. This is done by holding and delaying the flood and it is possible by means of storage volume behind the dam and its flood gates. The safe passage of sediments is not taken into account. The existing rating curve of the spillway as per the operational rule is shown below:

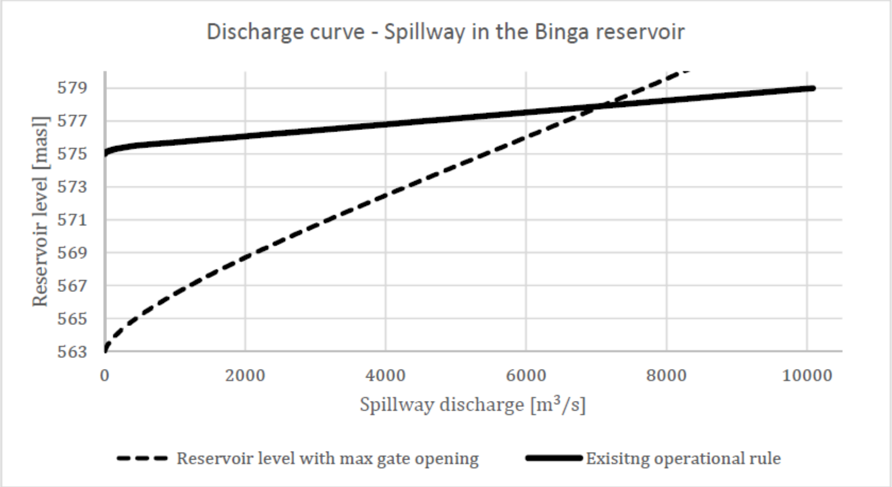

Figure 3. 7 Rating curve for Binga spillway, solid black line is existing rule whereas dotted line is technically possible

Source: (MulticonsultAS 2017)

In order to dampen the flood and consider the safe passage of sediments at the same time modification of operational rule curve is necessary. By doing this the flood discharges can be used to transport the sediment load as much as possible which is just opposite of the existing operation rule that facilitates the trapping of sediments in the reservoir.

The available tool that can be used to minimize sediment deposition and maximize sediment passage is gated spillway. The gates can be used to control water level during the flood events. If the water level is maintained at LRWL, it'll prevent bed load deposition in the live storage during floods and the suspended load that was previously deposited during lower flows can be stirred up and carried in suspension with higher velocity. Therefore, the reservoir should be operated for optimized condition of flood dampening and sediment passage.
There are some issues associated with the modified operational rule.

1. Will the lowering of reservoir level trigger the transportation of existing delta and pose threat to intake?
2. The passage of the sediments will be through the spillway and the coarser sediments can cause abrasion and structural failure of it. Can this threat be handled with maintenance and improvement of the spillway and what will be the cost associated to it?
3. How efficient is it to pass the sediments through the spillway for various discharges and water levels?
4. The distribution of sediments between spillway and intake is another issue for different discharges and water levels.

Since there is a risk of delta being unstable, sediment routing should most likely be combined with water level control. For this, hydraulic structures that can divert the flow around the intake and spillway can be designed and installed. (MulticonsultAS 2017) In the present study, a hydraulic structure to guide the flow around the intake and through the spillway is studied assuming that the spillway can withstand the possible damage caused by coarser sediments.

Chapter 4

SSIIM

4.1 Introduction

SSIIM (Sediment Simulation In Intakes with Multiblock option) is a CFD program made for hydraulic/river/environmental/sedimentation engineering. Originally this program was developed to simulate sediment movements in river/channel geometry but later used in other aspects of hydraulic engineering like spillway modeling, head loss in tunnels, etc. However, the main focus is on the computation of water velocities and sediment transport in river, channels, and reservoirs. The program solves Navier- Stokes equation in three- dimensional, almost non-orthogonal grid with k-e turbulence model. SSIIM solves convection-diffusion equation for sediments which gives deposition pattern and trapping efficiency. The bed changes over time along with the movement of free water surface can also be computed. (Olsen, Haastrup et al. 1985)

Like other CFD models, SSIIM has three computation steps namely, pre-processing, computations and post-processing. Pre-processing is basically the generation of grid and input. SSIIM has tools to generate input data and grid generators to make grids. There are modules in the program to calculate water velocity, water level changes, bed changes, etc. and these computations can also be combined. The post-processing is viewing the result. The user interface shows the velocity vectors and other scalar variables in plan, cross-section and longitudinal profile. Other packages like *Tecplot* or Para View can also be used to see the results. In SSIIM the computational module is directly connected with graphics which enables the user to see the results while the program performs computations and this is an advantage of SSIIM compared to other CFD programs. (Olsen, Haastrup et al. 1985)

There are two versions of SSIIM: SSIIM 1 and SSIIM 2. SSIIM 1 uses structured grid and SSIIM 2 uses unstructured grid. The advantage of unstructured grid over the structured is the ability to model wetting-drying condition, lateral movements of the river and complex geometry. Moreover, SSIIM 2 has some sediment transport algorithms which are missing in SSIIM 1. On the contrary, the structured grid used by SSIIM 1 uses less memory per cell and has faster solvers. (Olsen, Haastrup et al. 1985) Because of the above-mentioned advantages of SSIIM 2 over SSIIM 1 and the Binga reservoir having a complex geometry, SSIIM 2 is used for the simulations in the present study. This section will briefly describe the theoretical basis, input and output files used in the program and grid generation. For a detailed explanation about the model, it is recommended to see SSIIM user’s manual.

4.2 Theoretical Basis

4.2.1 Water Flow Calculation

SSIIM performs the hydraulic simulation by solving the Reynold’s averaged Navier- Stokes equation. To calculate turbulent shear stress, k-e turbulence model is used. For a constant density flow and non-compressible flow, the equation can be represented as:

$$\frac{\partial \mathrm{U_i}}{\partial \mathrm{t}} + U_j \frac{\partial \mathrm{U_i}}{\partial \mathrm{x_j}} = \frac{1}{\rho} \frac{\partial}{\partial \mathrm{x_j}} \left(-P\delta_{\mathrm{ij}} + \rho \overline{\mathrm{u_i u_j}}\right)$$

The velocity varying over time is divided as into two variables, average value and fluctuating value denoted by U and u respectively. The last term $\rho\overline{u_i u_j}$ is a turbulence term. Excluding this term gives the Navier- Stokes equation for laminar flow.
To model Reynold's stress term, the eddy viscosity concept is used and introduced by Boussinesq approximation.

$$-\rho\overline{u_i u_j} = \rho v_T \left(\frac{\partial U_i}{\partial x_j} + \frac{\partial U_j}{\partial x_i}\right) - \frac{2}{3}\rho k \delta_{ij}$$

where, K and v_T are the kinetic turbulent energy and eddy viscosity respectively.
Combining and arranging the terms in these two equations gives the following expression:

$$\frac{\partial U_i}{\partial t} + U_j \frac{\partial U_i}{\partial x_j} = \frac{1}{\rho}\frac{\partial}{\partial x_j}\left[-\left(P + \frac{2}{3}k\right)\delta_{ij} + \rho v_T \frac{\partial U_i}{\partial x_j} + \rho v_T \frac{\partial U_j}{\partial x_i}\right]$$

The transient and convective terms are denoted by the first and second terms on the left-hand side and on the right-hand side, the three terms represent pressure and kinetic energy, diffusion, and stress terms respectively.

The pressure term is solved by SIMPLE and SIMPLEC methods. The kinetic energy term is negligible in comparison to pressure. The SIMPLE (Semi-Implicit Method for Pressure-Linked Equations) method is default method and SIMPLEC can be used by using specific data set. The convective term is solved by First and Second Order Upwind Schemes and Power- Law Scheme. For static water level the transient term is by default neglected in SSIIM but in case of changing water level, for time, dependent computations, this can be invokes using certain data set in the *control* file. Due to less influence in the solution in many cases, the stress term is sometimes neglected. The diffusive term is solved with the same way as the solution of the convection-diffusion equation. In SSIIM 2, the gravity term is usually neglected, but in the cases where water level has higher gradients, this term can be invoked by using F36 data set. This is not relevant to the present study. (Olsen and Technology 2007)

4.2.2 Discretization Schemes

SSIIM involves the process of discretizing the whole geometry into a number of cells and then unknown variables are solved in each cell. The partial differential equations are solved where one cell is the function of the variable in the neighboring cells. The variables in the cells are computed as a weighted average of the concentration in the neighboring cells. The discretization schemes that are tested in the model are explained as follows:

First Order Upwind Scheme
The concentration in the target cell is calculated based on concentration in the upstream cell. The concentration of variable at cell surface is taken by using the cells upwind in the first order which means one cell upwind, not more.

Second Order Upwind Scheme
This scheme uses more accurate finite difference method to increase accuracy and remove false diffusion which can occur with first order upwind scheme. The false diffusion is due to the fact that the concentrations in the cells surrounding the target cell are based on the values in the center of these cells. The second order upwind scheme avoids this by using the concentration value on the target cell wall which separates the cell from the neighboring cells. Instead of

taking only the upstream cell in consideration, this scheme refers to two cells for the calculation of concentration value on the target cell wall.

Besides using the high order scheme, decreasing the grid cells size and aligning the grid with flow field can reduce false diffusion.

4.2.3 Sediment Flow Calculation

The sediment flow is calculated as suspended sediment transport and bed load transport. The sediment transport is modeled by convection-diffusion equation.

$$\frac{\partial \mathrm{c}}{\partial \mathrm{t}} + U_j \frac{\partial \mathrm{c}}{\partial \mathrm{x_j}} + w \frac{\partial \mathrm{c}}{\partial \mathrm{z}} = \frac{\partial}{\partial \mathrm{x_j}} \left(\Gamma \frac{\partial \mathrm{c}}{\partial \mathrm{x_j}} \right)$$

Where, c= sediment concentration, U= flow velocity, w= settling velocity, *Γ*= diffusion coefficient.

For suspended sediment load calculation, the most commonly used method is Van Rijn formula.

$$\mathrm{C}_{\mathrm{bed,\,susp,i}} = 0.015 \frac{d_i}{a} \frac{\left(\frac{\tau - \tau_{c,i}}{\tau_{c,i}} \right)^{1.5}}{\left[d_i \left(\frac{\frac{\rho_S}{(\rho_W - 1) g}}{v^2} \right)^{\frac{1}{3}} \right]^{0.3}}$$

Where, $\mathrm{C}_{\mathrm{bed,\,susp,i}}$ = concentration of sediment load at bed for ith fraction

d_i= diameter of the ith fraction, a= height of the bed cell set equal to the roughness height, $\boldsymbol{\tau}$= bed shear stress for d_i , $\boldsymbol{\tau_{c,i}}$ = critical shear stress for d_i calculated from shield's diagram, ρ_s= density of sediment, ρ_w= density of water, v= kinematic viscosity.

Bed load can be calculated by different formulae. Meyer- Peter and Muller formula, Van Rijn formula, Einstein formula, etc. In the present study, Van Rijn formula has been taken into consideration.

$$\frac{q_{bi}}{d_i^{1.5} \sqrt{((\rho_s - \rho_\mathrm{w})g)/\,\rho_\mathrm{w}}} = 0.053 \frac{\left(\frac{\boldsymbol{\tau} - \boldsymbol{\tau}_{c,i}}{\boldsymbol{\tau}_{c,i}} \right)^{2.1}}{d_i^{0.3} \left(\frac{(\rho_s - \rho_\mathrm{w})g}{\rho_\mathrm{w} v^2} \right)^{0.1}}$$

Where q_{bi}= transport rate of ith fraction of bed load per unit width. (Olsen and Technology 2007)

4.2.4 Boundary Conditions

The boundary conditions are initial values and functions set on the boundaries. The inflow boundaries use Dirichlet boundary conditions. For outflow, zero gradient boundary conditions are often used. For the water surface, zero gradient boundary conditions are used for ε and zero for turbulent kinetic energy, k. On the river bed and walls, the flux is zero, so boundary condition is not used. The concept of wall laws is used instead.

4.3 Input and Output Files

There are different input and output files used in SSIIM. The most relevant files to this work are discussed below:

Geodata file
This file contains the geometry of the river under consideration. In other words, it contains the topographic survey data in terms of X, Y and Z coordinates. The geodata file is used for bed interpolation to generate the bed level of the rivers/ reservoirs.

Control file
The control file is one of the most used and very important to run the simulations. In the control file, various parameters for grid properties, discharges, water levels, roughness coefficient, sediment properties, etc. are given. To invoke these parameters different data sets beginning with capital letters like F, G, W, K, S, etc. are used as per the SSIIM User's Manual.

Boogie file
While running the simulation, if there is a bug or the program crashes, the error is explained and written in boogie file. This file also shows the intermediate results from the computations.

Koordina file
This file contains the grid geometry or three-dimensional coordinates of the grid intersection points. The program generates the file itself after the grid is made.

Koomin file
This file is similar to *koordina* file, but it contains the grid geometry of the points where bed changes are not applicable. It is used in case of fixed bed fixed bed calculation.

Unstruc file
In SSIIM 2, this file stores the information about the grid coordinates and discharges.

Timei file
The information about variation in input parameters like discharge, water elevation, sediment concentration etc. are addressed by using *timei* file.

Result file
This is the output file containing result of hydraulic computation with velocities, pressure and turbulence. The result file can be written either after completion of prescribed iterations or from the menu.

Bedres file
The *bedres* file is used to see the changes in bed elevation and water level after computation.

ParaView file

This is the output file and can be read by software named *ParaView*. Through the *ParaView* software the results can be easily viewed and interpreted. Like *ParaView* file, there is another file called *Tecplot* which is an input for *Tecplot* software.

4.4 Convergence

Not Getting converged solution is a problem in SSIIM and in many other CFD programs. Important factors involved in convergence are described as follows:

A good grid

Slower convergence is caused by a higher degree of non-orthogonality of the grid. Also, if strong gradients are present, slower convergence can be experienced.

Relaxations coefficients

Various equations are solved iteratively starting from a guess value until the solution converges to give a final result. The relaxations coefficients are used to improve the guess value. During convergence, in general cases, lower relaxation coefficients give less instabilities but slower convergence and vice-versa. For most of the instability cases, lowering values on the K3 data set (in the *control* file) is advised.

Boundary conditions

In case of slow convergence and undesirable results, it’s good to check boundary conditions. Correct boundary conditions improve the convergence.

A fast solver

Choice of solver strongly influences the convergence speed. In most of the cases, the use of block correction (K 5 data set) will lead to faster convergence. The block correction option divides the whole grid into several coarser grids and iteration is carried from coarser grid to finer and vise-versa. This is carried out until convergence.

Numerical algorithms

Stable numerical algorithms should be invoked by different data sets in case of instabilities. (Olsen, Haastrup et al. 1985)

4.5 Grid Generation

The basic concept of CFD is to divide the whole area into a number of cells and to solve equation in each cell. The shape of cell is generally triangular or quadrilateral. The quality of grid affects the accuracy of result, convergence and computational time.

SSIIM 2 uses unstructured grid. The grid can move during computation. The grid that can move as per the solution of the equations is known as adaptive grid. For e.g. vertical movement of grid due to change in water level. Lateral movement of grid is also possible in case of a meandering river. (Olsen and Technology 2007)

To make a good quality grid following points are taken into consideration:

1. The grid lines are made as perpendicular to each other as possible. This factor is taken into consideration since the degree of orthogonality affects the convergence.
2. To avoid false diffusion the grid lines are aligned to the stream flow direction as much as possible.
3. The distortion ratio (ratio of two perpendicular sides of a cell) and the ratio of two neighboring grid cell size are taken into consideration. The ratios are tried to keep as low as possible.

Before making the grid, information of topography of the reservoir is necessary. This information can be obtained by the bathymetric survey. The data used is basically the x, y, z coordinates of the reservoir bed. At first, the model boundary is set with the help of drawing in *AutoCAD* software. This data is extracted from *AutoCAD* in excel file format and then transferred to *geodata* file which is the only file readable by SSIIM. This file contains a number of x, y, z coordinates. The letter E is used before each coordinate and Z is used at the end to indicate the last line in the file. (Olsen, Haastrup et al. 1985) An example of geodata file is presented as follows:

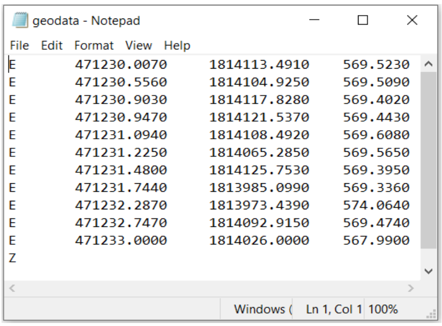

```
E       471230.0070     1814113.4910    569.5230
E       471230.5560     1814104.9250    569.5090
E       471230.9030     1814117.8280    569.4020
E       471230.9470     1814121.5370    569.4430
E       471231.0940     1814108.4920    569.6080
E       471231.2250     1814065.2850    569.5650
E       471231.4800     1814125.7530    569.3950
E       471231.7440     1813985.0990    569.3360
E       471232.2870     1813973.4390    574.0640
E       471232.7470     1814092.9150    569.4740
E       471233.0000     1814026.0000    567.9900
Z
```

Figure 4. 1 Geodata file

After preparation of *geodata* file, the points are viewed in the graphical interface of SSIIM called as *grid editor*. The points are seen in different colors according to the water depth. After viewing the points, a plan view of grid is prepared in xy- plane. During the preparation of plan view, grid size is given. When the plan view looks ok, 3D grid is generated with varying number of cells in vertical direction. This can be done in *grid editor* interface by choosing *Generate-> Bed levels* and *Generate-> 3D grid*. The grid can either be multi-block or one single block. (Olsen, Haastrup et al. 1985)

4.5.1 Grid Options

SSIIM 2 has multi-block and one block options for grid generation. Multi-block means more than one block can be created covering the water surface and then joined together. At last there will be one unstructured grid covering the whole water surface.

The natural water bodies normally don't have rectangular or square shapes and therefore, the grid has to be fitted according to their irregular shapes. This can be done in the graphical interface itself by dragging the points on the boundary of blocks to desired location. This can be done in a special mode of the grid editor called *NoMovePoints* mode. This can be used in case of multi-block grid.

There is another approach that involves making one single grid bigger than the water body. If the points in the geodata file are for the area of water surface only, additional points have to be added with elevation higher than the water surface in order to define the outer limits of water body. After defining the water level, the grid is generated at this water level with only the cells which are wet and *unstruc* file is written. Inflow and outflow are specified in this file. Usually, at the start of computation, the water level is below the highest water level. To lower down the grid to this level, F 112 1 data set is invoked in the control file. Before this a *koordina* file is made with initial water level by modifying data from file called *koordina.t*. The F 112 1 data set reads the original *unstruc* file and water level from *koordina* file and hence the grid is generated at the required water level as a single block. (Olsen, Haastrup et al. 1985) This approach is adopted to make grid in the present study as shown in Figure 4. 2.

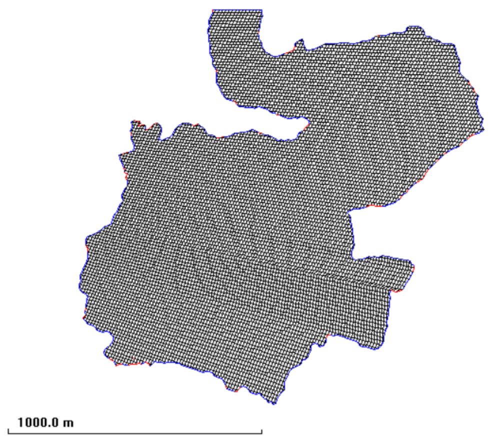

Figure 4. 2 One block grid

The advantage with this approach is quick way to make a good fitting geometry. Moreover, the grid cells are uniform in size and are orthogonal leading to more stable and faster computations compared to multi-block approach. The time required for simulation while using multi-block grid is higher because of extra boundaries. It is also possible to make a single block grid with graphical adjustments, but it can be a problem in complex geometries during adjustments. In complex geometries, it is very difficult to make grid cells uniform and meet other criteria of a well-functioning grid. (Hoven 2010)

4.5.2 Discharge Input

Since the grid is unstructured in SSIIM 2, it's not possible to give the discharge directly in the *control* file. Therefore, the discharge is given in a special interface called *Discharge Editor*. In this interface, the inflow and outflow locations are given along with the discharge values. There can be more than one inflow and outflow discharge groups but to achieve continuity, the total inflow discharge should be equal to total outflow discharge. (Hoven 2010)

After discharge input, the file should be saved as *unstruc* file. To do this, an option called *Write unstruc file* should be chosen from the menu. The program now generates an *unstuc* file which contains information of the grid and discharge.

4.5.3 Grid of Binga

The grid of Binga is made with one-block grid option as shown in Figure 4. 2. The multiblock option was also an alternative but convergence is faster for the grid with only one block than multiblock for equal situations. (Hoven 2010)

Grid size affects computation time, coarse grid gives convergence faster than fine grid hence reducing the simulation time. Therefore, the model was generated with coarse grid with a block size of 121*121 and cell size of 12m * 16m in xy- plane. Total number of cells were about 58356 at the start when discharge was 1000 m^3/s and water level at 575.71 masl. The grid has upto 10 cells in verticle direction but varies according to the depth and when the water level goes down or bed level increase due to sedimentation. The cell number decreases on the xy-plane also when the cells dry up.

4.5.3.1 Problems faced

While making the grid, initially, the water level was kept very high and *unstruc* file was written. After that the grid was lowered to the required water level. On doing so, some points were interpolated outside the reservoir boundary which caused instabilities during computation. Therefore, those points were removed by adding other points around the boundary with higher elevation than the points on the boundary. But adding very high elevation points near inlet and outlet would also cause the bed level to be higher than the water level and this would prevent water inflow and outflow. So, too high elevation points should not be added around the boundary.

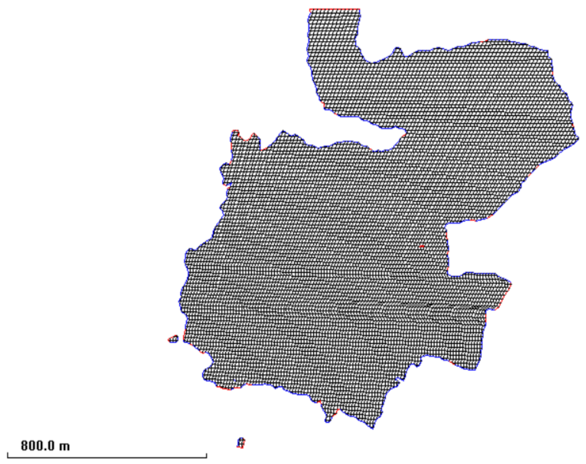

Figure 4. 3 Interpolated points outside the boundary of reservoir

Chapter 5

Simulation of Hydraulics

After preparation of grid, the hydraulic simulation is carried out and should be stable before carrying out sediment simulation. The parameters obtained from hydraulic simulation are important for sediment simulation. Different hydraulic variables like velocity, pressure, bed shear stress, etc. are obtained from hydraulic simulation. The discharges, downstream water level, discretization schemes, grid size, boundary roughness, etc. are finalized for the use in sediment simulation.

5.1 Input Data

The hydraulic simulation was carried out for 1 in 2-year flow of 1000 m^3/s and 1 in 10-year flow of 3000 m^3/s. Hydraulic simulation was carried out for 500 m^3/s also but the bed shear stress obtained from the simulation was too low which would not affect the sediment transport. Hence higher flows were simulated to observe the sedimentation.

It was decided to test these flows without flow to the turbine. This is done for simplicity and compared to these floods the flow to the turbine is very small i.e. 76 m^3/s.

The simulations were carried out for 4 cases as tabulated below. Full gate opened condition is the situation where the water level drops down and accelerate in the reservoir. This creates a river like situation with hydraulic capacity to erode and transport the carrying as well as deposited sediments through the reservoir.

Table 5. 1 Flood values with corresponding reservoir levels at different operational rule

Simulation No.	**Flood**	**Flood Value (m^3/s)**	**D/S water level (masl)**	**Operational Rule**
1.	Q_2	1000	575.71	Existing
2.	Q_2	1000	568	Full gate opening
3.	Q_{10}	3000	576.46	Existing
4.	Q_{10}	3000	571.4	Full gate opening

The downstream water levels are based on the rating curve for Binga spillway, Figure 3. 7. The technical possibility of flushing is restricted by spillway crest level at 563 masl and 6 gates with total length of 72m. The water levels for full gate opening scenarios were also confirmed by using the following formula:

$$Q = C * L_{eff} * H_0^{3/2} = 2 * (72m - 12 * 0.1 * H_0) * H_0^{3/2}$$

For 1000 m^3/s at full gate opening condition the d/s water level is 566.8 masl according to this formula. However, at this level the grid cut the bed and was split so the continuity of the flow could not be maintained. This is because free surface computation was not used. Free surface computation is more complex and hence it was avoided. Therefore, a higher water level of 568 masl was considered for simulation.

5.2 Simulation Time

For shorter time periods, the distribution pattern of the sediments can be viewed for the given time span. For the simulations with long time durations, the computational time can be shortened by using time steps, which means the number of seconds one iteration comprises. This is not relevant for steady-state hydraulic computations.

In the present study, the sediment concentration and bed changes are to be simulated. The time span used in the simulation was the number of days corresponding to a typical duration of the discharges. The flood values were simulated for 3.7 days (~319700 secs) as mentioned in Table 3. 3.

5.3 Starting Simulation

The simulation can be started by invoking run options in F 2 data set in *control* file or manually from the user interface. The algorithm used for hydraulic simulation is F 2 UW.

5.4 Input Files

The most important file used in hydraulic simulation is the *control* file. In addition to the *control* file, *unstruc* and *koordina* files are also important for the simulation.

Control file

For the simulation, less computational time demanding settings were used. The data sets used in the control file for hydraulic simulation of 1000 m^3/s at existing operational level is explained in Appendix B. Only a part of it is explained in this section.

The simulation used the roughness in the reservoir as input. The value was set to 0.1 meters in the F 16 data set. The time step of the simulation was taken 100 with 100 inner iterations per time step in the F 33 data set. To avoid the instabilities caused by cells with very small depths F 94 data set was invoked. An algorithm that changes the shape of the cells close to the boundary and improves bank smoothness was used and is given by F 102 data set. The F 113 and F 235 data sets were also included to stabilize the triangular cells. To improve stability by avoiding grid problems, the F 159 data set was used. The choice of discretization scheme was made by invoking K 6 data set.

(Almeland, Olsen et al. 2019) observed different flow situation in sand trap for first and second order upwind scheme. In this case also both of these discretization schemes were tested and the flow patterns in these two cases were different from each other as seen in Figure 5. 1. But the flow pattern obtained from the second-order upwind scheme was chosen for further study. The reason to do so it that the use of SOU scheme would reduce false diffusion and give a better solution.

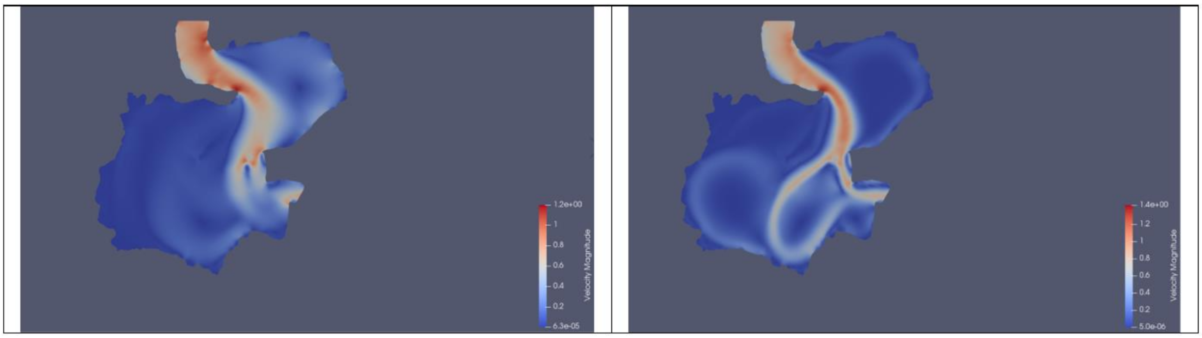

Figure 5. 1 Flow situation when using first order (left) and second order (right) upwind scheme - 1000 cumecs at existing operational level

For the simulation of 1000 m^3/s at full gate opened condition, the water level was changed in *koordina* file and W 1 data set and all the other data sets and parameters were kept same. For the simulation of 3000 m^3/s at existing operational level, the discharge inflow and outflow were changed in *Discharge Editor* interface, water level in *koordina* file and discharge and water level in W 1 data set. Similarly, for 3000 m^3/s at full gate opened condition, the water level was changed in *koordina* file and W 1 data set.

5.5 Simplifications

- The time step of 100 and coarse grid (cell size 12m*16m) were used which reduced the computational time significantly.
- During the simulations at full gate opening, the time period of gate opening and a varying water level were not taken into consideration. Only the water level after the gates have been fully opened was taken.

5.6 Results

The results of the simulation are stored in the *result* file. The results can be viewed from the user interface of the program itself or from the *ParaView* software. The horizontal velocities and bed shear stress observed for all the four cases are shown in the figures below. As seen from the figures, there is a small island that separates the flow into two distinct flow paths in all the four cases. The horizontal velocities shown in all the cases are at the surface.

Note: the scales in the figures vary. So, it is recommended to see the legends.

a) 1000 m^3/s at existing operational level

The main flow has velocity of around 1.2m/s and decreases gradually as it reaches the reservoir downstream. The bed shear stress is around 2.2 N/m^2 at the inlet and to the middle portion of the reservoir but decreases further downstream. At the right bend near the inlet, the bed shear stress is around 10 N/m^2 and bank erosion can take place here.

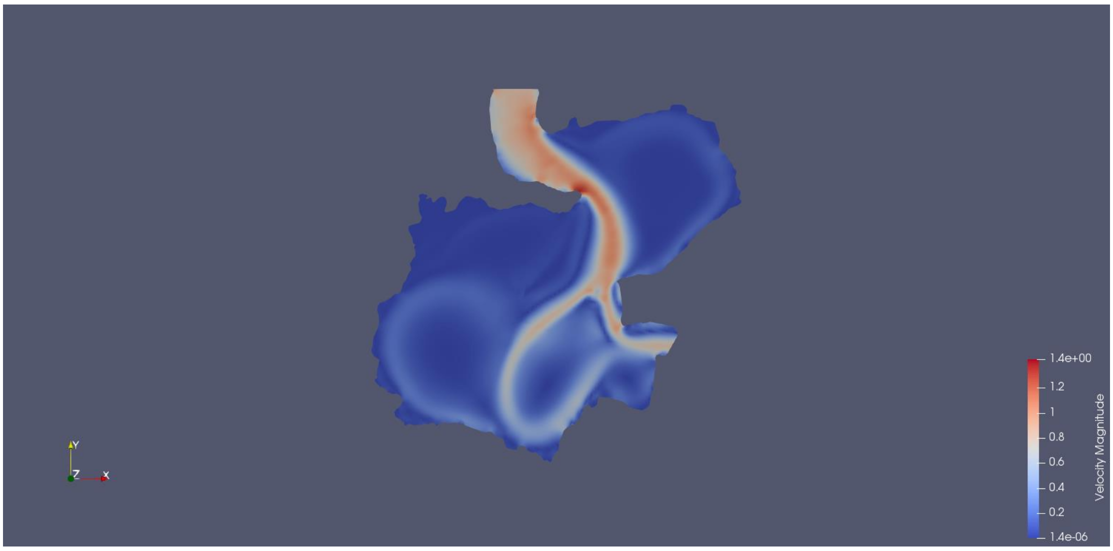

Figure 5. 2 Horizontal velocity

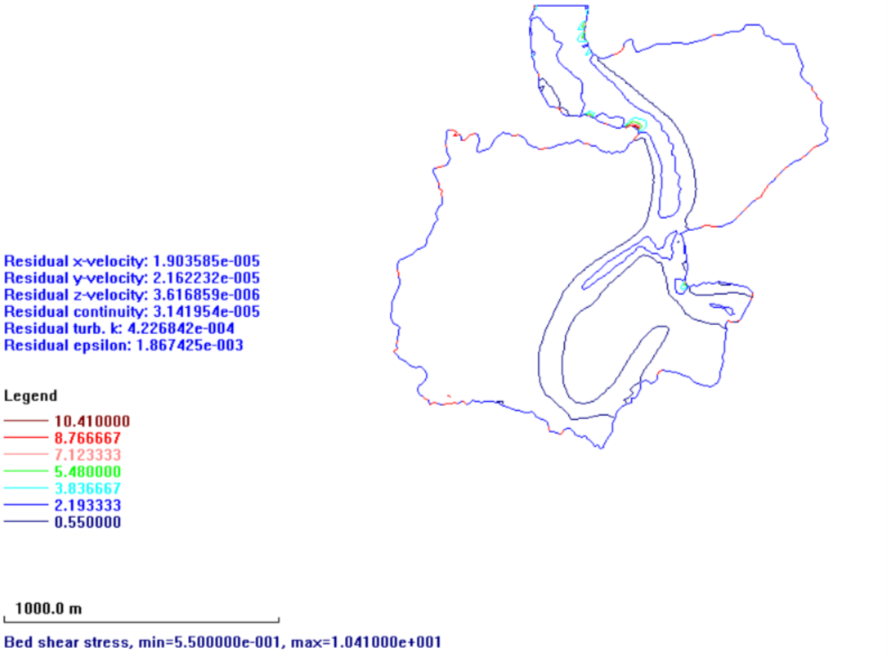

```
Residual x-velocity: 1.903585e-005
Residual y-velocity: 2.162232e-005
Residual z-velocity: 3.616859e-006
Residual continuity: 3.141954e-005
Residual turb. k: 4.226842e-004
Residual epsilon: 1.867425e-003
```

Figure 5. 3 Bed shear stress

b) 1000 m^3/s at full gate opening

The water level is decreased and the grid is lowered down to a level of 568 masl. The grid cuts bed at this elevation and cells get dry at many places. Due to this reason, the inlet portion is seen constricted and high velocity can be seen in this portion. Since the water level is dropped down the velocity can be seen increased in the reservoir. The velocity is above 15 m/s at the inlet and then gradually decreases.

The accelerated water increased the bed shear stress in the reservoir. The bed shear stress is very high at he inflow area and reduces to around 35 N/m^2 and then to 17 N/m^2 towards the middle portion of the reservoir. With this result, it can be said that bed load will be transported further downstream as compared to the situation in existing operational level.

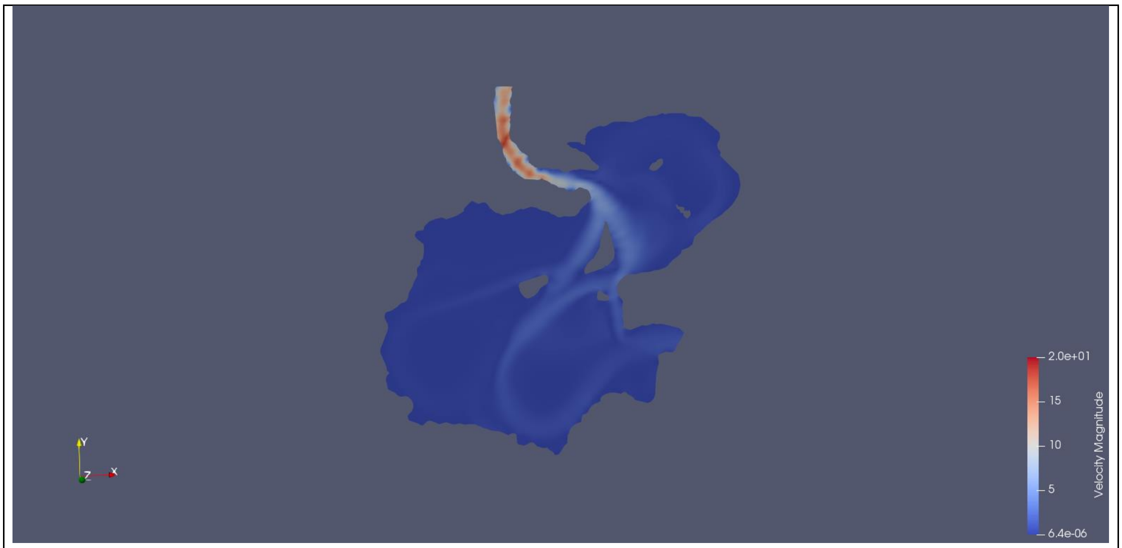

Figure 5. 4 Horizontal velocity

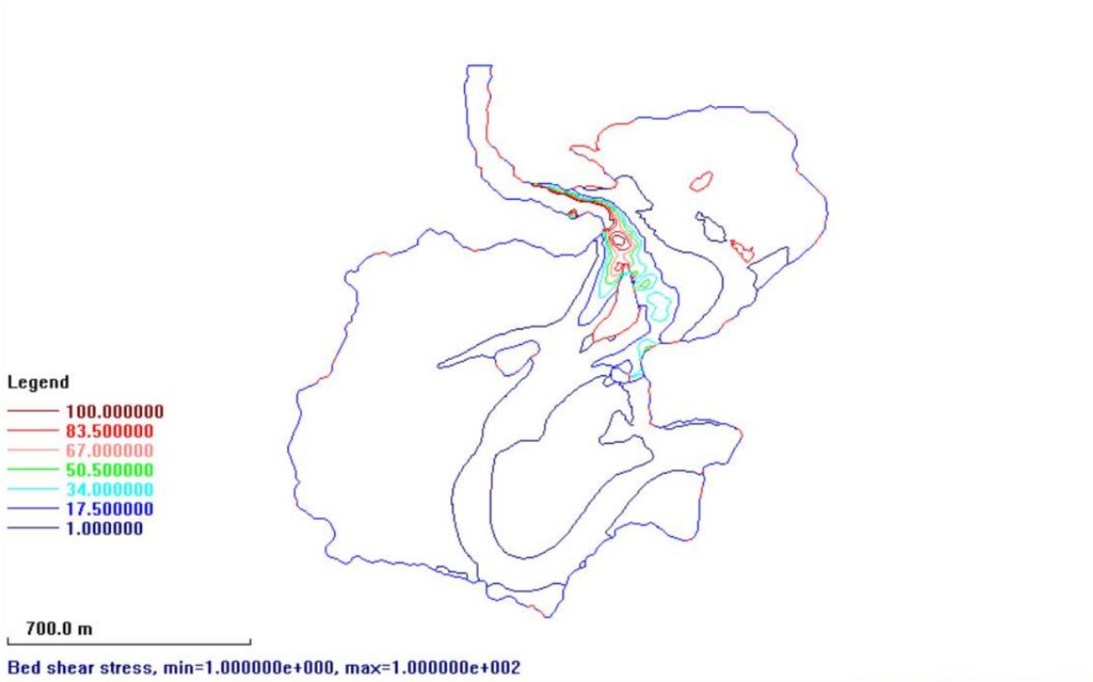

Figure 5. 5 Bed shear stress

c) 3000 m^3/s at existing operational level

The average velocity of the main channel is above 3 m/s and the bed shear stress is around 20 N/m^2 and then decreases to 11 N/m^2 and even less as the flow approaches towards spillway.

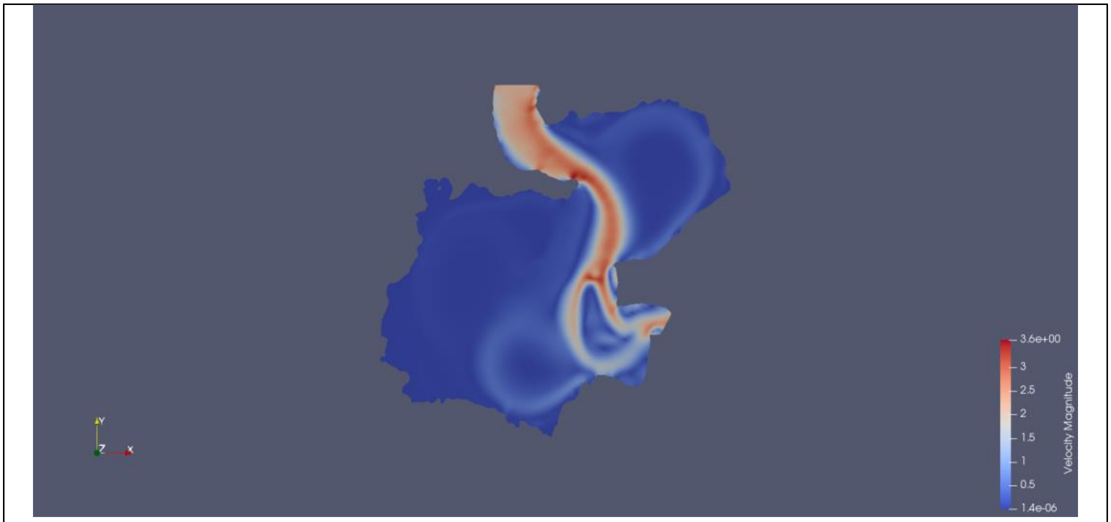

Figure 5. 6 Horizontal velocity

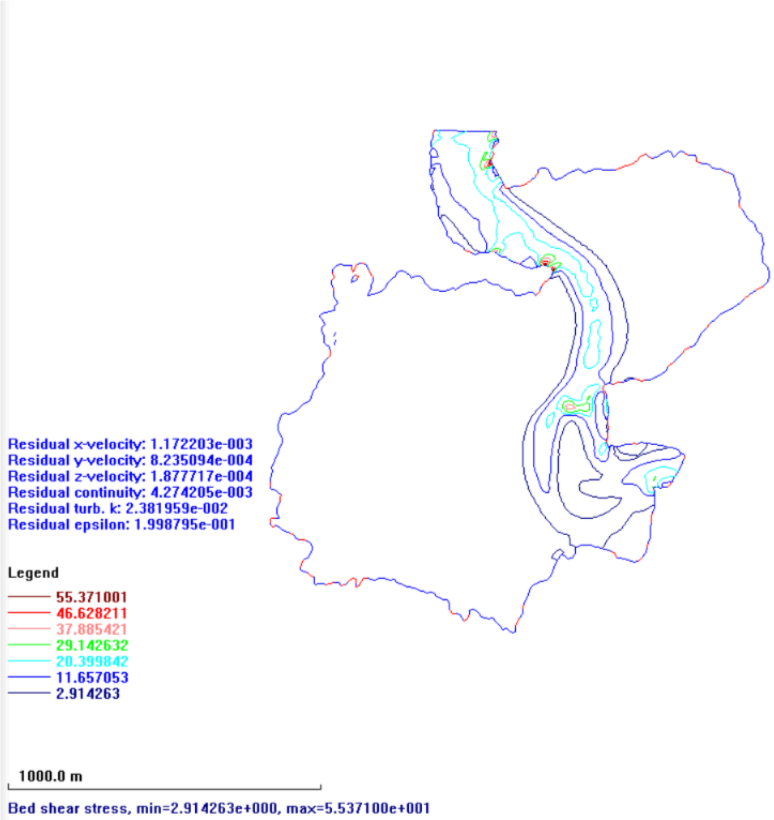

```
Residual x-velocity: 1.172203e-003
Residual y-velocity: 8.235094e-004
Residual z-velocity: 1.877717e-004
Residual continuity: 4.274205e-003
Residual turb. k: 2.381959e-002
Residual epsilon: 1.998795e-001
```

Figure 5. 7 Bed shear stress

d) 3000 m^3/s at full gate opening

The velocity is seen increased as compared to the existing operational rule. At the inflow area, the velocity is more than 8 m/s and then gradually decreases to 6 m/s and to around 5 m/s. The bed shear stress is very high in the uppermost part of the reservoir. The bed shear stress gradually decreases to 45 N/m^2 and to around 30 N/m^2 and lesser towards intake and spillway. Comparatively, the bed shear stress is highest in this case. So, it can be said that the bed load transportation takes place to farthest downstream and bed changes will be more in the downstream of the reservoir in comparison to the previous cases.

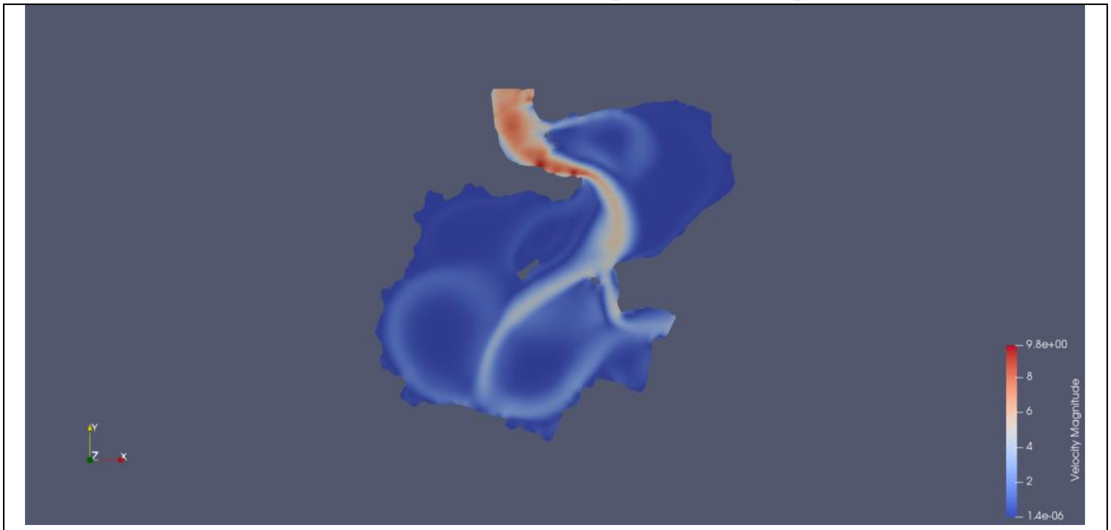

Figure 5. 8 Horizontal velocity

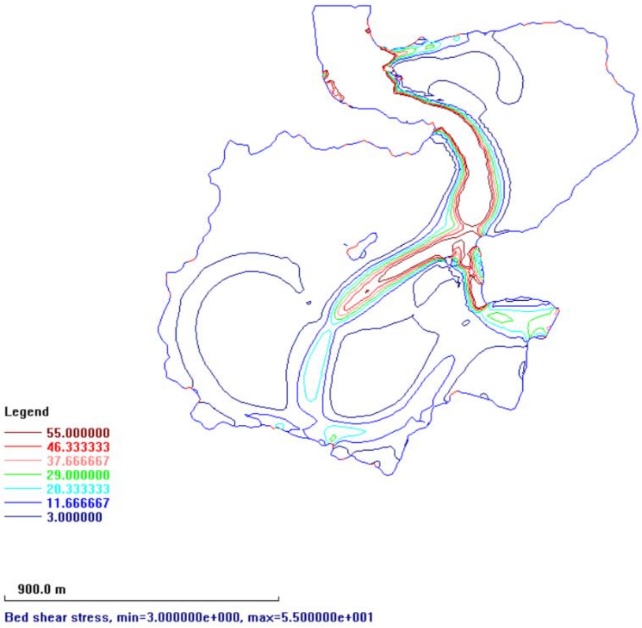

Figure 5. 9 Bed shear stress

5.7 Problem Faced

The problem faced during hydraulic computation was poor convergence in case of 1000 m^3/s at full gate opening. The flow is constricted at the inlet and the number of wet cells is very less in both horizontal and vertical directions. This might be the reason for the convergence problem. Making the grid finer/ increasing the cell numbers may solve the problem.

Chapter 6

Simulation of Sediments

It is beneficial to know the sediment deposition/ erosion and their locations to deal with the sediment problem of Binga. It can be a matter of interest to see what will happen to the inflowing sediments transported by different floods at different operational rules. The bed shear stress in hydraulic simulation gave a rough idea about the sediment transportation and deposition. The bed level changes can be observed more clearly by sediment simulation. SSIIM helps to see what happens to the inflowing sediments in different flood occasions.

6.1 Input Data

Detail sediment data were not available during the simulation. The duration of different floods in a year were known but the corresponding sediment loads carried by these floods were not known. So, some assumptions have been made to simplify the work.

For simulating the sediment deposition, four different scenarios as stated in Table 5. 1 were used. Two discharges, Q_2 and Q_{10} each at existing operational rule and full gate opening condition were studied.

The input data for sediment simulation are sediment sizes, sediment fall velocities, and sediment concentrations. The sediment sizes are taken based on grain size distribution given in Figure 3. 5 in such a way that they cover the range of distribution. The sediment sizes are 100mm, 10mm, 1mm and 0.06 mm. The sediment concentration of 5000 ppm is assumed to be carried by both floods. The calculation of sediment concentration of individual sediment size is shown below:

A constant sediment inflow is assumed throughout the period of flood and that is 5000ppm which is equivalent to 5kg/m^3. With standard sediment density of 2650 kg/m^3, the sediment concentration is equal to 0.001887 m^3/m^3. Now based on Table 3. 5 the concentration is divided as per the granulometry. 10% of cobble small has concentration of 10%*0.001887= 0.000189 m^3/m^3, 35% of gravel medium has concentration of 0.000660 m^3/m^3, concentration of 35% of coarse sand is 0.000660 m^3/m^3 and that of 20% of coarse silt is 0.000377 m^3/m^3

Table 6. 1 Sediment inflow

	1000 m^3/s	3000 m^3/s
100mm (cobble small)	10%	10%
10mm (gravel medium)	35%	35%
1mm (coarse sands)	35%	35%
0.06mm (coarse silts)	20%	20%
Discharge duration	3.7 days	3.7 days

Table 6. 2 Sediment concentration

Sediment sizes	Sediment Concentrations (m^3/m^3)
100mm (cobble small)	0.000189
10mm (gravel medium)	0.000660
1mm (coarse sands)	0.000660
0.06mm (coarse silts)	0.000377

The fall velocities of the sediments are calculated from the simplified Rubey's formula which can be expressed as follows:

$$\omega = \frac{\left(1636(\rho_s - \rho)d^3 + 9\mu^2\right)^{0.5} - 3\mu}{500d}$$

where, ω = terminal fall velocity m/s, ρ_s = density of sediments kg/m^3 , ρ = density of water kg/m^3, μ = dynamic viscosity N*s/m^2, d= diameter of particle m. (Morris and Fan 1998)

Table 6. 3 Fall velocities of sediment particles

Sediment sizes	Fall velocity (m/s)
100mm (cobble small)	1.04
10mm (gravel medium)	0.33
1mm (coarse sands)	0.098
0.06mm (coarse silts)	0.0032

6.2 Simulation Time

The simulation for all the four scenarios are conducted for 3.7 days which is approximately 319700 secs as mentioned in Table 3. 3.

6.3 Starting Simulation

To start the sediment simulation right after the start of the program, the algorithm F 2 UIS is used in the control file.

6.4 Input Files

The *control* file and *timei* file are the two important files for sediment simulation. The control file for sediment simulation is same as the control file for hydraulic simulation but some data sets are added to the existing data sets. The added data sets for sediment simulation are S, N, B and some F data sets. The *timei* file has inputs of time, discharge, water levels, and sediment concentrations. In addition to these files, same *unstruc* file has been used as in the hydraulic simulation for four different cases. The *koordina* file that stores information about the grid is also another important file used in the simulation.

Control file

All the algorithms used in the control file are similar to those used during hydraulic simulation. Apart from those, there are some additional algorithms used during sediment simulation which are explained in Appendix C. Only some important data sets are explained in this section.

To calculate the sediment concentrations at the bed, van Rijn formula was used in the simulation. This was invoked by F 84 data set. The F 6 data set invoked the coefficient for the formula. The simulation is transient sediment computation and this is specified on F 37 data set. The S data set gives the sediment sizes and fall velocities of the sediments under consideration. It is important to mention the same number of sediment sizes used in G 1 data as used in S data set. The N data set was invoked which gives the size fraction of different sediment groups.

Timei file

The *timei* file comprises of the simulation start and end time. It is possible to use intermediate time steps as well. For every time step used the discharge, water level and sediment concentrations entering the reservoir are stated. Due to lack of data, constant concentration of the sediments was considered throughout the time period of 3.7 days. The example of *timei* file for 1000 m^3/s at existing operational level is shown below:

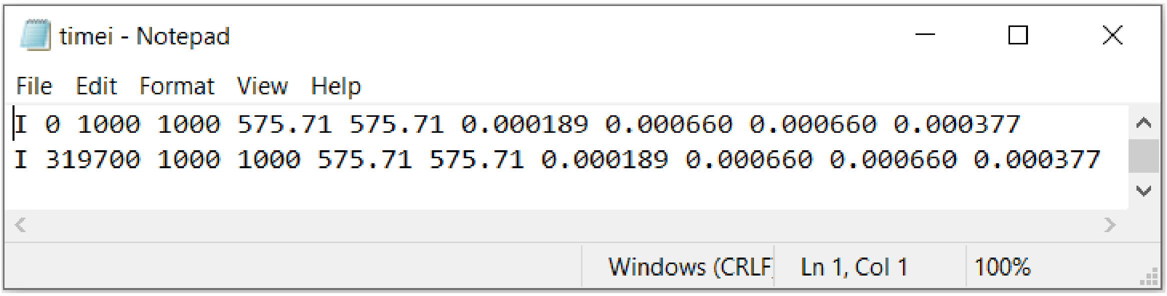

```
I 0 1000 1000 575.71 575.71 0.000189 0.000660 0.000660 0.000377
I 319700 1000 1000 575.71 575.71 0.000189 0.000660 0.000660 0.000377
```

Figure 6. 1 Timei file for 1000 m3/s at existing operational level

The I data set reads the time in seconds as its first float. The second and third floats are upstream and downstream discharges respectively. The fourth float indicates upstream water level and the fifth float is downstream water level. If any variable(s) is unknown, then a negative value is inserted and the program will calculate the value. The four floats, in the end, are concentration of four sediment groups given in S data set.

6.5 Simplifications

- Four different sediment sizes of 100mm, 10mm, 1mm, and 0.06mm were used according to the grain size distribution curve.
- A constant sediment concentration of 5000 ppm was used throughout the flood period.
- Assumptions were made for the size fraction of sediments under consideration i.e. 10%, 35%, 35%, 20% for cobble small, gravel medium, coarse sands and coarse silts respectively.
- For the full gate opening simulations, the time period of gate opening and varying water level were neglected. Simulations were carried out with the water level achieved after all the gates have been opened.
- Less computational time demanding settings- coarse grid and time step of 100 were used.

6.6 Results

The bed level changes for two floods at two different operational levels are shown below. Negative numbers indicate erosion and positive numbers indicate deposition. A lot of depositions are seen in the upper part of the reservoir. For full gate opening condition, it is seen that the bed changes are more in the downstream part compared to the existing operational level situations. This is due to the fact that, in full gate open condition, the increase in bed shear stress results in transportation of bed loads further downstream and hence significant bed changes are seen in the downstream part of the reservoir.

Incase of 1000 m^3/s at existing operational level the deposition at the inflow area is upto 10m and has gradually decreased to 4m and then to around 0.8m towards the middle portion of the reservoir and 0.1m close to intake location. When the water level is lowered by full gate opening, the deposition of the sediments are significant further downstream of the reservoir. Deposition, as well as some erosion, are observed at the inflow area. The deposition of 9m and also around 2m is seen prominently towards the middle portion. The deposition of around 0.33m is observed very close to intake.

Similarly, in case of 3000 m^3/s at existing operational level, the major deposition is around 4.5m (8m at few locations) at the inflow area with very few erosion. Towards the middle portion of the reservoir the deposition has increased to 8 to 13 m and has decreased to 4.5m near spillway. The deposition is seen to be 1 m and decreased to around 0.15m very close to the intake. The sedimentation pattern for the same discharge at full gate opening is different. Erosion can be seen at the inflow area. The bed changes can be seen very far downstream. This is due to high bed shear stress and transportation of bed load from the upstream end of the reservoir. Deposition of 0.16m to 13m is observed at the inflow area. At the middle portion of the reservoir, it is around 4.5 m to 13 m. Near the intake location, deposition is 2m and decreased to 0.16m. These sediment simulations show that the bed load during high floods and full gate opening operation can be transported downstream of the reservoir and result in bed changes near the intake. Therefore, during flushing of the reservoir, there is a higher risk of intake being clogged.

Note: the scales in the figures vary. So, it is recommended to see the legends.

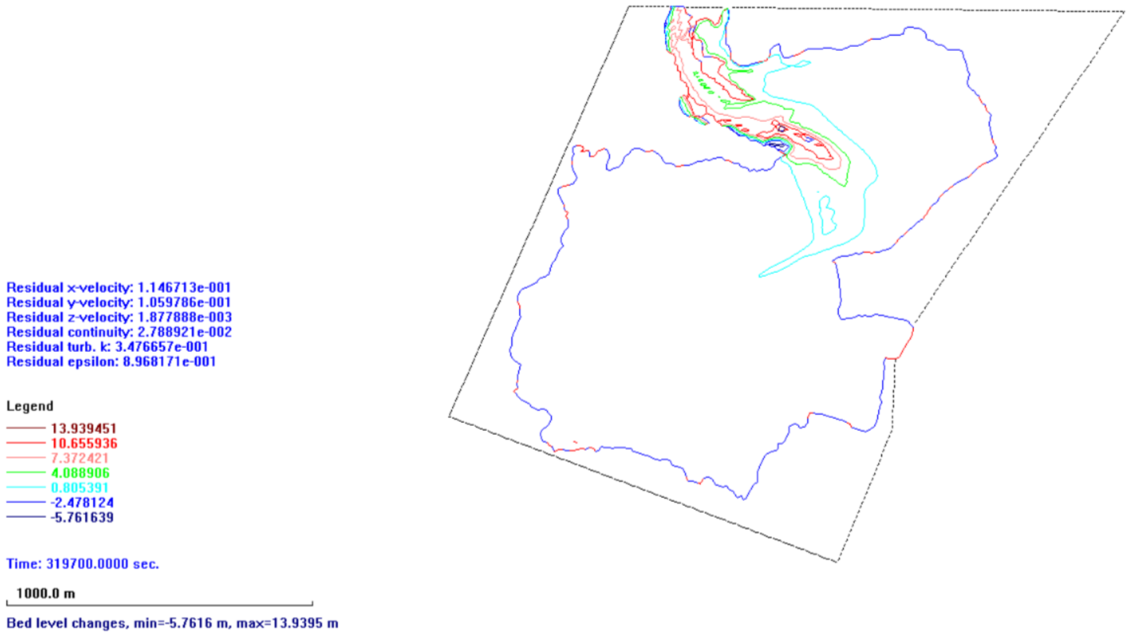

Figure 6. 2 Bed level changes for 1000 cumecs at existing operational level

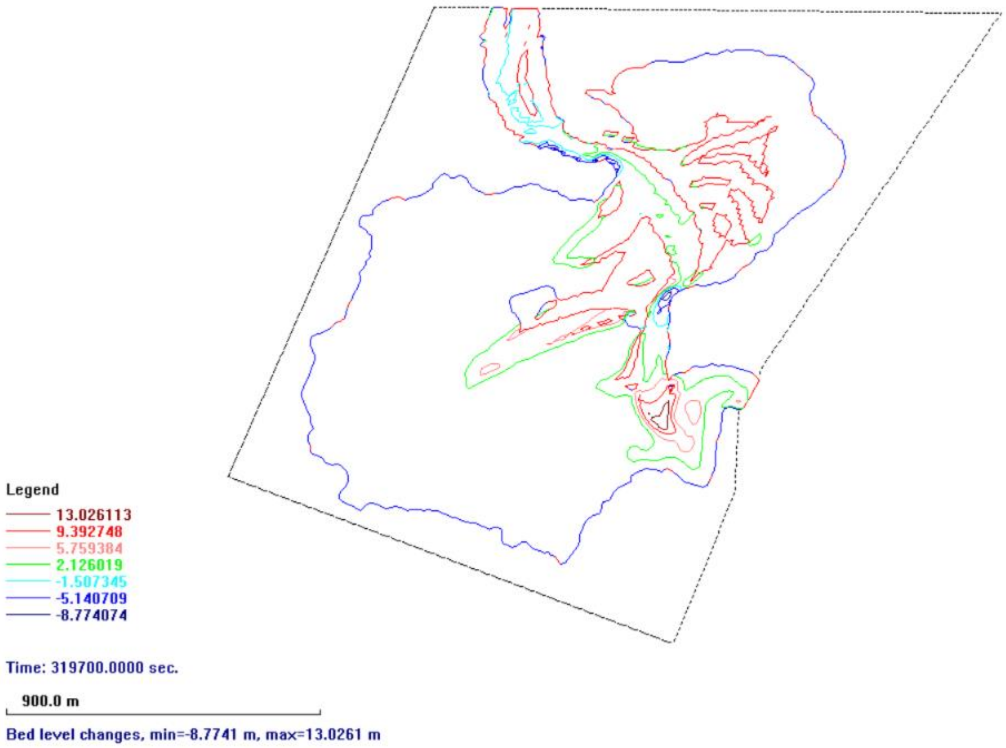

Figure 6. 3 Bed level changes for 1000 cumecs at full gate opening

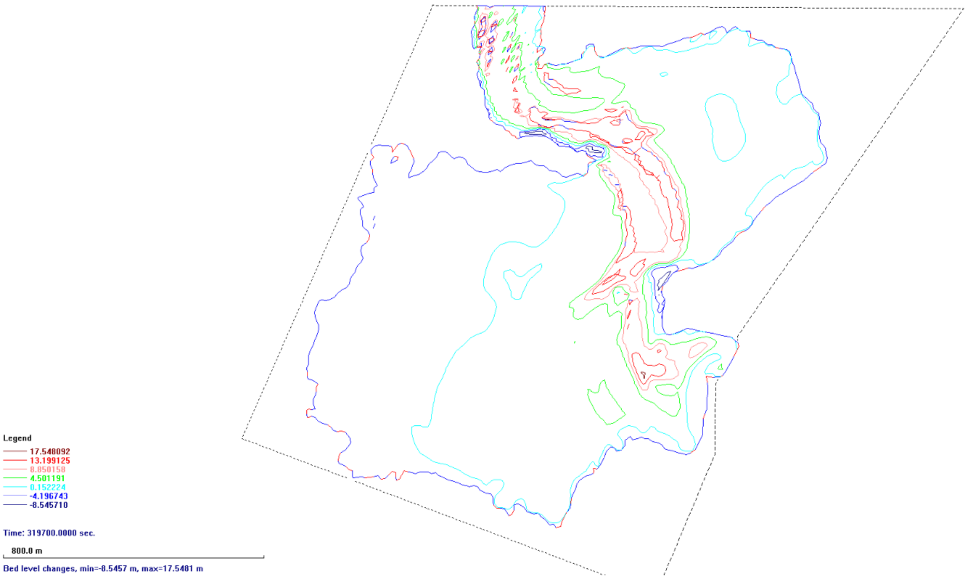

Figure 6. 4 Bed level changes for 3000 cumecs at existing operational level

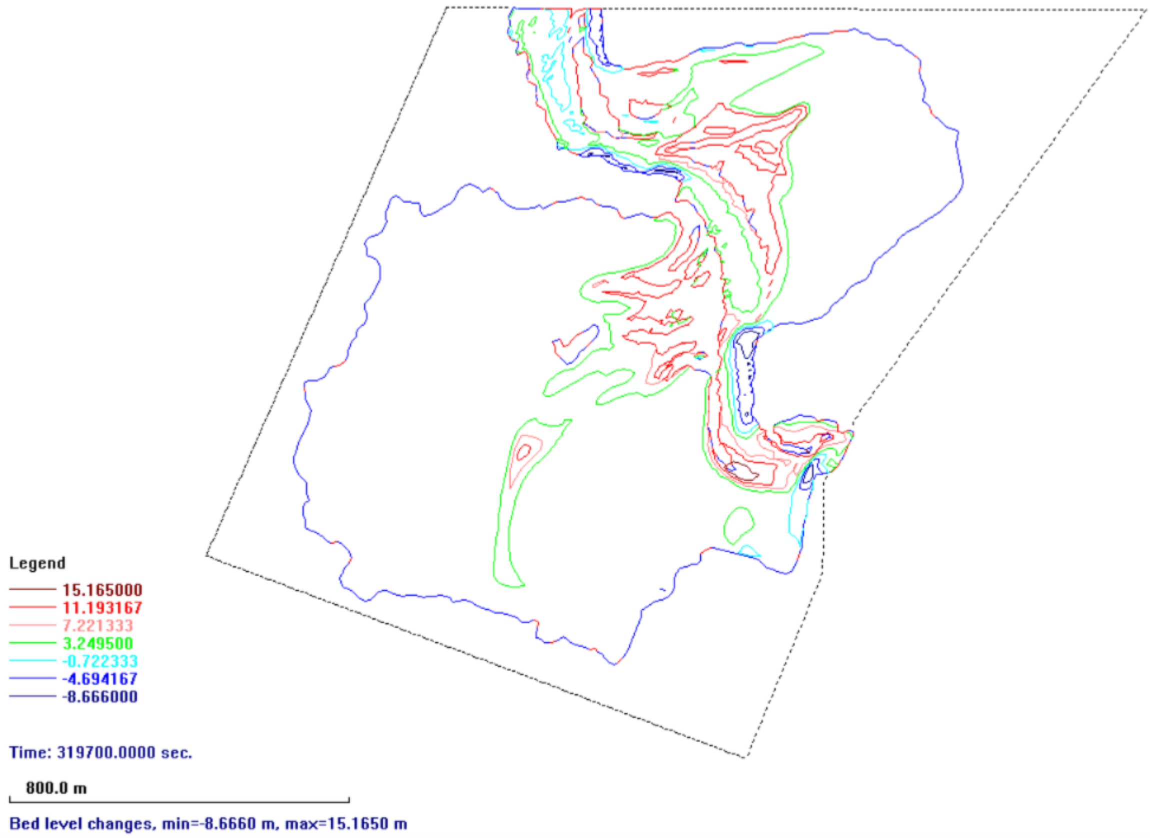

Figure 6. 5 Bed level changes for 3000 cumecs at full gate opening

The sediment deposition has led to drying up of several areas in the reservoir. Because of deposition, the velocities and flow patterns have been changed in all four cases which can be seen from the figures below:

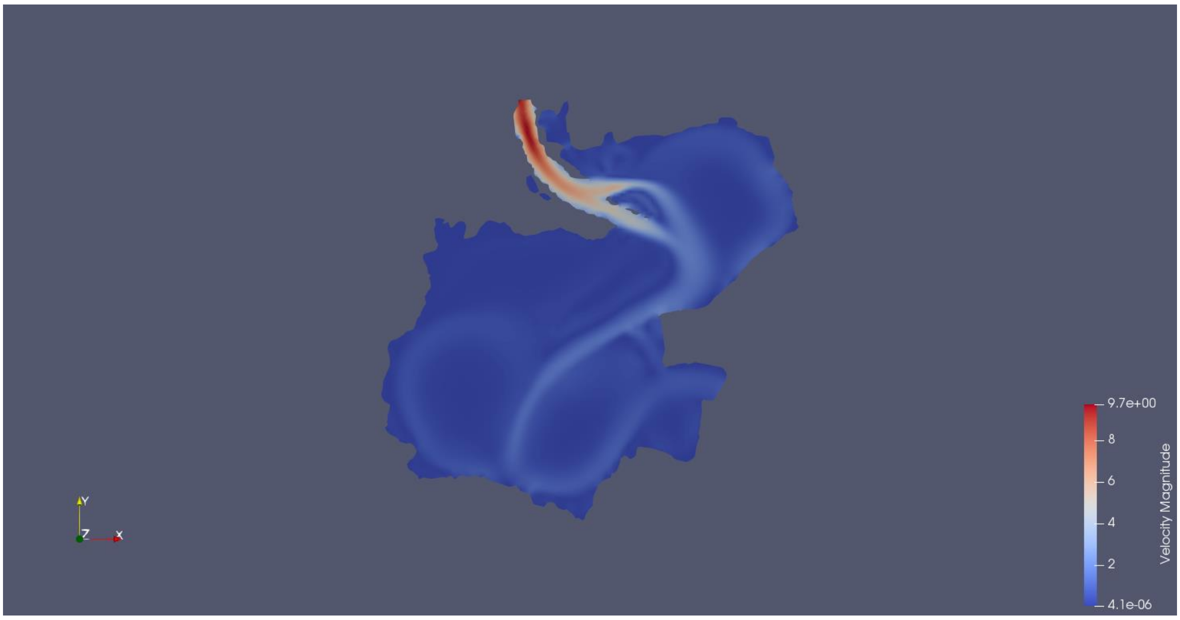

Figure 6. 6 Horizontal velocity for 1000 cumecs at existing operational level

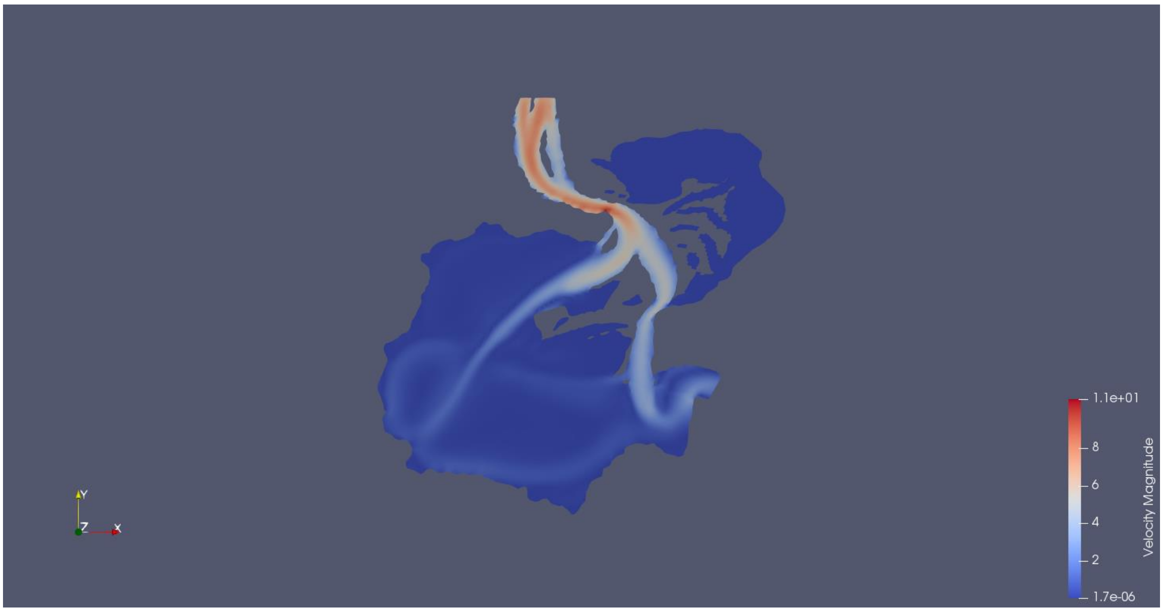

Figure 6. 7 Horizontal velocity for 1000 cumecs at full gate opening

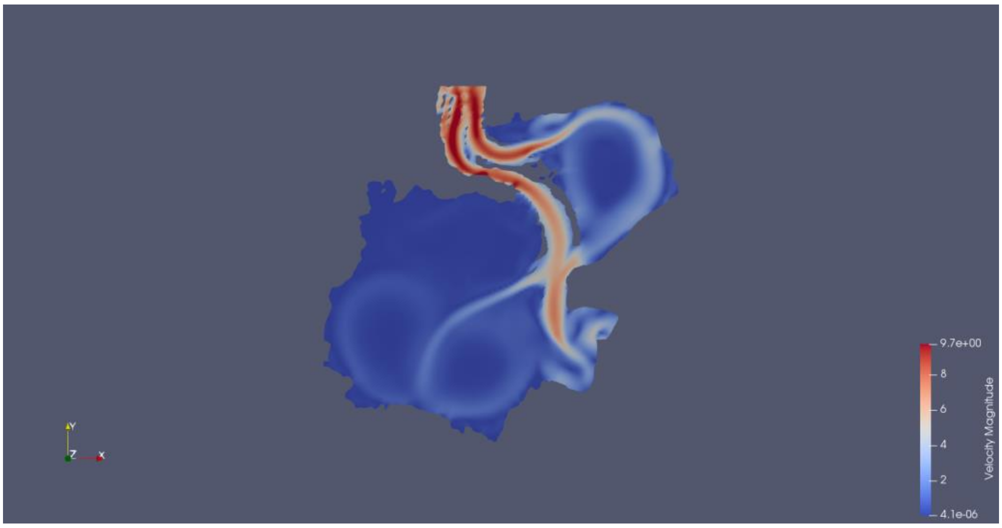

Figure 6. 8 Horizontal velocity for 3000 cumecs at existing operational level

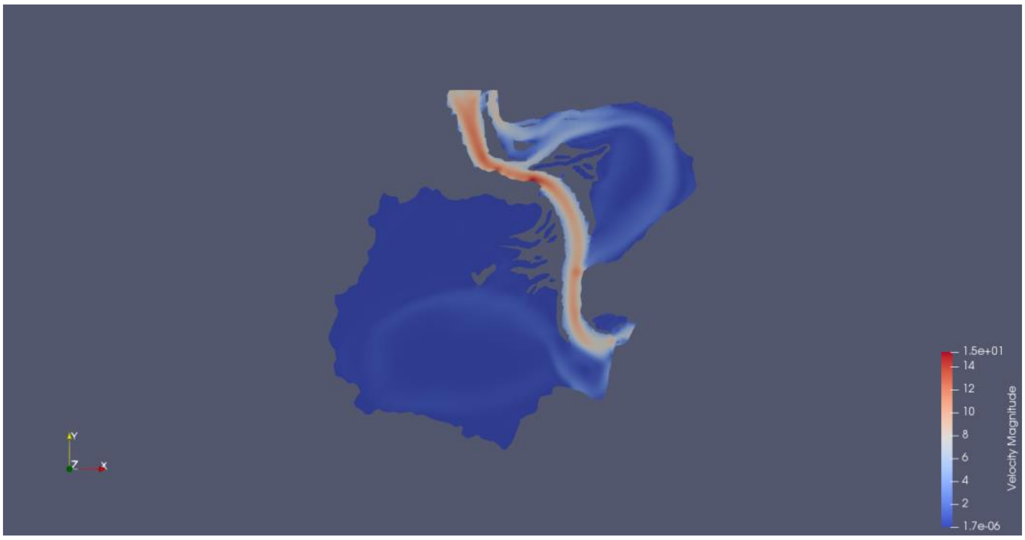

Figure 6. 9 Horizontal velocity for 3000 cumecs at full gate opening

6.7 Problems Faced

The problem faced was divergence of solution after some iterations in case of 3000 m3/s at full gate opening. During the simulation, a time step of 100 and inner iteration of 100 was used in F 33 data set. Parameter sensitivity analysis, explained later in section 8.2 page 41, was performed during hydraulic simulation and it was found that decreasing time step and/ or increasing inner iteration helps to improve convergence. Therefore, a reduction of time step from 100 to 10 was made and F 292 1 1 data set was invoked inorder to solve the problem. Similarly, the convergence was not good when running 3000 m^3/s at existing operational level but was improved by using time step of 10 instead of 100 and inner iteration 200 instead of 100 in F 33 data set. However, this took a long time (3 full days) to complete the simulation and also changed the result, see Appendix C.2 Problems Faced.

Chapter 7

Sediment Management in Binga Reservoir

Sediment Management in the reservoir should cover the following objectives:

- Prevent clogging of intake and stoppage in production
- Provide safe passage of flood from the spillway
- Ensure the safety of the dam and spillway
- Maintain ability to produce power

It is seen from the sediment simulation that the transportation of the sediments is towards spillway and also in the direction of the intake. Flushing by spillway gate opening is one of the measures to handle sediments, but during flushing, the transport of bed load is seen further downstream towards the intake. It is of great importance to stop the sediment load that is progressing towards the intake. In order to do this, a guide wall to direct the flow towards the spillway can be made from the island that is in the middle part of the reservoir, see Figure 7. 1.

Figure 7. 1 Dikes to guide the flow towards spillway

The general idea of the guide wall is to modify the flow pattern and the velocity to keep the sedimentation problem far away from the intake and to direct the sediments towards the spillway during flushing. The intake will take water from around the end of the guide wall.

It is important to design the guide wall in such a way that it withstands erosion caused by overtopping. But the upstream and downstream water level difference in the reservoir is not that much to cause the erosion. Therefore, scour protection work will be limited. (MulticonsultAS 2017)

For the simulation, the crest level width of guide wall is taken 4.5 m, length of the guide wall at right side of the island 336 m, at left side of island 396 m and assumed to be at the elevation of HRWL, 575 masl. The reason to do so is that during normal operation, the guide wall will not be overtopped by the water and the sediments will be trapped and diverted from upstream of the guide wall. The simulation is carried out for the flood of 3000 m^3/s at full gate opening because it is the case with highest bed shear stress transporting bed load to farthest downstream.

7.1 Input Data

The simulation was done with the same input data as in sediment simulation for 3000 m^3/s at full gate opening in existing geometry.

7.2 Simulation Time

The simulation time is 3.7 days i.e. 319700 secs.

7.3 Starting Simulation

To start the sediment simulation, the algorithm F 2 UIS is used in the control file.

7.4 Input Files

The points representing guide walls were added using different software called AutoCAD, so the *geodata* file was modified. The *unstruc* file, therefore, changed because the grid was remade. However, the grid size is kept same and attempts were made to keep the changes in grid orientation as less as possible.

Control file

All the algorithms in the control file are same except the time step in F 33 data set and F 292 data set. As stated in section 6.7 page 35, during the simulation of 3000 m^3/s at full gate opening in existing geometry, a problem of simulation crashing was observed, so time step was reduced to 10 and F 292 data set was invoked. Now during this simulation of improved geometry with the guide wall, the time step is put to 50 and inner iteration to 200 and also the F 292 data set is removed to save computational time.

Timei file

The *timei* file is same as that for 3000 m^3/s at full gate opening in existing geometry.

7.5 Simplifications

The simplifications are same as stated in section 6.5.

7.6 Results

In the improved geometry, the sediment deposition of 4 to 12 m is seen at the mid-portion of the reservoir. Erosion of around 0.11m to 4m can be seen in the inflow area.

A comparison of sediment deposition pattern and flow situation after sediment deposition in existing and improved geometry is presented below. The guide wall has diverted the sediment deposits towards the spillway and there are no bed changes towards the intake location. The improved geometry thus fulfills our objective to prevent clogging of intake.

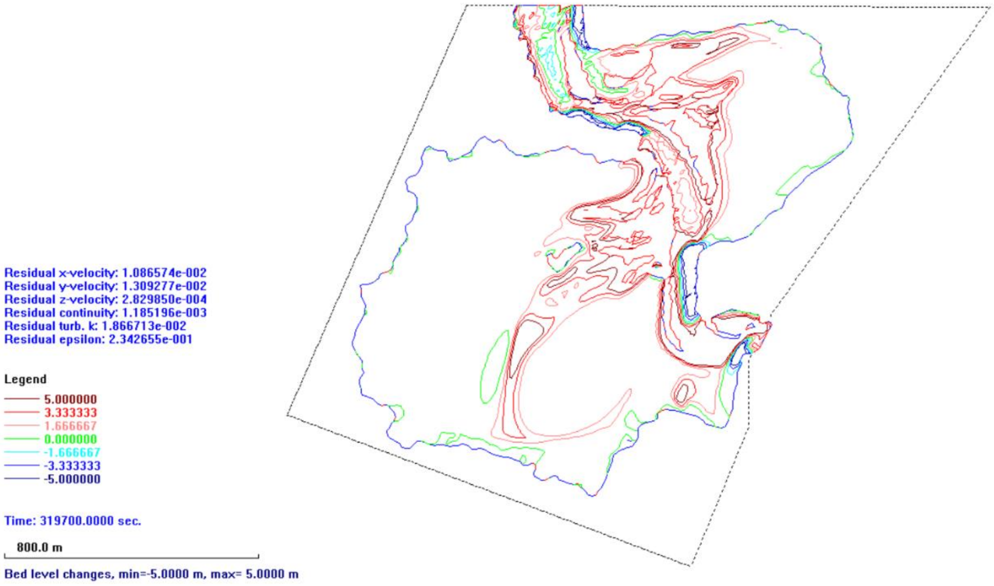

Figure 7. 2 Bed changes in existing geometry

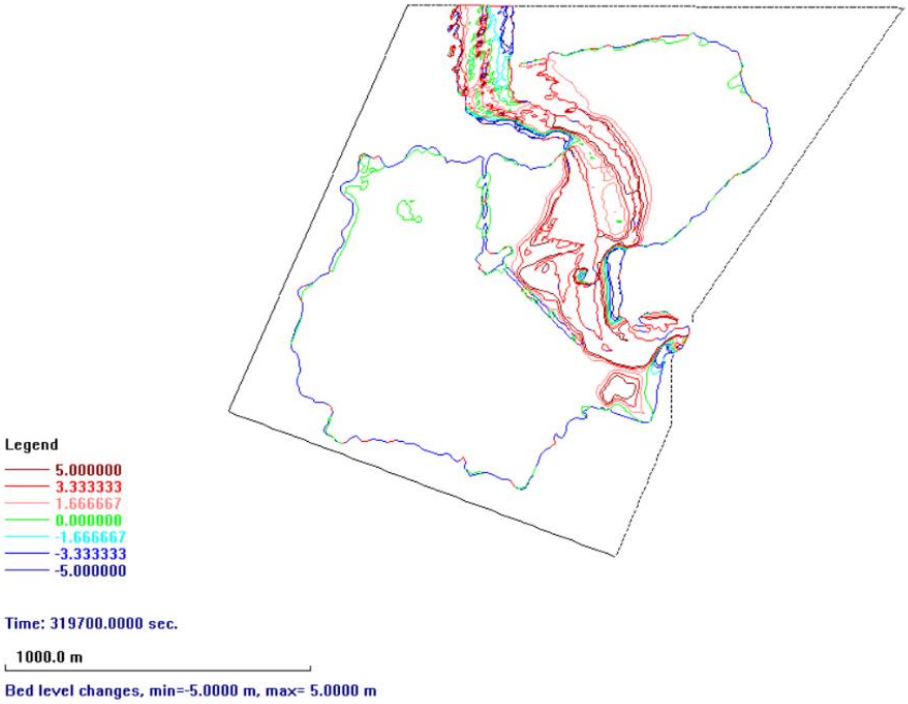

Figure 7. 3 Bed changes in improved geometry

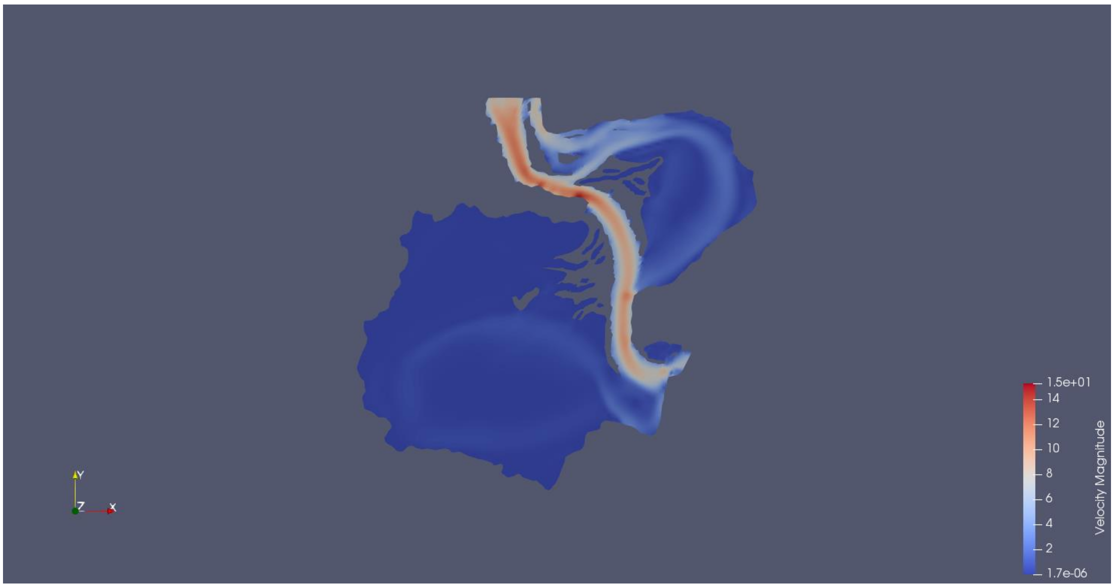

Figure 7. 4 Horizontal velocity in existing geometry

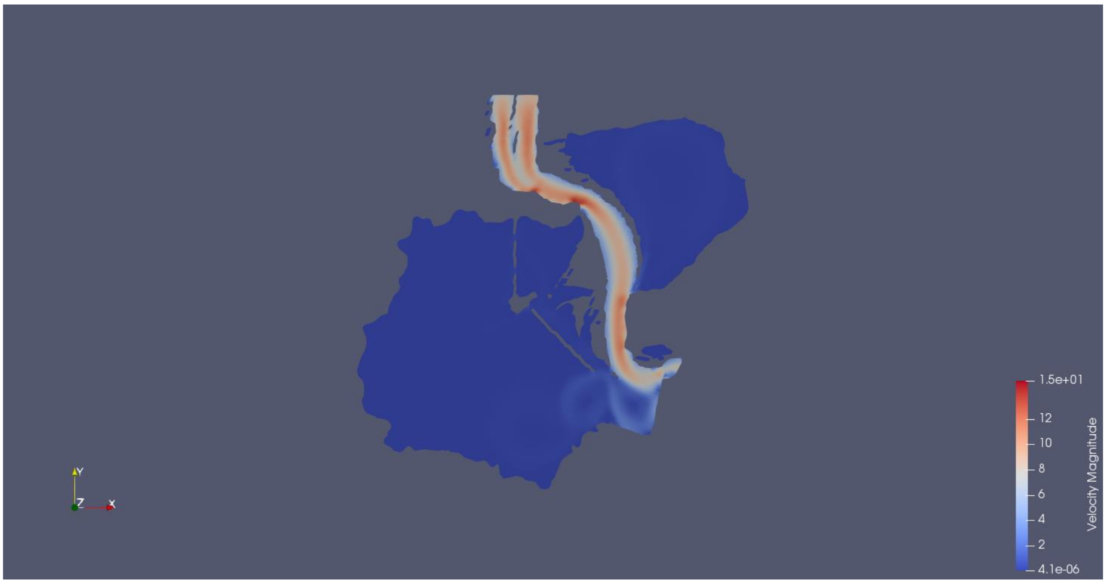

Figure 7. 5 Horizontal velocity in improved geometry

7.7 Problems Faced

Convergence problem was seen during the simulation. In many simulations, the convergence had been seen improved by decreasing the time step and/ or increasing the number of iterations in F 33 data set. This can be done in this case also. Due to computational delays, a higher time step of 100 was used for this simulation process. Similarly, due to sedimentation, the cells get dry in many places reducing the number of wet cells which can also influence the result. So, making the grid finer can also be tried to improve convergence.

7.8 Alternative Concepts

The guide wall length used in the simulation is long which can be economically unfeasible. Therefore, the length can be reduced. From the simulation, it is seen that the right guide wall can be omitted. The right guide wall was used in the simulation with an assumption that the flow direction of the main channel will be changed towards the right bank after it hits the lower guide wall. However, the main channel tends to flow towards spillway and the transport of sediment load will be towards spillway rather than the right bank.

The elevation of the guide wall crest used in the simulation is 575 masl. On doing so, the guide wall will not be overtopped in normal operation and the sediments will be trapped behind it. However, if the height of guide wall is reduced without compromising the extent of sediment transport downstream, then the project can be more economical.

Another sediment handling approach can be a bypass tunnel at the entrance of the reservoir. The main idea is to catch the bed load upstream of the reservoir and to transport the incoming sediment load towards downstream river of the plant through a tunnel. If the bypass tunnel is made on the upstream part then all the sediments will be filtered out right away with very low discharge or very often occurring discharge in general. On the other hand, if the water level is lowered more or higher discharge is used, the bypass tunnel can be made downstream due to the transport of sediment further downstream of the reservoir. This can reduce the cost of bypass tunnel. The feasibility and effectiveness of this approach can also be studied.

Chapter 8

Discussion

8.1 Result verification

The sediment deposition simulations were carried out for the future flood events using the recent bathymetry, so there are no measurements to compare the results. However, the verification can be done by comparing these results with the simulation results from physical model in the future. The physical model is under construction in hydraulic lab at the Department of Civil and Environmental Engineering, NTNU. Another way to verify the results can be the use of other computer programs like HEC-RAS.

8.2 Parameter Sensitivity Analysis

Changing the algorithms and/or parameters of algorithms used in the simulations might affect the result and computational time. Some parameters were tested for the hydraulic simulation to see if the change can have a significant influence on the results. This sensitivity analysis is presented in Appendix B in tabulated form. The following parameters are explained in this section:

- Roughness coefficient
- Time step and inner iterations
- Grid size

The roughness coefficient in the original simulation was 0.1. By reducing it to half i.e. 0.05, the bed shear stress was reduced slightly at some locations. However, there was no significant change in the horizontal velocity. When the roughness was doubled i.e. 0.2, there was a change in horizontal velocity and flow pattern and there was a slight increase in bed shear stress. The roughness coefficient was again changed to 0.3 and the flow pattern was observed similar to that in case of 0.2 and there was a slight increase in bed shear stress.

After many simulations, it was found out that, decrease in time step and/ or increase in inner iterations in F 33 data set improve the convergence and increase the simulation time.

The change was made on grid size. The initial grid had 12m * 16m cell size in xy- direction. The cell size was reduced to half i.e. 6m * 8m and simulation was carried out. There was no significant change in the result. Unfortunately, the convergence was not so good which was later solved by decreasing the time step and increasing the inner iterations and the simulation was computational time demanding.

8.3 Simulation of Sediments

During the simulation of sediments, due to lack of data, assumptions had been made for concentration and sediment size fraction. Change in these parameters can produce different sedimentation pattern. The time period of gate opening and varying water level was not considered during the simulation of full gate opening conditions. However, the period of the floods under consideration is 3.7 days and the time period of gate opening will be in some hours which is considered negligible in the study.

During the simulation of sediment at full gate opening conditions, high erosion and less deposition were expected but the deposition is observed to be more than erosion. This is due to the use of coarser sediments with high critical bed shear stress and assumption of constant sediment concentration throughout the flood period.

8.4 Sediment Simulation in Improved Geometry

In the model, to calculate the sediment transport rate, van Rijn approach was used. However, the determination of sediment transport rates is one of the most challenging topics. There exist many formulae, but a general unifying formula is not available yet. Therefore, more approaches are to be used to determine the expected range of transport rates.

An algorithm F 84 5 was used instead of F 84 1. F 84 5 invokes Meyer- Peter and Muller's formula for sediment transport and F 84 1 indicated bed load formula by van Rijn. The purpose to test this algorithm is to see if a change in the sediment transport formula can have any significant effect on the result.

The velocity of main channel flow when using Meyer- Peter and Muller's formula was seen lower than when using van Rijn formula. The flow and deposition patterns were also observed different. The total bed changes when using van Rijn approach and Meyer- Peter and Mullers approach were 1.42 mill. m^3 and 1.65 mill. m^3 respectively, see Appendix D.

For the simulation of reservoir flushing, the varying water level during gate opening of spillway was neglected with an assumption that this time period wouldn't influence the result. This assumption was checked by including varying water level in the *timei* file. The timei file is shown in Appendix D. G 6 data set which calculates water surface elevation with an adaptive grid and F 36 3 data set which invokes the movement of water surface up and down equally in all cells according to the d/s water level given in *timei* file were used. The time step and number of iterations in F 33 data set were set to 100 and 100 to save computational time. Total change in bed levels when varying water level was not considered was 1.42 mill. m^3 whereas when varying water level was considered, it was 1.45 mill. m^3. The pattern of bed changes was in close relation to each other, see Appendix D.

8.5 Reasons for Inaccuracies

The errors and uncertainties mentioned in section 2.3.2 page 5 are relevant in this case. They are discussed as follows:

1. Errors in numerical approximations: Efforts have been made to align the grid with the flow field. Discretization scheme that is used in simulation is the second-order upwind scheme and this reduces false diffusion.

2. Modelling errors: This can be relevant in this study. An example can be lowering of water level during full gate opening. In this case, inflow should be much smaller than outflow. However, SSIIM is unable to handle differences between inflow and outflow, so, the same discharge is used in both inflow and outflow.

3. Errors due to not complete convergence: The time-dependent computations are used and convergence has not been reached for every time step. To achieve complete convergence, the simulations would be very time-consuming. Therefore, there is a risk of inaccurate result due to incomplete convergence.

4. Round- off errors: 64 bits floating point numbers with 12 digits accuracy is used by SSIIM. So, rounding- off error should not be a problem in this case.

5. Errors in input data: There are uncertainties while deciding input data and assumptions have been made during sediment simulation. This can cause inaccuracies in the result.

6. Programming errors: SSIIM has not been tested widely and has been used by a limited number of people, so there might be many bugs which can produce inaccurate results.

Other reasons for errors can be due to the reduced number of cells especially in case of full gate opening simulations. When the water level is lowered down, the width and depth of channel decreases and the number of cells gets reduced. This can affect the result.

It is also seen that the result varies with the choice of parameters. An example is a change in time step and iterations in F 33 data set. The decrease in time step and increase in inner iterations influenced convergence and also the sediment transport and deposition pattern for the sediment simulation of 3000 m^3/s at existing operational level.

Chapter 9

Conclusion

The objective of this present study was to perform the three-dimensional modeling of flow structures and bed load movement at Binga Hydropower Plant. The task mainly included documentation of flow situation based on the recent bathymetry, presenting a working hypothesis on how to convey the bed load through the reservoir and documenting the flow situations and bed load movement. To fulfill these objectives, SSIIM was used to perform the hydraulic simulation based on the recent bathymetry which gave the flow situation in the reservoir. Similarly, the sediment simulation was carried out to see how the sediments are eroded, transported and deposited. Four scenarios were studied for this purpose which are 1000 m^3/s at existing operational level & full gate opening condition and 3000 m^3/s at existing operational level & full gate opening condition. The sediment simulations showed that the risk of intake clogging will increase if proper sediment handling approach is not adopted. Therefore, a working hypothesis was made to divert sediments away from the intake and through the spillway. This could be achieved by making a guide wall across the reservoir. Finally, simulation was performed in an improved geometry with guide wall for 3000 m^3/s flood at full gate opening because this is the situation where the bed shear stress was highest and would likely transport the bed load far downstream of the reservoir and close to the intake.

It has been found that the choice of algorithms and choice of parameters in various data sets affect the result. For example, the time step and inner iterations in F 33 data set, choice of discretization scheme in K 6 data set, choice of roughness coefficient in F 16 data set, etc. During the simulations, least computation demanding parameter settings were used to save simulation time which was crucial because of time limitation.

During the initial phase of hydraulic simulation, problems were faced while selecting the algorithms to make the model stable. It has been observed that for time-dependent computation, low time steps facilitates in good convergence of the computations but on the other hand, it increases the computational time as well. A conclusion that is drawn from the hydraulic simulation which can be useful for future physical modeling is that, below 1000 m^3/s, at existing operational level, the bed shear stress is too low to transport bed loads downstream and everything gets deposited at the inflow area. So, to simulate bed load movement higher flood or lower flood at full gate opening can be tested.

Some assumptions had to be made during the sediment simulation, because of the lack of data. The assumptions were made on the size fraction and sediment concentration. This can affect the erosion, transportation, and deposition taking place in the reservoir. There are many other possibilities for inaccuracies in the results of the simulations. Therefore, further testing of the simulations has to be done and also verification of the results is recommended.

Chapter 10

The way forward

To improve the results a lot of further work can be done. Firstly, simulations can be done using old bathymetry data, calibrate the model to get present bathymetric condition and then use this calibrated model to predict future scenarios and validate the results.

For the sediment simulation, missing data of sediment concentration and sediment size fraction should be measured. An approach to put up a 2D simulation model can also be made in the future to estimate the shear stress in the river upstream in order to see what’s coming in and to have a boundary condition for reservoir simulation. In addition, measurements of inflow and outflow discharges and water levels during flushing have to be done. This will make the flushing simulations more realistic.

During simulation of flushing, the water level is lowered down. This results in the reduction of cell numbers. Therefore, a finer grid size can be tested which is neither computational time demanding nor compromises the quality of result.

During low and frequently occurring floods, the sediments tend to deposit at reservoir upstream. Therefore, using a bypass tunnel that can tap sediments from upstream can be more effective than making a guide wall. This can be studied further.

References

Almeland, S. K., et al. (2019). "Multiple solutions of the Navier-Stokes equations computing water flow in sand traps." Engineering Applications of Computational Fluid Mechanics 13(1): 199-219.

Anderson, J. D. and J. Wendt (1995). Computational fluid dynamics, Springer.

Fan, J. and G. L. J. J. o. H. E. Morris (1992). "Reservoir sedimentation. II: Reservoir desiltation and long-term storage capacity." 118(3): 370-384.

Hauer, C., et al. (2018). "State of the art, shortcomings and future challenges for a sustainable sediment management in hydropower: A review." Renewable and Sustainable Energy Reviews 98: 40-55.

Hoven, L. E. (2010). Three-dimensional numerical modelling of sediments in water reservoirs, Norges teknisk-naturvitenskapelige universitet, Fakultet for ….

IHA, I. H. A. (2017). "Case Study Binga, Philippines."

Morris, G. L. and J. Fan (1998). Reservoir sedimentation handbook: design and management of dams, reservoirs, and watersheds for sustainable use, McGraw Hill Professional.

Mouris, K., et al. (2018). Three-dimensional numerical modeling of hydraulics and morphodynamics of the Schwarzenbach reservoir. E3S Web of Conferences, EDP Sciences.

MulticonsultAS (2017). "Binga HPP- towards a robust and reliable run- of- river operation, concept report V2 ".

Olsen, J. V., et al. (1985). "Users Manual."

Olsen, N. R. B. (2010). Result assessment methods for 3D CFD models in sediment transport computations. 1st Conference of the European section of the IAHR, Edinburgh, Scotland.

Olsen, N. R. B. J. T. N. U. o. S. and T. Technology (2007). "Numerical modelling and hydraulics."

Schellenberg, G., et al. (2017). "Dealing with Sediment: Effects on Dams and Hydropower Generation." Hydro Review Worldwide.

StøleAS, S. S. D. I. H. (2018). "Binga Sediment Challenges Study- Operational Impacts of Alternatives A0, AL, AR and "AR- DO Almost Nothing"."

Appendix A

Task Description

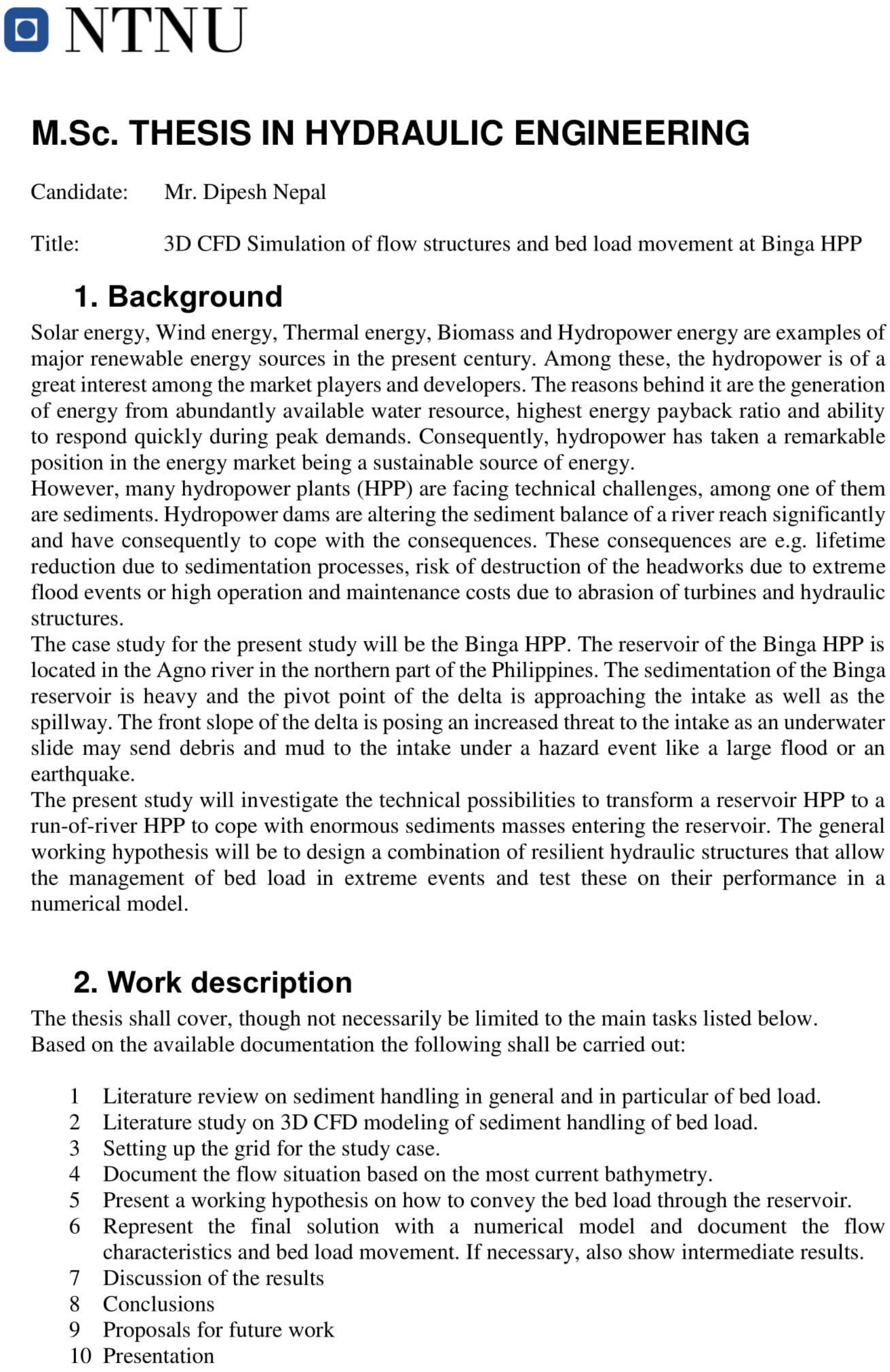

NTNU

M.Sc. THESIS IN HYDRAULIC ENGINEERING

Candidate: Mr. Dipesh Nepal

Title: 3D CFD Simulation of flow structures and bed load movement at Binga HPP

1. Background

Solar energy, Wind energy, Thermal energy, Biomass and Hydropower energy are examples of major renewable energy sources in the present century. Among these, the hydropower is of a great interest among the market players and developers. The reasons behind it are the generation of energy from abundantly available water resource, highest energy payback ratio and ability to respond quickly during peak demands. Consequently, hydropower has taken a remarkable position in the energy market being a sustainable source of energy.

However, many hydropower plants (HPP) are facing technical challenges, among one of them are sediments. Hydropower dams are altering the sediment balance of a river reach significantly and have consequently to cope with the consequences. These consequences are e.g. lifetime reduction due to sedimentation processes, risk of destruction of the headworks due to extreme flood events or high operation and maintenance costs due to abrasion of turbines and hydraulic structures.

The case study for the present study will be the Binga HPP. The reservoir of the Binga HPP is located in the Agno river in the northern part of the Philippines. The sedimentation of the Binga reservoir is heavy and the pivot point of the delta is approaching the intake as well as the spillway. The front slope of the delta is posing an increased threat to the intake as an underwater slide may send debris and mud to the intake under a hazard event like a large flood or an earthquake.

The present study will investigate the technical possibilities to transform a reservoir HPP to a run-of-river HPP to cope with enormous sediments masses entering the reservoir. The general working hypothesis will be to design a combination of resilient hydraulic structures that allow the management of bed load in extreme events and test these on their performance in a numerical model.

2. Work description

The thesis shall cover, though not necessarily be limited to the main tasks listed below.
Based on the available documentation the following shall be carried out:

1. Literature review on sediment handling in general and in particular of bed load.
2. Literature study on 3D CFD modeling of sediment handling of bed load.
3. Setting up the grid for the study case.
4. Document the flow situation based on the most current bathymetry.
5. Present a working hypothesis on how to convey the bed load through the reservoir.
6. Represent the final solution with a numerical model and document the flow characteristics and bed load movement. If necessary, also show intermediate results.
7. Discussion of the results
8. Conclusions
9. Proposals for future work
10. Presentation

NTNU

The literature review should outline the previous contributions in a condensed manner and result in the motivation for the current study.

3. Supervision

Associate Prof. Nils Rüther will be the main supervisor. Diwash Lal Maskey and Adjunct Associate Prof. Siri Stokseth are appointed as co-supervisors. The supervisors shall assist the candidate and make relevant information, documents and data available.

Discussion with and input from other research or engineering staff at NTNU or other institutions are recommended. Significant inputs from others shall be referenced in a convenient manner.

The research and engineering work carried out by the candidate in connection with this thesis shall remain within an educational context. The candidate and the supervisors are free to introduce assumptions and limitations, which may be considered unrealistic or inappropriate in a contract research or a professional/commercial context.

4 Report format and submission

The report should be written with a text editing software. Figures, tables and photos shall be of high quality. The report format shall be in the style of scientific reports and must contain a summary, a table of content, and a list of references.

The report shall be submitted electronically in B5-format .pdf-file in Blackboard, and three paper copies should be handed in to the institute. Supplementary working files such as spreadsheets, numerical models, program scripts, figures and pictures shall be uploaded to Blackboard. The summary shall not exceed 450 words. The Master's thesis should be submitted within 15th of June 2019.

The candidate shall present the work at a MSc. seminar towards the end of the master period. The presentation shall be given with the use of powerpoint or similar presentation tools. The date and format for the MSc. seminar will be announced during the semester.

Trondheim, 14. January 2019

____
Nils Rüther
Associate Professor
Department of Civil and Environmental Engineering
NTNU

Appendix B

Simulation of Hydraulics

B.1 Input Files

The algorithms used in the control file for the simulation of 1000 cumecs at existing operational level are explained in detail as follows:

F 2 UW: Automatic execution of hydraulic simulation is carried out by introducing this data set where *U* stands for reading *unstruc* file and *W* stands for water flow computation.

F 16 0.1: The roughness of the river bed is set to 0.1.

F 33 100 100: This data set activates transient term in the model where the time step (100) and number of inner iterations (100) per iteration per time step are defined.

F 64 11: This algorithm generates body-fitted grid lines in longitudinal and lateral directions giving priority to hexahedral cells close to bed. The hexahedral cells give better performance than tetrahedral cells and also give true portrait of bed cells.

F 65 10000000 10000000 10000000 100000 10000: This data set assigns number of grid cells in the grid, maximum number of surfaces in the grid, maximum number of grid corner points, maximum number of surfaces in connection between blocks, maximum number of connection points.

F 94 0.5 0.5: This sets the maximum and minimum grid corner height to 0.5 each. The cells with very small depths can cause instabilities.

F 102 1: The algorithm is invoked to change the shape of grid cells close to the boundary and improve the bank smoothness.

F 112 1: This algorithm is added after the water level in the *koordina* file has been added. The grid is regenerated after reading the *unstruc* file.

F 113 7: F 113 data set stabilizes the solution in very shallow regions near to the side walls. Integer 7 is used as flux limiter which means the extra term from Rhie and Chow interpolation should be less than 20% of the linear interpolation term.

F 159 1 9 0 1 0: This data set is used to avoid grid problems. The data set reads five integers. The first integer invokes algorithm that tries to remove dead-end with width of only one cell. The second integer deals with the problem of ridges between wet cells. Integer 9 sets internal walls in the ridges. The third integer tries to remove holes in the grid, where there is only one cell that is not connected to side neighbors. This algorithm is not used in the simulation. The fourth integer removes single wet cells with dry neighboring cells in 2D. The fifth integer tries to increase water level in partially dry cells by lowering bed levels. This algorithm is not used in the simulation.

F 168 8: Multi-block solver for pressure- correction equation. The integer 8 indicates the number of levels in grid nesting.

F 235 10: This algorithm is invoked to improve stability in triangular cells. 10 is a successful algorithm which gives extra relaxation in the triangular cells.

G 1 502 502 11 4: The first, second and third integers indicate maximum number of grid lines in x, y and z directions respectively. The fourth integer is the number of sediment sizes.

W 1 13.33 1000 575.71: The three integers are Strickler's number, discharge and d/s water level respectively.

K 1 3197 50000: The two integers invoke algorithms for number of iterations for the flow procedure and number of minimum iterations between water surface updates. The simulation uses a time step of 100. So, to simulate 3.7 days, 3197 iterations are necessary.

K 2 0 1: The two integers indicate if the wall laws are used for water flow computation on the side walls and on the surface respectively. 0 indicate use of wall laws and 1 indicate zero gradients are used.

K 3 0.8 0.8 0.8 0.2 0.5 0.5: Six floats are read. The first three are relaxation factors for three velocity equations. Fourth float is for pressure correction equation and last two are for k and e equations. Higher relaxation coefficients give more instabilities than lower relaxation factors but the computational time is faster. Higher coefficients are to be used initially to see if the solution converges well, if not the coefficients are lowered gradually.

K 4 1 1 1 5 1 1: Six integers are read indicating number of iterations for each equation

K 5 0 0 0 10 0 0: Multiblock solver used to increase the convergence speed of the water flow computation.

K 6 1 1 1 0 0 0: Six integers in this data set are for six water flow equations. The integers indicate the choice of discretization scheme for convective terms. 1 represent second- order upwind (SOU) scheme and 0 represent first order power law (POW). The options apply to velocity and turbulence equations only.

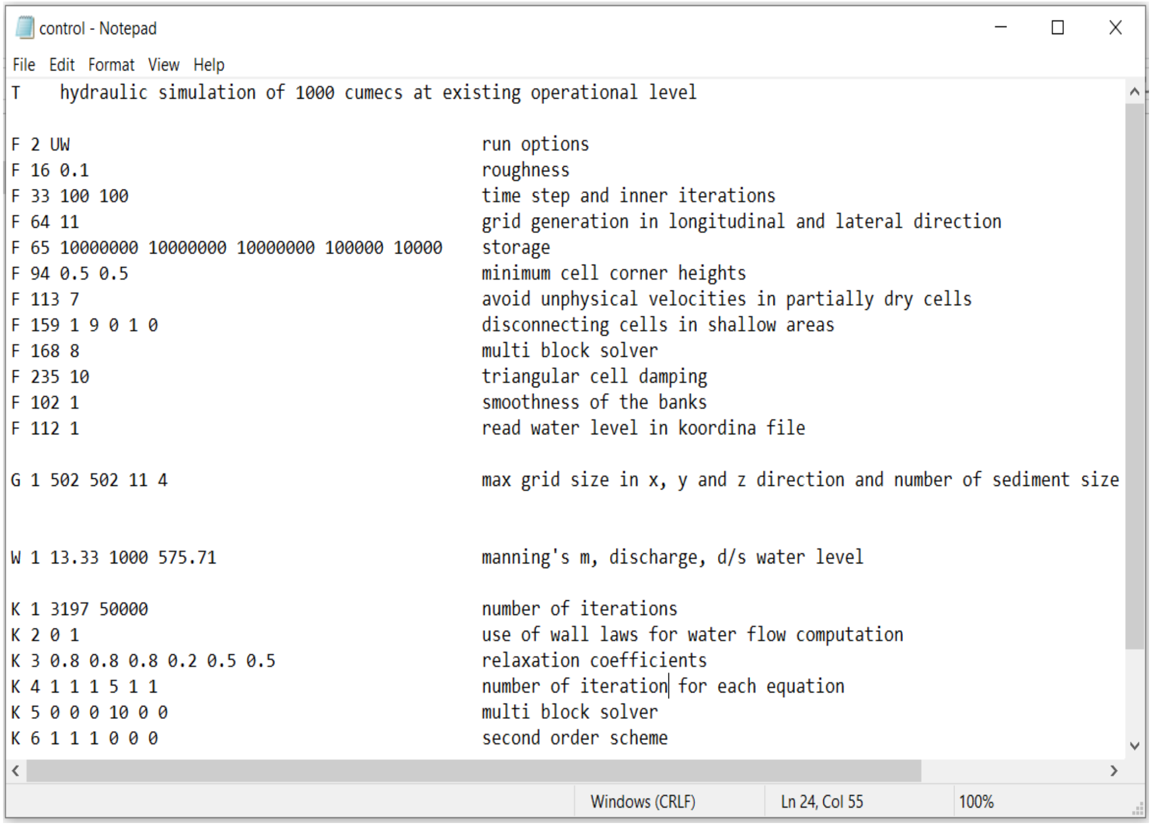

```
T    hydraulic simulation of 1000 cumecs at existing operational level

F 2 UW                                          run options
F 16 0.1                                        roughness
F 33 100 100                                    time step and inner iterations
F 64 11                                         grid generation in longitudinal and lateral direction
F 65 10000000 10000000 10000000 100000 10000    storage
F 94 0.5 0.5                                    minimum cell corner heights
F 113 7                                         avoid unphysical velocities in partially dry cells
F 159 1 9 0 1 0                                 disconnecting cells in shallow areas
F 168 8                                         multi block solver
F 235 10                                        triangular cell damping
F 102 1                                         smoothness of the banks
F 112 1                                         read water level in koordina file

G 1 502 502 11 4                                max grid size in x, y and z direction and number of sediment size


W 1 13.33 1000 575.71                           manning's m, discharge, d/s water level

K 1 3197 50000                                  number of iterations
K 2 0 1                                         use of wall laws for water flow computation
K 3 0.8 0.8 0.8 0.2 0.5 0.5                     relaxation coefficients
K 4 1 1 1 5 1 1                                 number of iteration for each equation
K 5 0 0 0 10 0 0                                multi block solver
K 6 1 1 1 0 0 0                                 second order scheme
```

Figure B. 1 Sample control file for 1000 cumecs at existing operational level

B.2 Parameter Sensitivity Analysis

<table>
<tr><th>Comparison No.</th><th>Free surface algorithm (F36 data set)</th><th>Relaxation coefficients (K3 data set values)</th><th>Roughness coefficient (F 16 data set)</th><th colspan="2">Time Step and inner iteration (F 33 data set)</th><th>Grid cell size (m)</th><th>Highest residual</th><th>Run time (secs)</th></tr>
<tr><td>Initial Simulation</td><td>Used</td><td>0.2 0.2 0.2 0.05 0.2 0.2</td><td>0.1</td><td>100</td><td>100</td><td>12*16</td><td>3.22e^-3</td><td>319700</td></tr>
<tr><td>1.</td><td>Not used</td><td>0.2 0.2 0.2 0.05 0.2 0.2</td><td>0.1</td><td>100</td><td>100</td><td>12*16</td><td>2.1e^-3</td><td>122600</td></tr>
<tr><td colspan="9">Comment: Compared to initial simulation, the flow pattern is same. Even if free surface algorithm is used, the increase in u/s water level is by 9 cms which is negligible.</td></tr>
<tr><td>2.</td><td>Used</td><td>0.8 0.8 0.8 0.2 0.5 0.5</td><td>0.1</td><td>100</td><td>100</td><td>12*16</td><td>1.9e^-3</td><td>319700</td></tr>
<tr><td colspan="9">Comment: Relaxation coefficients are set to default. Compared to initial simulation, there was no change in the results.</td></tr>
</table>

3.	Not used	0.8 0.8 0.8 0.2 0.5 0.5	0.1	100	100	12*16	1.8e^-3	319700
Comment: Free surface algorithm was removed, and relaxation coefficients were set to default and compared to initial simulation. There’s no change in the results.								
4. a)	Not used	0.8 0.8 0.8 0.2 0.5 0.5	0.05	100	100	12*16	1.8e^-3	319700
Comment: Compared to 3, the roughness coefficient was reduced to half. No significant change was seen in horizontal velocity but at some locations the bed shear stress was reduced.								
4. b)	Not used	0.8 0.8 0.8 0.2 0.5 0.5	0.2	100	100	12*16	4.4e^-2	213800
Comment: The roughness coefficient was doubled and compared to 3. There was a change in flow pattern. The main flow bends towards spillway sooner than in 3. An argument can be that when the roughness is increased there is decrease in velocity and the main flow channel doesn’t have enough energy to go further downstream. The bed shear stress was seen increased.								
5.	Not used	0.8 0.8 0.8 0.2 0.5 0.5	0.1	10	100	12*16	1.50e^-3	319700
Comment: The time step in f33 data set was reduced to 10 from 100 and compared to 3. There were no significant changes in the results but the computational time increased.								
6.	Not used	0.8 0.8 0.8 0.2 0.5 0.5	0.1	100	200	12*16	1.89e^-3	319700
Comment: The inner iteration for each time step was increased to 200 from 100 in f33 data set and compared to 3. No change in the results was seen. The computational time increased.								
7.	Not used	0.8 0.8 0.8 0.2 0.5 0.5	0.1	1	20	12*16	2.2e^-3	3197
Comment: Both the time step and inner iteration were changed and compared to 3. The flow pattern was seen different than in 3. The flow was not developed throughout the reservoir. This was later solved in comparison 7. a)								
7.a)	Not used	0.8 0.8 0.8 0.2 0.5 0.5	0.1	1	20	12*16	1.91e^-3	47917
Comment: As compared to 7, the change made here is the first integer in K 1 data set i.e. number of iterations for flow procedure. After increasing this number, the flow was developed fully in the reservoir and the flow is seen similar to comparison 3. The computational time increased.								

<table>
<tr><td>8</td><td>Not used</td><td>0.8 0.8
0.8 0.2
0.5 0.5</td><td>0.1</td><td>100</td><td>100</td><td>6*8</td><td>1.23e^2</td><td>162800</td></tr>
<tr><td colspan="9">Comment: Change is made on the grid size. The cell size is reduced to half of what was before and compared to 3. The problem of poor convergence was seen which was solved later on comparison no. 11.</td></tr>
<tr><td>9</td><td>Not used</td><td>0.8 0.8
0.8 0.2
0.5 0.5</td><td>0.1</td><td>1</td><td>100</td><td>12*16</td><td>1.93e^-3</td><td>3197</td></tr>
<tr><td colspan="9">Comment: A compared to 3, the time step was further reduced to 1 from 100. The flow pattern was not fully developed throughout the reservoir (similar problem as in 7). To save time, simulation with increased time step in K1 data set was not performed but based on the result of 7.a) it can be said that the flow will develop further d/s if time step is increased.</td></tr>
<tr><td>10</td><td>Not used</td><td>0.8 0.8
0.8 0.2
0.5 0.5</td><td>0.1</td><td>10</td><td>20</td><td>12*16</td><td>1.80e^-3</td><td>319700</td></tr>
<tr><td colspan="9">Comment: Compared to 5, the inner iteration was changed from 100 to 20. No change was seen in the result but there was change in computational time.</td></tr>
<tr><td>11</td><td>Not used</td><td>0.8 0.8
0.8 0.2
0.5 0.5</td><td>0.1</td><td>10</td><td>500</td><td>6*8</td><td>8.2e^-1</td><td>161700</td></tr>
<tr><td colspan="9">Comment: To solve instability in comparison 8, the time step was reduced from 100 to 10 and inner iteration was increased from 100 to 500. On doing this the convergence improved but it was a computational time demanding simulation.</td></tr>
<tr><td>12</td><td>Not used</td><td>0.8 0.8
0.8 0.2
0.5 0.5</td><td>0.1</td><td>-</td><td>-</td><td>12*16</td><td>1.03e^2</td><td>319700</td></tr>
<tr><td colspan="9">Comment: The F 33 data set was removed and compared to 3. The flow pattern was different, and the simulation was unstable. The convergence couldn’t be made better even after many manipulations and addition of algorithms.</td></tr>
<tr><td>13</td><td>Not used</td><td>0.8 0.8
0.8 0.2
0.5 0.5</td><td>0.3</td><td>100</td><td>100</td><td>12*16</td><td>2.09e^-2</td><td>Try with 0.3 roughness</td></tr>
<tr><td colspan="9">Comment: Roughness coefficient was increased from 0.1 to 0.3 and compared to 3. The flow pattern was changed (main flow channel curved sooner towards spillway than in 3). Increase in bed shear stress was observed.</td></tr>
</table>

The following figures are comparisons of outcomes of sensitivity analysis performed.

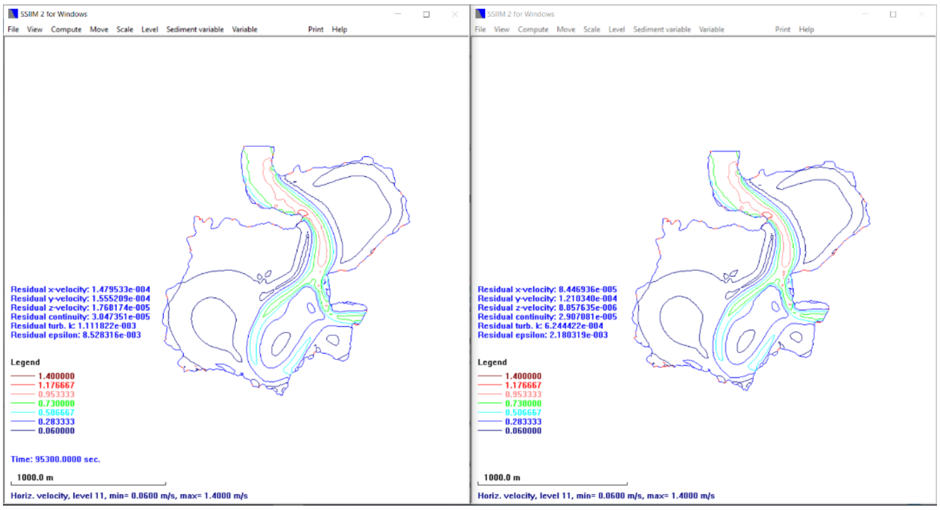

Residual x-velocity: 1.479533e-004
Residual y-velocity: 1.555209e-004
Residual z-velocity: 1.768174e-005
Residual continuity: 3.047351e-005
Residual turb. k: 1.111822e-003
Residual epsilon: 8.528316e-003

Legend
1.400000
1.176667
0.953333
0.730000
0.506667
0.283333
0.060000

Time: 95300.0000 sec.

1000.0 m

Horiz. velocity, level 11, min= 0.0600 m/s, max= 1.4000 m/s

Residual x-velocity: 8.446936e-005
Residual y-velocity: 1.210340e-004
Residual z-velocity: 8.857635e-006
Residual continuity: 2.907081e-005
Residual turb. k: 6.244422e-004
Residual epsilon: 2.180319e-003

Legend
1.400000
1.176667
0.953333
0.730000
0.506667
0.283333
0.060000

1000.0 m

Horiz. velocity, level 11, min= 0.0600 m/s, max= 1.4000 m/s

Figure B.2. 1 Comparison no. 1

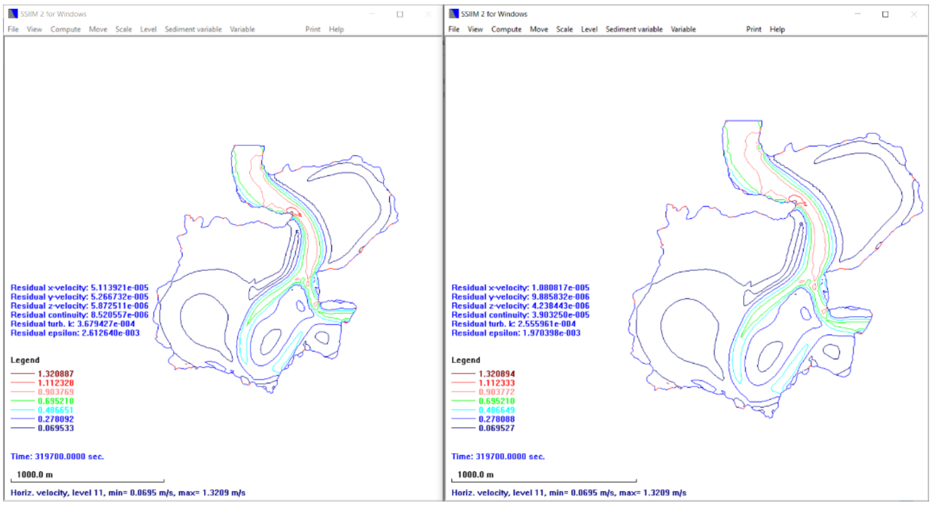

Residual x-velocity: 5.113921e-005
Residual y-velocity: 5.266732e-005
Residual z-velocity: 5.872511e-006
Residual continuity: 8.520557e-006
Residual turb. k: 3.679427e-004
Residual epsilon: 2.612640e-003

Legend
1.320887
1.112328
0.903769
0.695210
0.486651
0.278092
0.069533

Time: 319700.0000 sec.

1000.0 m

Horiz. velocity, level 11, min= 0.0695 m/s, max= 1.3209 m/s

Residual x-velocity: 1.080817e-005
Residual y-velocity: 9.885832e-006
Residual z-velocity: 4.238443e-006
Residual continuity: 3.903250e-005
Residual turb. k: 2.555961e-004
Residual epsilon: 1.970398e-003

Legend
1.320894
1.112333
0.903772
0.695210
0.486649
0.278088
0.069527

Time: 319700.0000 sec.

1000.0 m

Horiz. velocity, level 11, min= 0.0695 m/s, max= 1.3209 m/s

Figure B.2. 2 Comparison no. 2

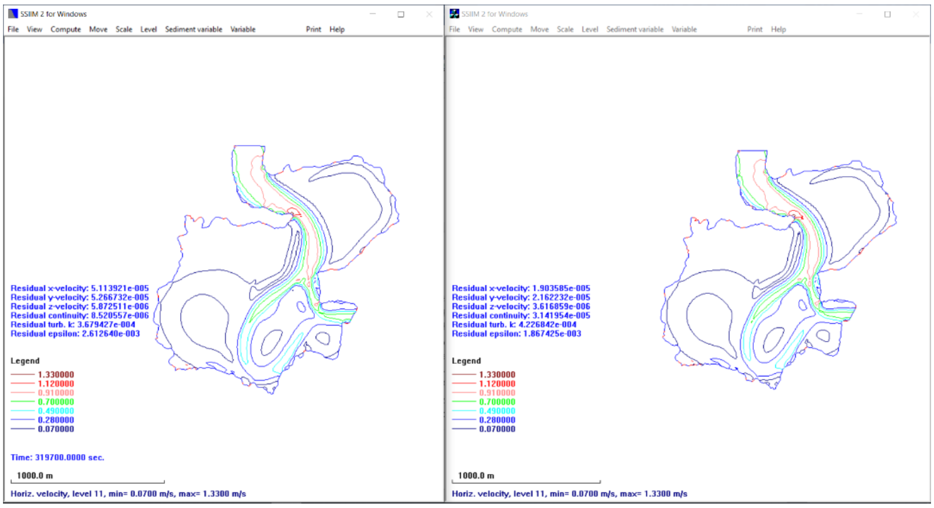

Residual x-velocity: 5.113921e-005
Residual y-velocity: 5.266732e-005
Residual z-velocity: 5.872511e-006
Residual continuity: 8.520557e-006
Residual turb. k: 3.679427e-004
Residual epsilon: 2.612640e-003

Legend
1.330000
1.120000
0.910000
0.700000
0.490000
0.280000
0.070000

Time: 319700.0000 sec.

1000.0 m

Horiz. velocity, level 11, min= 0.0700 m/s, max= 1.3300 m/s

Residual x-velocity: 1.903585e-005
Residual y-velocity: 2.162232e-005
Residual z-velocity: 3.616859e-006
Residual continuity: 3.141954e-005
Residual turb. k: 4.226842e-004
Residual epsilon: 1.867425e-003

Legend
1.330000
1.120000
0.910000
0.700000
0.490000
0.280000
0.070000

1000.0 m

Horiz. velocity, level 11, min= 0.0700 m/s, max= 1.3300 m/s

Figure B.2. 3 Comparison no. 3

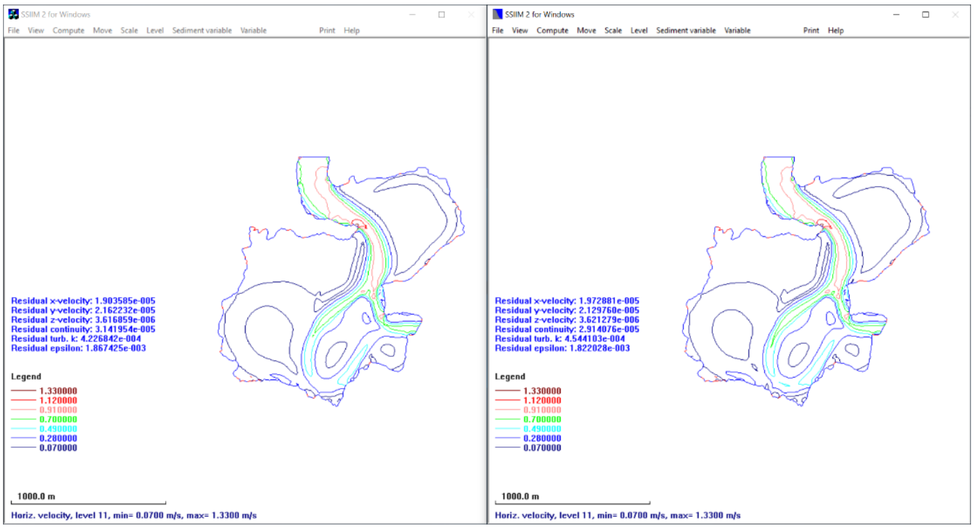

```
Residual x-velocity: 1.903585e-005
Residual y-velocity: 2.162232e-005
Residual z-velocity: 3.616859e-006
Residual continuity: 3.141954e-005
Residual turb. k: 4.226842e-004
Residual epsilon: 1.867425e-003
```

Legend
1.330000
1.120000
0.910000
0.700000
0.490000
0.280000
0.070000

1000.0 m

Horiz. velocity, level 11, min= 0.0700 m/s, max= 1.3300 m/s

```
Residual x-velocity: 1.972881e-005
Residual y-velocity: 2.129760e-005
Residual z-velocity: 3.621279e-006
Residual continuity: 2.914076e-005
Residual turb. k: 4.544103e-004
Residual epsilon: 1.822028e-003
```

Legend
1.330000
1.120000
0.910000
0.700000
0.490000
0.280000
0.070000

1000.0 m

Horiz. velocity, level 11, min= 0.0700 m/s, max= 1.3300 m/s

Figure B.2. 4 Comparison no. 4 a)

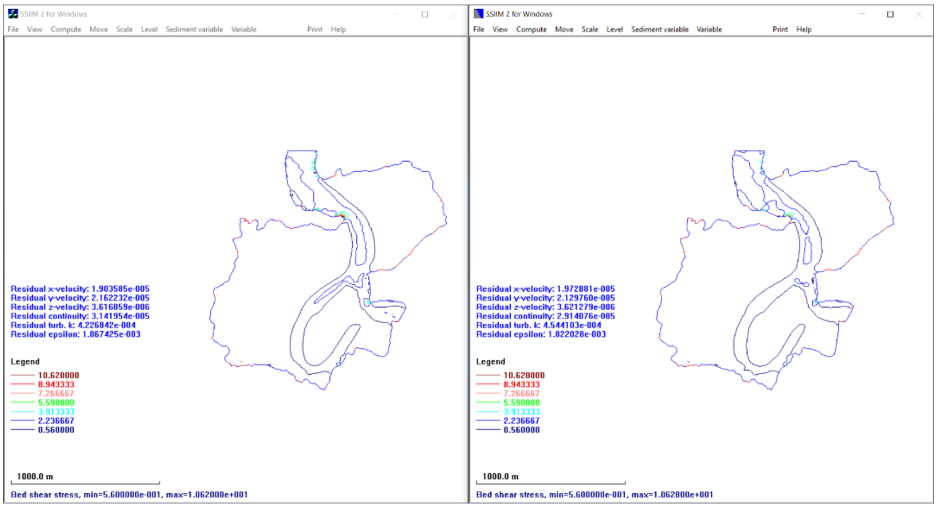

```
Residual x-velocity: 1.903585e-005
Residual y-velocity: 2.162232e-005
Residual z-velocity: 3.616859e-006
Residual continuity: 3.141954e-005
Residual turb. k: 4.226842e-004
Residual epsilon: 1.867425e-003
```

Legend
10.620000
8.943333
7.266667
5.590000
3.913333
2.236667
0.560000

1000.0 m

Bed shear stress, min=5.600000e-001, max=1.062000e+001

```
Residual x-velocity: 1.972881e-005
Residual y-velocity: 2.129760e-005
Residual z-velocity: 3.621279e-006
Residual continuity: 2.914076e-005
Residual turb. k: 4.544103e-004
Residual epsilon: 1.822028e-003
```

Legend
10.620000
8.943333
7.266667
5.590000
3.913333
2.236667
0.560000

1000.0 m

Bed shear stress, min=5.600000e-001, max=1.062000e+001

Figure B.2. 5 Comparison no. 4 a) bed shear stress

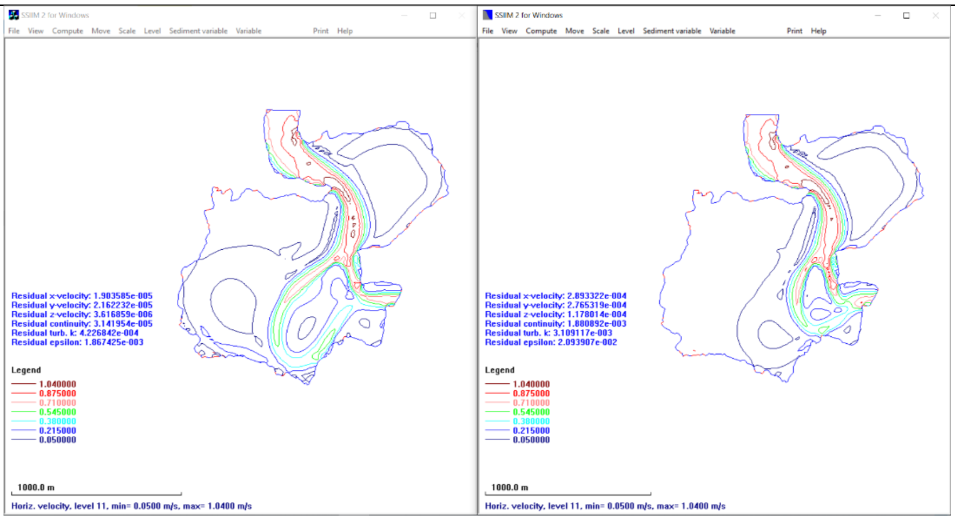

```
Residual x-velocity: 1.903585e-005
Residual y-velocity: 2.162232e-005
Residual z-velocity: 3.616859e-006
Residual continuity: 3.141954e-005
Residual turb. k: 4.226842e-004
Residual epsilon: 1.867425e-003
```

Legend
1.040000
0.875000
0.710000
0.545000
0.380000
0.215000
0.050000

1000.0 m

Horiz. velocity, level 11, min= 0.0500 m/s, max= 1.0400 m/s

```
Residual x-velocity: 2.893322e-004
Residual y-velocity: 2.765319e-004
Residual z-velocity: 1.178014e-004
Residual continuity: 1.880892e-003
Residual turb. k: 3.109117e-003
Residual epsilon: 2.093907e-002
```

Legend
1.040000
0.875000
0.710000
0.545000
0.380000
0.215000
0.050000

1000.0 m

Horiz. velocity, level 11, min= 0.0500 m/s, max= 1.0400 m/s

Figure B.2. 6 Comparison no. 4 b)

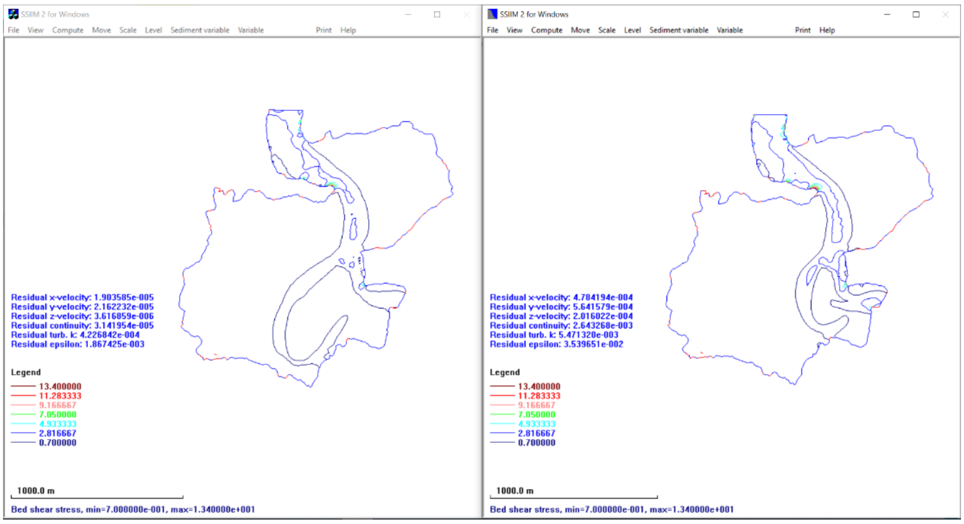

```
Residual x-velocity: 1.903585e-005
Residual y-velocity: 2.162232e-005
Residual z-velocity: 3.616859e-006
Residual continuity: 3.141954e-005
Residual turb. k: 4.226842e-004
Residual epsilon: 1.867425e-003

Legend
13.400000
11.283333
9.166667
7.050000
4.933333
2.816667
0.700000

1000.0 m
Bed shear stress, min=7.000000e-001, max=1.340000e+001
```

```
Residual x-velocity: 4.784194e-004
Residual y-velocity: 5.641579e-004
Residual z-velocity: 2.016022e-004
Residual continuity: 2.643268e-003
Residual turb. k: 5.471320e-003
Residual epsilon: 3.539651e-002

Legend
13.400000
11.283333
9.166667
7.050000
4.933333
2.816667
0.700000

1000.0 m
Bed shear stress, min=7.000000e-001, max=1.340000e+001
```

Figure B.2. 7 Comparison no. 4 b) bed shear stress

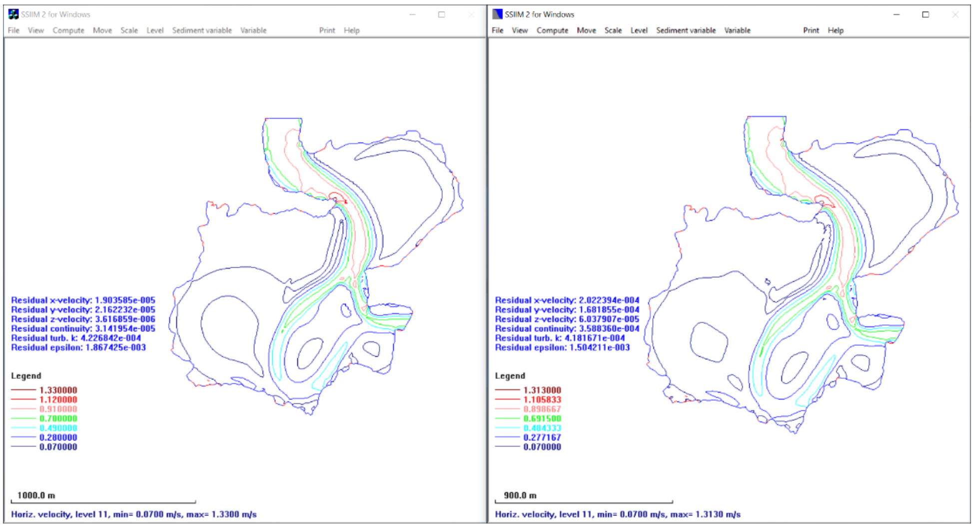

```
Residual x-velocity: 1.903585e-005
Residual y-velocity: 2.162232e-005
Residual z-velocity: 3.616859e-006
Residual continuity: 3.141954e-005
Residual turb. k: 4.226842e-004
Residual epsilon: 1.867425e-003

Legend
1.330000
1.120000
0.910000
0.700000
0.490000
0.280000
0.070000

1000.0 m
Horiz. velocity, level 11, min= 0.0700 m/s, max= 1.3300 m/s
```

```
Residual x-velocity: 2.022394e-004
Residual y-velocity: 1.681855e-004
Residual z-velocity: 6.037907e-005
Residual continuity: 3.588360e-004
Residual turb. k: 4.181671e-004
Residual epsilon: 1.504211e-003

Legend
1.313000
1.105833
0.898667
0.691500
0.484333
0.277167
0.070000

900.0 m
Horiz. velocity, level 11, min= 0.0700 m/s, max= 1.3130 m/s
```

Figure B.2. 8 Comparison no. 5

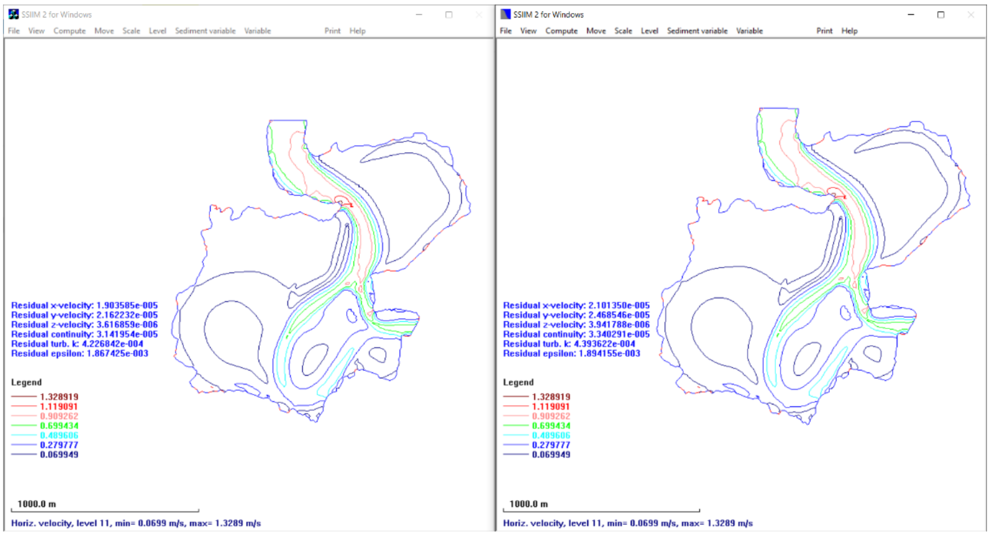

```
Residual x-velocity: 1.903585e-005
Residual y-velocity: 2.162232e-005
Residual z-velocity: 3.616859e-006
Residual continuity: 3.141954e-005
Residual turb. k: 4.226842e-004
Residual epsilon: 1.867425e-003

Legend
1.328919
1.119091
0.909262
0.699434
0.489606
0.279777
0.069949

1000.0 m
Horiz. velocity, level 11, min= 0.0699 m/s, max= 1.3289 m/s
```

```
Residual x-velocity: 2.101350e-005
Residual y-velocity: 2.468546e-005
Residual z-velocity: 3.941788e-006
Residual continuity: 3.340291e-005
Residual turb. k: 4.393622e-004
Residual epsilon: 1.894155e-003

Legend
1.328919
1.119091
0.909262
0.699434
0.489606
0.279777
0.069949

1000.0 m
Horiz. velocity, level 11, min= 0.0699 m/s, max= 1.3289 m/s
```

Figure B.2. 9 Comparison no. 6

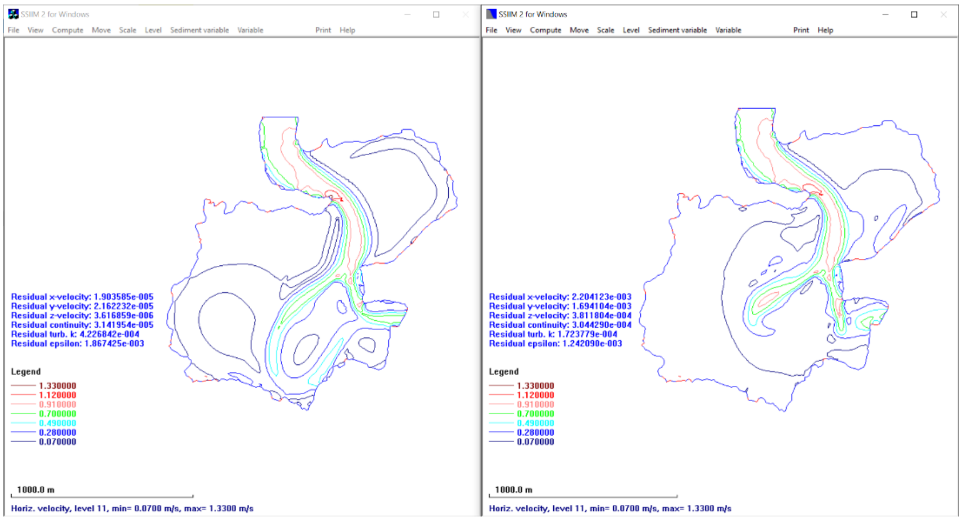

```
Residual x-velocity: 1.903585e-005
Residual y-velocity: 2.162232e-005
Residual z-velocity: 3.616859e-006
Residual continuity: 3.141954e-005
Residual turb. k: 4.226842e-004
Residual epsilon: 1.867425e-003
```

```
Horiz. velocity, level 11, min= 0.0700 m/s, max= 1.3300 m/s
```

```
Residual x-velocity: 2.204123e-003
Residual y-velocity: 1.694104e-003
Residual z-velocity: 3.811804e-004
Residual continuity: 3.044290e-004
Residual turb. k: 1.723779e-004
Residual epsilon: 1.242090e-003
```

```
Horiz. velocity, level 11, min= 0.0700 m/s, max= 1.3300 m/s
```

Figure B.2. 10 Comparison no. 7

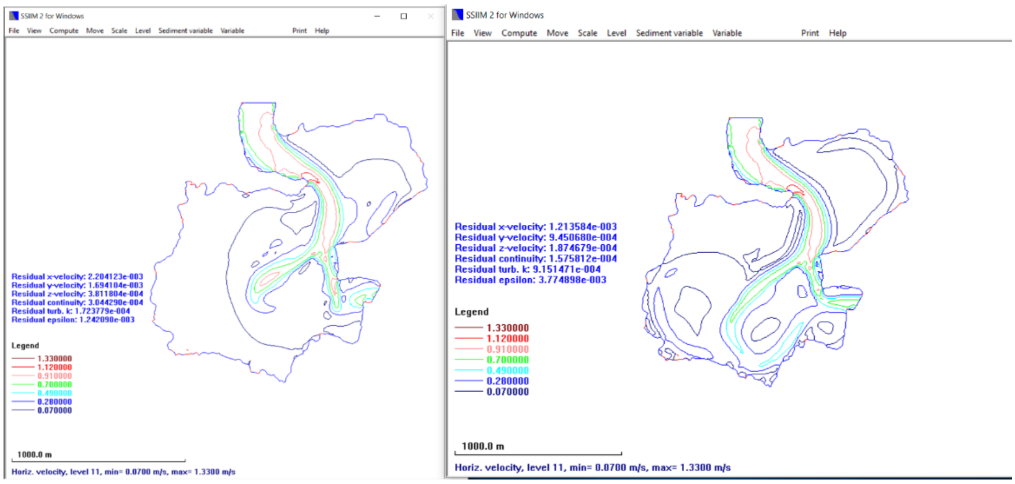

```
Residual x-velocity: 2.204123e-003
Residual y-velocity: 1.694104e-003
Residual z-velocity: 3.811804e-004
Residual continuity: 3.044290e-004
Residual turb. k: 1.723779e-004
Residual epsilon: 1.242090e-003
```

```
Horiz. velocity, level 11, min= 0.0700 m/s, max= 1.3300 m/s
```

```
Residual x-velocity: 1.213584e-003
Residual y-velocity: 9.450680e-004
Residual z-velocity: 1.874679e-004
Residual continuity: 1.575812e-004
Residual turb. k: 9.151471e-004
Residual epsilon: 3.774898e-003
```

```
Horiz. velocity, level 11, min= 0.0700 m/s, max= 1.3300 m/s
```

Figure B.2. 11 Comparison no. 7 a)

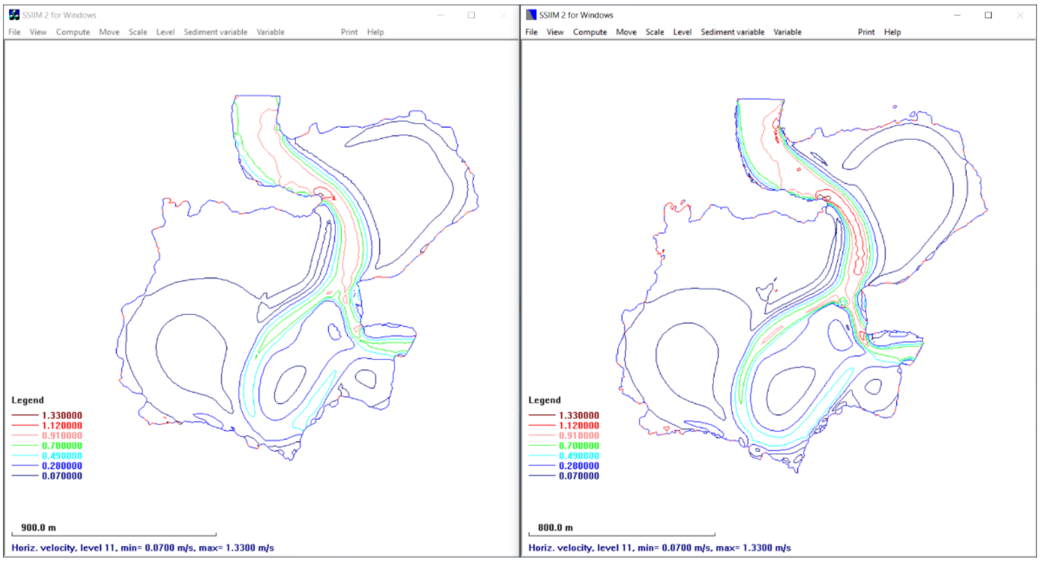

```
Horiz. velocity, level 11, min= 0.0700 m/s, max= 1.3300 m/s
```

```
Horiz. velocity, level 11, min= 0.0700 m/s, max= 1.3300 m/s
```

Figure B.2. 12 Comparison no. 8

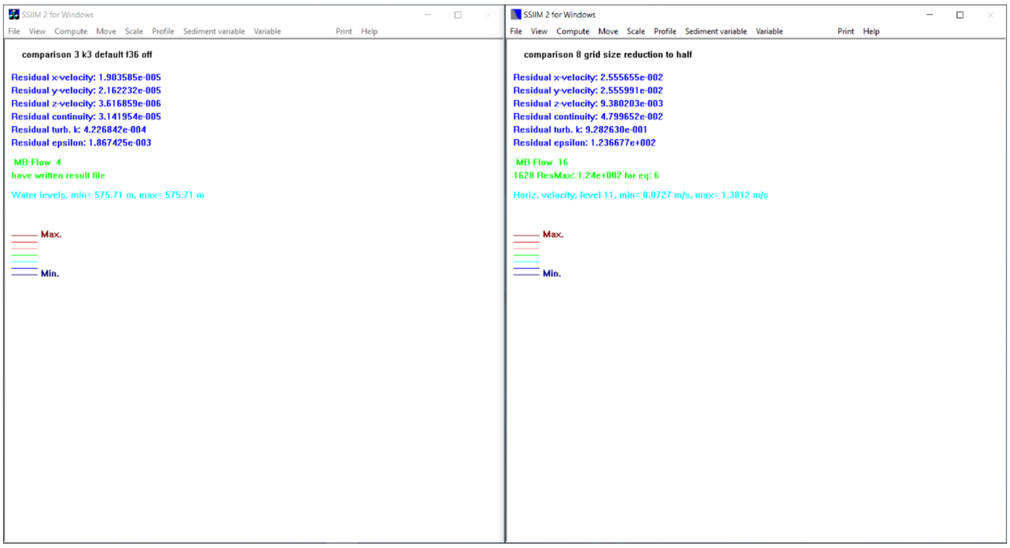

```
comparison 3 k3 default f36 off

Residual x-velocity: 1.903585e-005
Residual y-velocity: 2.162232e-005
Residual z-velocity: 3.616859e-006
Residual continuity: 3.141954e-005
Residual turb. k: 4.226842e-004
Residual epsilon: 1.867425e-003

 MB-Flow  4
have written result file

Water levels, min= 575.71 m, max= 575.71 m
```

```
comparison 8 grid size reduction to half

Residual x-velocity: 2.555655e-002
Residual y-velocity: 2.555991e-002
Residual z-velocity: 9.380203e-003
Residual continuity: 4.799652e-002
Residual turb. k: 9.282630e-001
Residual epsilon: 1.236677e+002

 MB-Flow  16
1628 ResMax: 1.24e+002 for eq: 6

Horiz. velocity, level 11, min= 0.0727 m/s, max= 1.3812 m/s
```

Figure B.2. 13 Comparison no. 8 poor convergence (right)

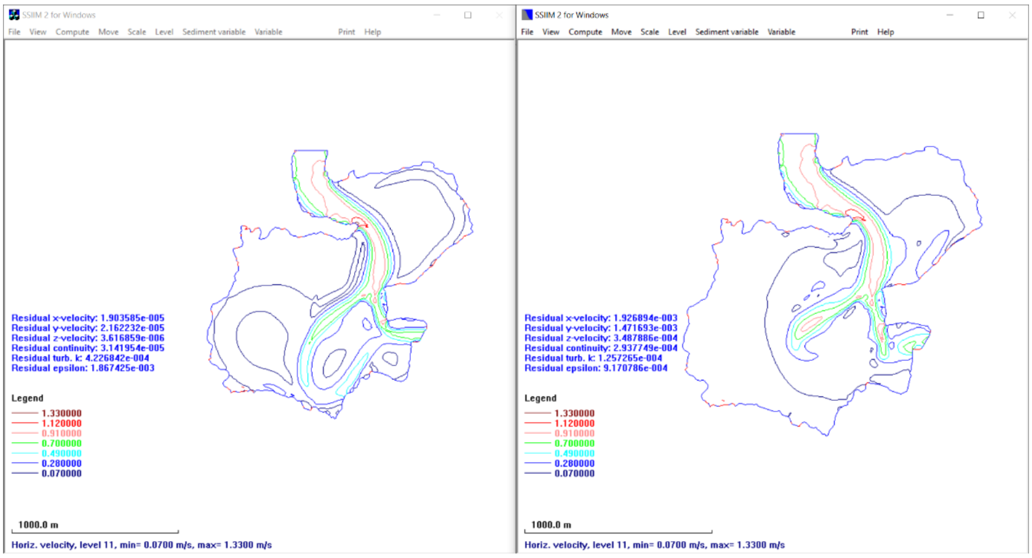

```
Residual x-velocity: 1.903585e-005
Residual y-velocity: 2.162232e-005
Residual z-velocity: 3.616859e-006
Residual continuity: 3.141954e-005
Residual turb. k: 4.226842e-004
Residual epsilon: 1.867425e-003

Legend
1.330000
1.120000
0.910000
0.700000
0.490000
0.280000
0.070000

1000.0 m
Horiz. velocity, level 11, min= 0.0700 m/s, max= 1.3300 m/s
```

```
Residual x-velocity: 1.926894e-003
Residual y-velocity: 1.471693e-003
Residual z-velocity: 3.487886e-004
Residual continuity: 2.937749e-004
Residual turb. k: 1.257265e-004
Residual epsilon: 9.170786e-004

Legend
1.330000
1.120000
0.910000
0.700000
0.490000
0.280000
0.070000

1000.0 m
Horiz. velocity, level 11, min= 0.0700 m/s, max= 1.3300 m/s
```

Figure B.2. 14 Comparison no. 9

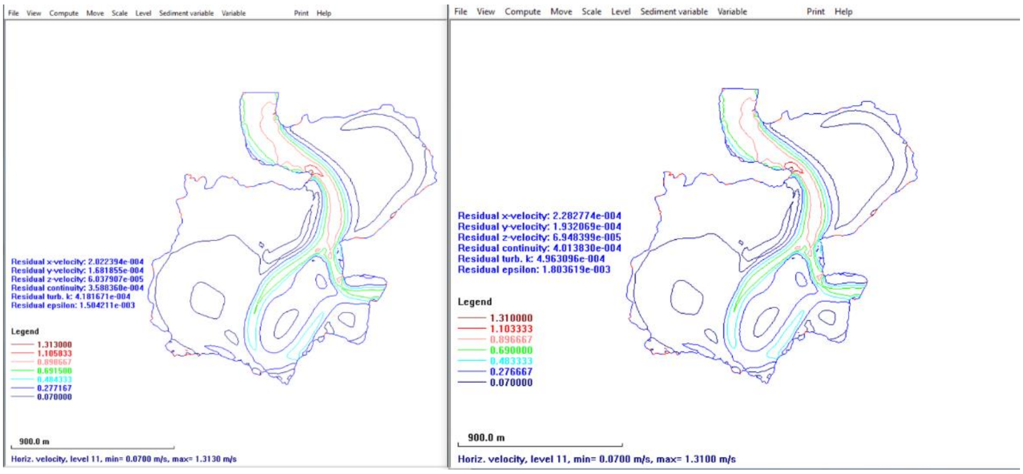

```
Residual x-velocity: 2.022394e-004
Residual y-velocity: 1.681855e-004
Residual z-velocity: 6.037907e-005
Residual continuity: 3.588360e-004
Residual turb. k: 4.181671e-004
Residual epsilon: 1.504211e-003

Legend
1.313000
1.105833
0.898667
0.691500
0.484333
0.277167
0.070000

900.0 m
Horiz. velocity, level 11, min= 0.0700 m/s, max= 1.3130 m/s
```

```
Residual x-velocity: 2.282774e-004
Residual y-velocity: 1.932069e-004
Residual z-velocity: 6.948399e-005
Residual continuity: 4.013830e-004
Residual turb. k: 4.963096e-004
Residual epsilon: 1.803619e-003

Legend
1.310000
1.103333
0.896667
0.690000
0.483333
0.276667
0.070000

900.0 m
Horiz. velocity, level 11, min= 0.0700 m/s, max= 1.3100 m/s
```

Figure B.2. 15 Comparison no. 10

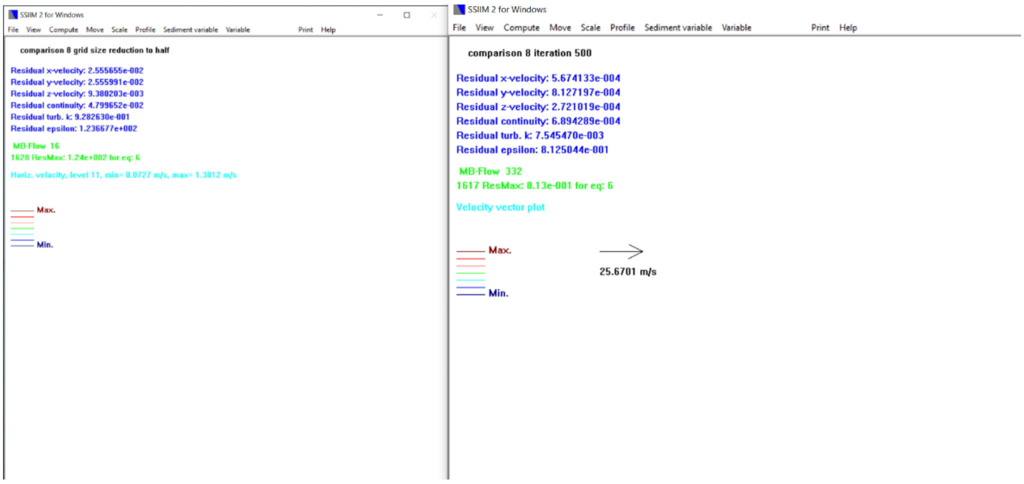

```
comparison 8 grid size reduction to half

Residual x-velocity: 2.555655e-002
Residual y-velocity: 2.555991e-002
Residual z-velocity: 9.380203e-003
Residual continuity: 4.799652e-002
Residual turb. k: 9.282630e-001
Residual epsilon: 1.236677e+002

 MB-Flow  16
1628 ResMax: 1.24e+002 for eq: 6

Horiz. velocity, level 11, min= 0.0727 m/s, max= 1.3812 m/s
```

```
comparison 8 iteration 500

Residual x-velocity: 5.674133e-004
Residual y-velocity: 8.127197e-004
Residual z-velocity: 2.721019e-004
Residual continuity: 6.894289e-004
Residual turb. k: 7.545470e-003
Residual epsilon: 8.125044e-001

 MB-Flow  332
1617 ResMax: 8.13e-001 for eq: 6

Velocity vector plot
```

Figure B.2. 16 Comparison no. 11

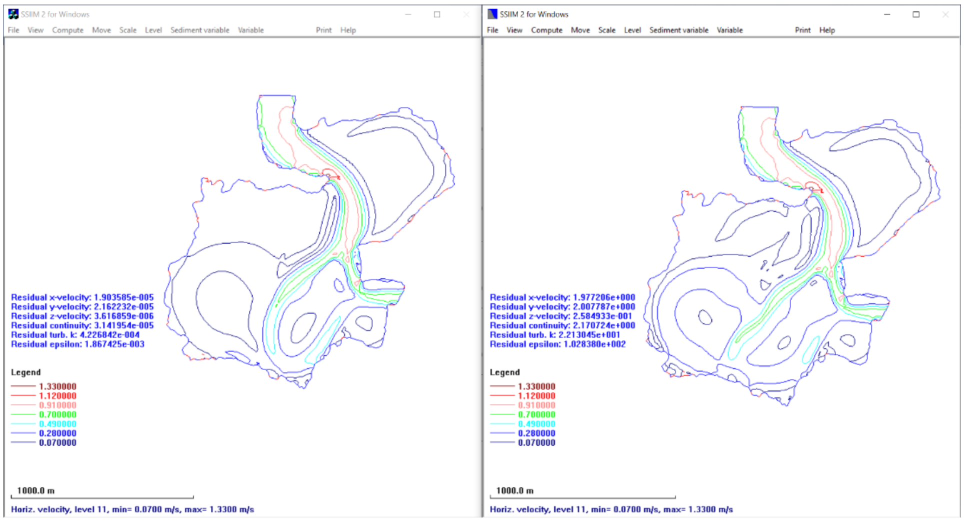

```
Residual x-velocity: 1.903585e-005
Residual y-velocity: 2.162232e-005
Residual z-velocity: 3.616859e-006
Residual continuity: 3.141954e-005
Residual turb. k: 4.226842e-004
Residual epsilon: 1.867425e-003

Horiz. velocity, level 11, min= 0.0700 m/s, max= 1.3300 m/s
```

```
Residual x-velocity: 1.977206e+000
Residual y-velocity: 2.007787e+000
Residual z-velocity: 2.584933e-001
Residual continuity: 2.170724e+000
Residual turb. k: 2.213045e+001
Residual epsilon: 1.028380e+002

Horiz. velocity, level 11, min= 0.0700 m/s, max= 1.3300 m/s
```

Figure B.2. 17 Comparison no. 12

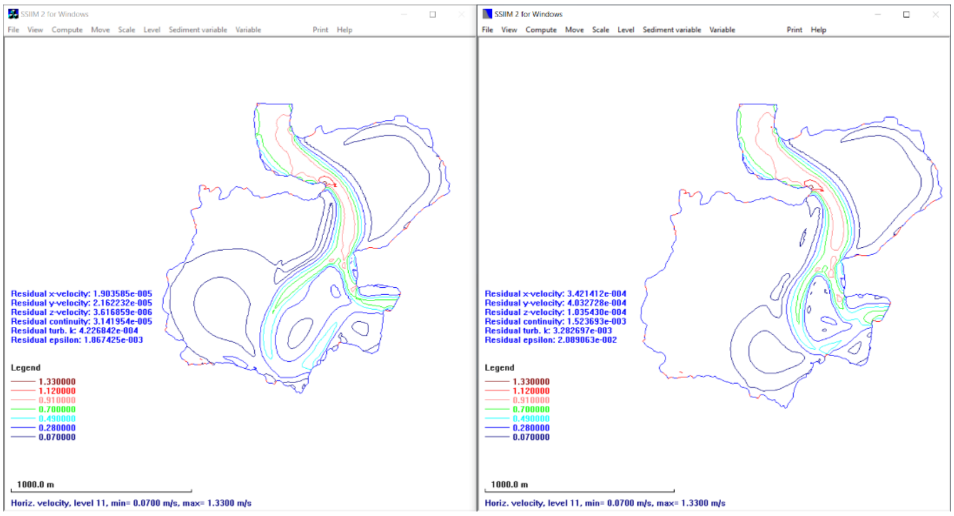

```
Residual x-velocity: 1.903585e-005
Residual y-velocity: 2.162232e-005
Residual z-velocity: 3.616859e-006
Residual continuity: 3.141954e-005
Residual turb. k: 4.226842e-004
Residual epsilon: 1.867425e-003

Horiz. velocity, level 11, min= 0.0700 m/s, max= 1.3300 m/s
```

```
Residual x-velocity: 3.421412e-004
Residual y-velocity: 4.032728e-004
Residual z-velocity: 1.035430e-004
Residual continuity: 1.523693e-003
Residual turb. k: 3.282697e-003
Residual epsilon: 2.089063e-002

Horiz. velocity, level 11, min= 0.0700 m/s, max= 1.3300 m/s
```

Figure B.2. 18 Comparison no. 13

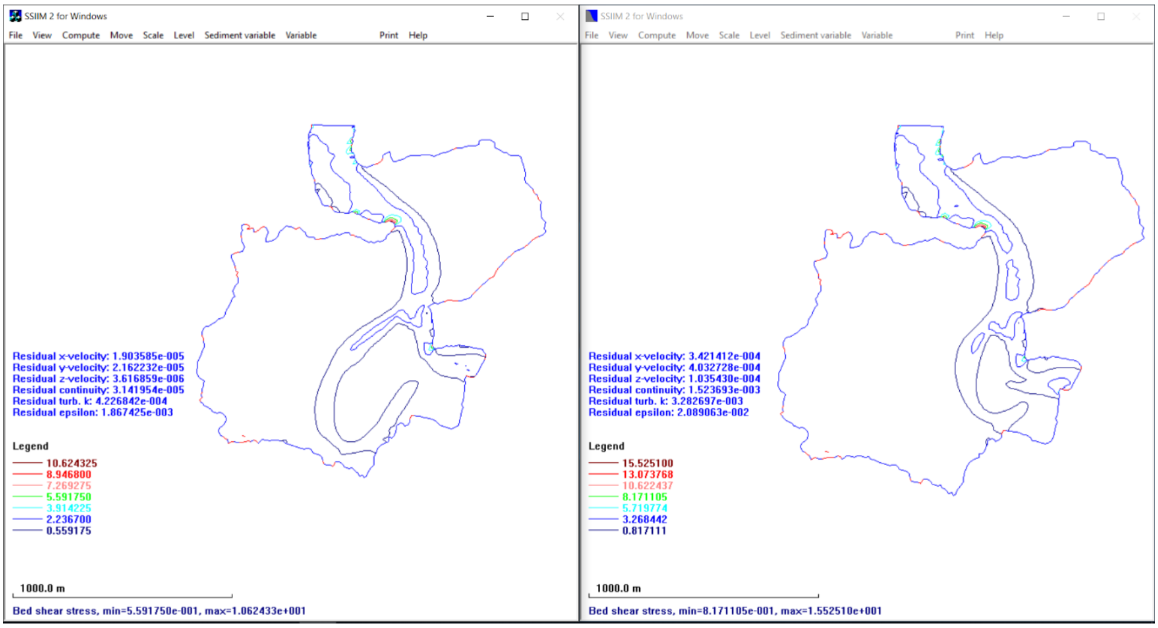

```
Residual x-velocity: 1.903585e-005
Residual y-velocity: 2.162232e-005
Residual z-velocity: 3.616859e-006
Residual continuity: 3.141954e-005
Residual turb. k: 4.226842e-004
Residual epsilon: 1.867425e-003

Legend
10.624325
8.946800
7.269275
5.591750
3.914225
2.236700
0.559175

1000.0 m
Bed shear stress, min=5.591750e-001, max=1.062433e+001
```

```
Residual x-velocity: 3.421412e-004
Residual y-velocity: 4.032728e-004
Residual z-velocity: 1.035430e-004
Residual continuity: 1.523693e-003
Residual turb. k: 3.282697e-003
Residual epsilon: 2.089063e-002

Legend
15.525100
13.073768
10.622437
8.171105
5.719774
3.268442
0.817111

1000.0 m
Bed shear stress, min=8.171105e-001, max=1.552510e+001
```

Figure B.2. 19 Comparison no. 13 bed shear stress

Appendix C

Simulation of Sediments

C.1 Input Files

The additional data sets used in sediment simulation are explained as follows.

F 2 UIS: Execution of sediment simulation is carried out by the use of this data set where U reads *unstruc* file, I initialize sediment concentration computation and S calculates sediment concentration.

F 6 0.025 1.5 0.3: The F 6 data set invokes coefficients for bed concentration formula. The coefficients 0.025, 1.5, 0.3 are van Rijn's coefficients.

F 37 2: Transient sediment computation. This data set invokes time-dependent computation of sediment transport. The integer 2 denotes different algorithm for bed cells where sediment concentration formula is converted into an entrainment rate.

F 84 1: F 84 data set indicates the use of sediment transport formula. Integer 1 invokes bed load formula by van Rijn.

S data set: This data set gives the size and fall velocity of the sediments under consideration. At first, an integer is read which indicates the size group. After that sediment size in meter and fall velocity in m/s is given. Example: S 1 0.1 1.04. Four different sediment size groups are used with their corresponding diameters and fall velocities.

N data set: This data set comprises of size fractions of different sediment groups. The first integer indicates the group; the first group has index 0. The second integer indicates the sediment size. There a float read at last which indicates the fraction of size in the group. Example: N 0 1 0.1. This means bed sediment is 10% cobble small which is group S 1. Like this, the N data set is written for four different sediment sizes.

B 0 0 0 0 0: B data sets invokes algorithm to distribute different sediment groups to different locations of the geometry. The first integer indicates group number. Second and third integers are cell numbers in the streamwise direction. The last two integers are cell numbers in the lateral direction. The information on sediment distribution at different locations are not available, so the integers are 0.

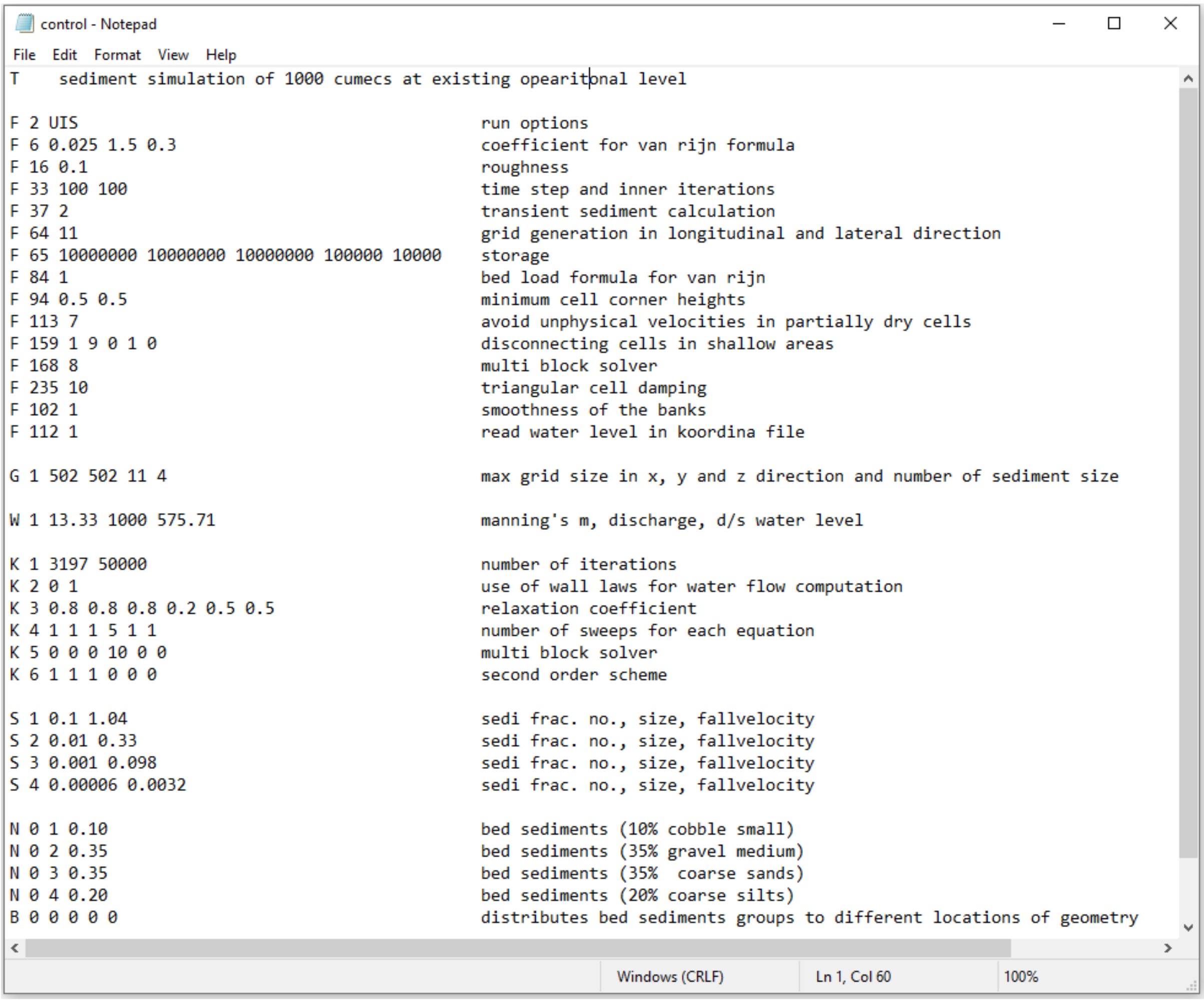

```
T    sediment simulation of 1000 cumecs at existing opearitonal level

F 2 UIS                                         run options
F 6 0.025 1.5 0.3                               coefficient for van rijn formula
F 16 0.1                                        roughness
F 33 100 100                                    time step and inner iterations
F 37 2                                          transient sediment calculation
F 64 11                                         grid generation in longitudinal and lateral direction
F 65 10000000 10000000 10000000 100000 10000    storage
F 84 1                                          bed load formula for van rijn
F 94 0.5 0.5                                    minimum cell corner heights
F 113 7                                         avoid unphysical velocities in partially dry cells
F 159 1 9 0 1 0                                 disconnecting cells in shallow areas
F 168 8                                         multi block solver
F 235 10                                        triangular cell damping
F 102 1                                         smoothness of the banks
F 112 1                                         read water level in koordina file

G 1 502 502 11 4                                max grid size in x, y and z direction and number of sediment size

W 1 13.33 1000 575.71                           manning's m, discharge, d/s water level

K 1 3197 50000                                  number of iterations
K 2 0 1                                         use of wall laws for water flow computation
K 3 0.8 0.8 0.8 0.2 0.5 0.5                     relaxation coefficient
K 4 1 1 1 5 1 1                                 number of sweeps for each equation
K 5 0 0 0 10 0 0                                multi block solver
K 6 1 1 1 0 0 0                                 second order scheme

S 1 0.1 1.04                                    sedi frac. no., size, fallvelocity
S 2 0.01 0.33                                   sedi frac. no., size, fallvelocity
S 3 0.001 0.098                                 sedi frac. no., size, fallvelocity
S 4 0.00006 0.0032                              sedi frac. no., size, fallvelocity

N 0 1 0.10                                      bed sediments (10% cobble small)
N 0 2 0.35                                      bed sediments (35% gravel medium)
N 0 3 0.35                                      bed sediments (35%  coarse sands)
N 0 4 0.20                                      bed sediments (20% coarse silts)
B 0 0 0 0 0                                     distributes bed sediments groups to different locations of geometry
```

Figure C. 1 Sample control file for 1000 cumecs at existing operational level

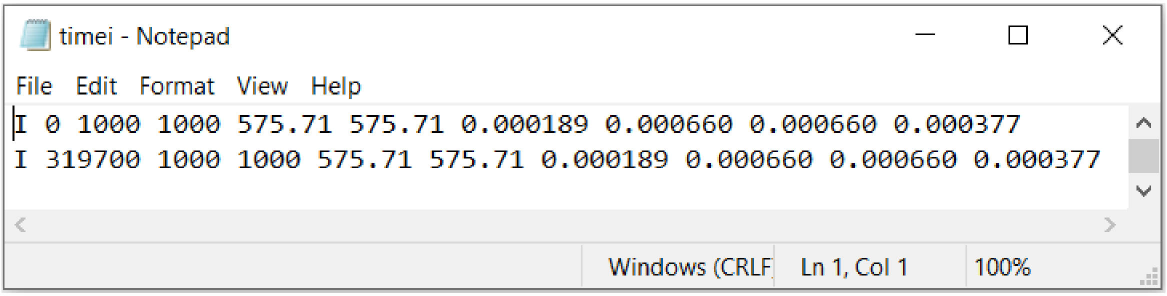

```
I 0 1000 1000 575.71 575.71 0.000189 0.000660 0.000660 0.000377
I 319700 1000 1000 575.71 575.71 0.000189 0.000660 0.000660 0.000377
```

Figure C. 2 Sample timei file for 1000 cumecs at existing operational level

C.2 Problems Faced

Comparison of problem faced and its solution in case of 3000 m3/s at full gate opening

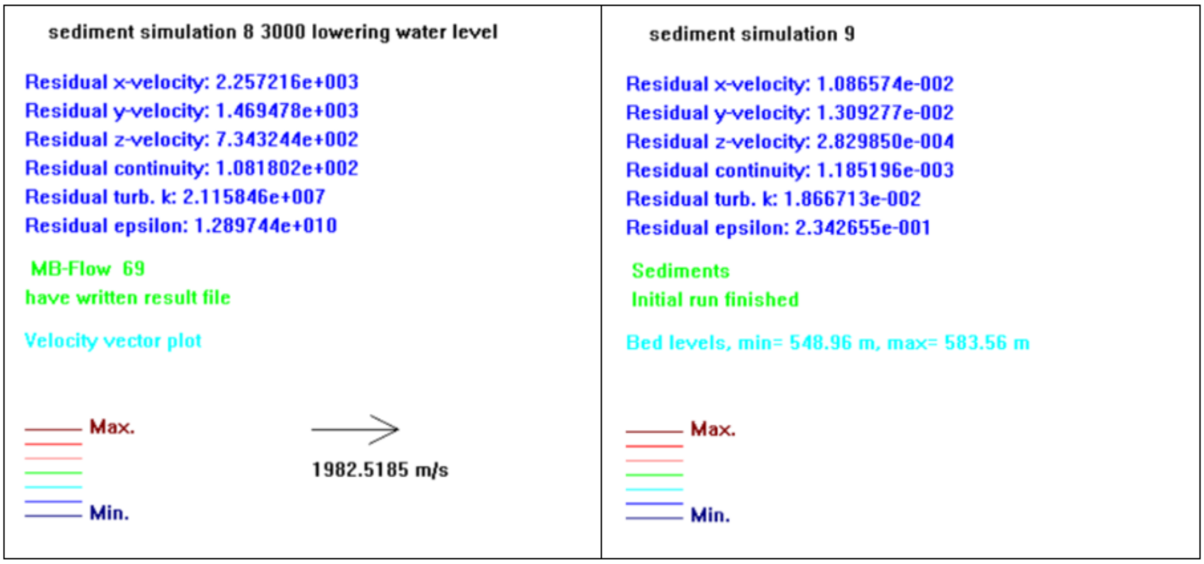

```
sediment simulation 8 3000 lowering water level

Residual x-velocity: 2.257216e+003
Residual y-velocity: 1.469478e+003
Residual z-velocity: 7.343244e+002
Residual continuity: 1.081802e+002
Residual turb. k: 2.115846e+007
Residual epsilon: 1.289744e+010

 MB-Flow  69
have written result file

Velocity vector plot
```

```
sediment simulation 9

Residual x-velocity: 1.086574e-002
Residual y-velocity: 1.309277e-002
Residual z-velocity: 2.829850e-004
Residual continuity: 1.185196e-003
Residual turb. k: 1.866713e-002
Residual epsilon: 2.342655e-001

 Sediments
 Initial run finished

Bed levels, min= 548.96 m, max= 583.56 m
```

Figure C. 3 Improvement of convergence 3000 cumecs at full gate opening

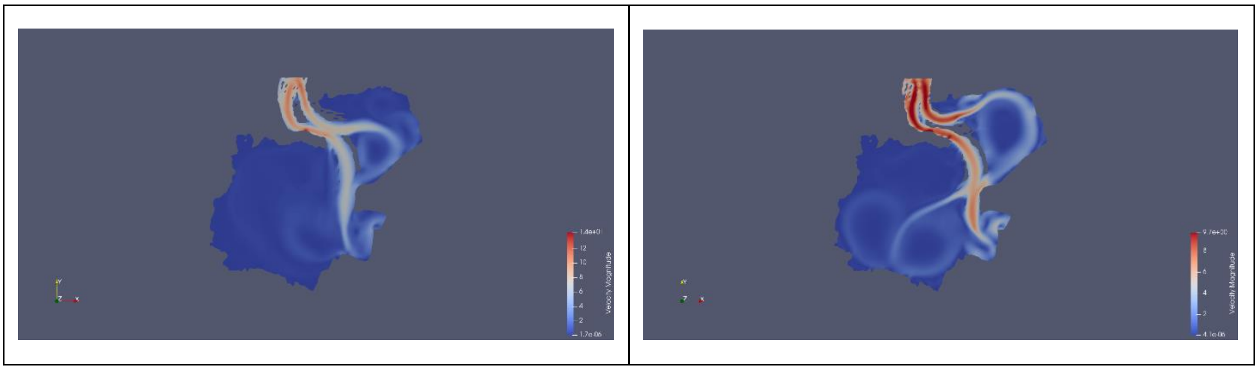

Figure C. 4 Result influenced by change in parameters in F 33 data set 3000 at existing operational level (before and after)

Appendix D

Discussion

D.1 Van Rijn and Meyer- Peter Muller’s Approaches

The comparison between the results obtained from van Rijn and Meyer- Peter Muller’s approaches is as follows:

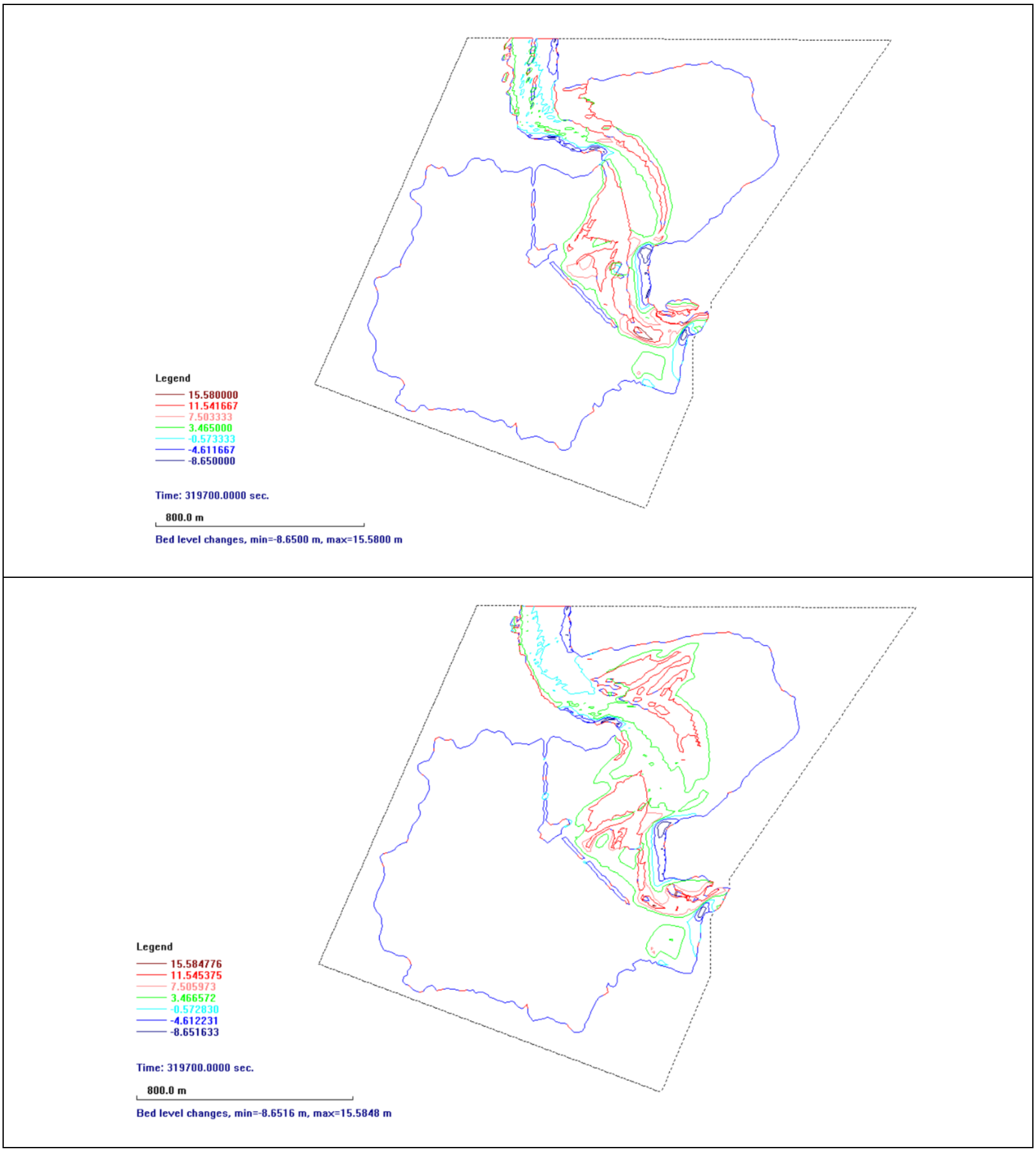

Figure D. 1 Bed changes using van Rijn (top) and Meyer- Peter Muller (bottom) formulae

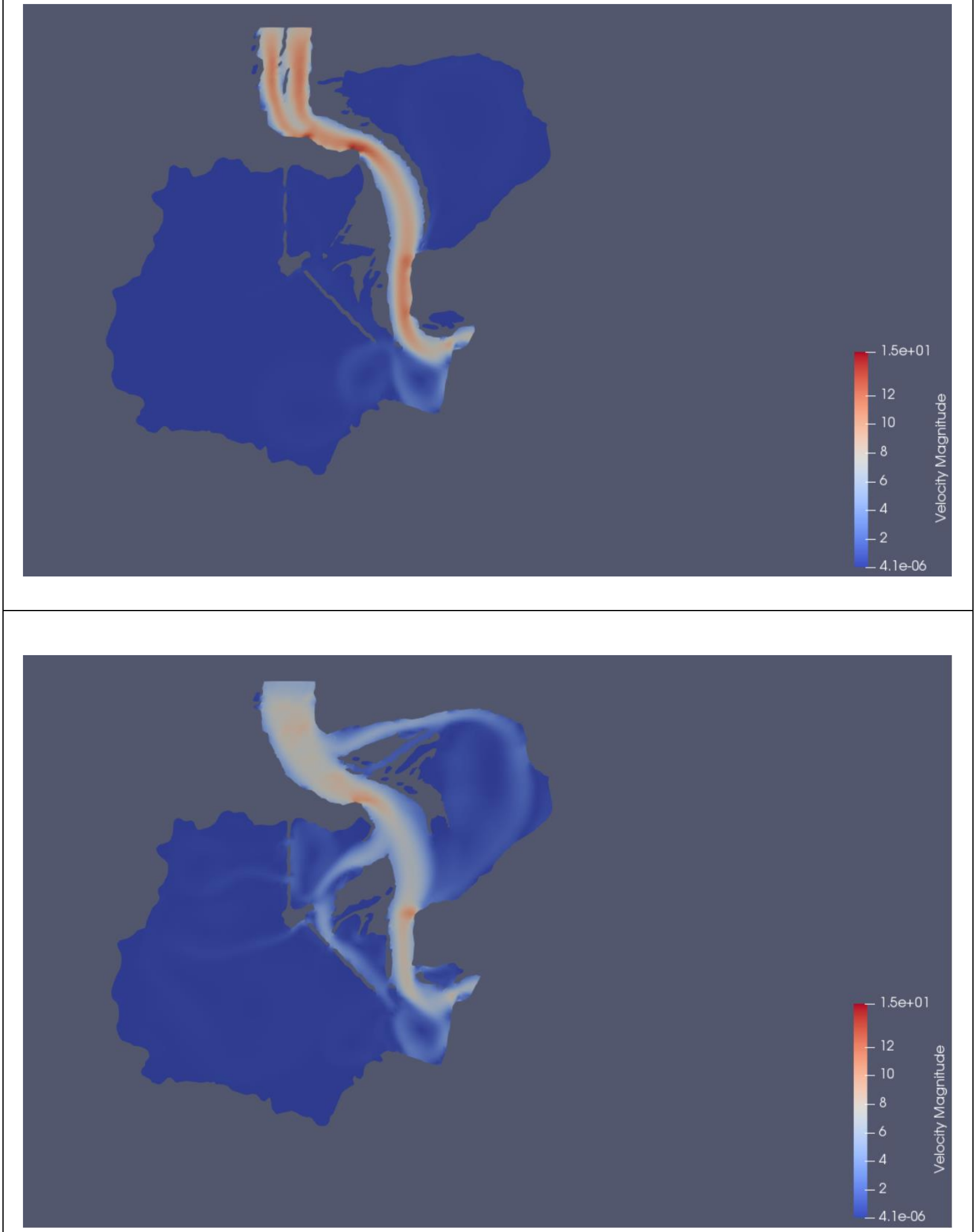

Figure D. 2 Horizontal velocity using van Rijn (top) and Meyer- Peter Muller (bottom) formulae

D.2 Simulation Considering Varying Water Level

The control file and timei file for varying water level simulation are as follows:

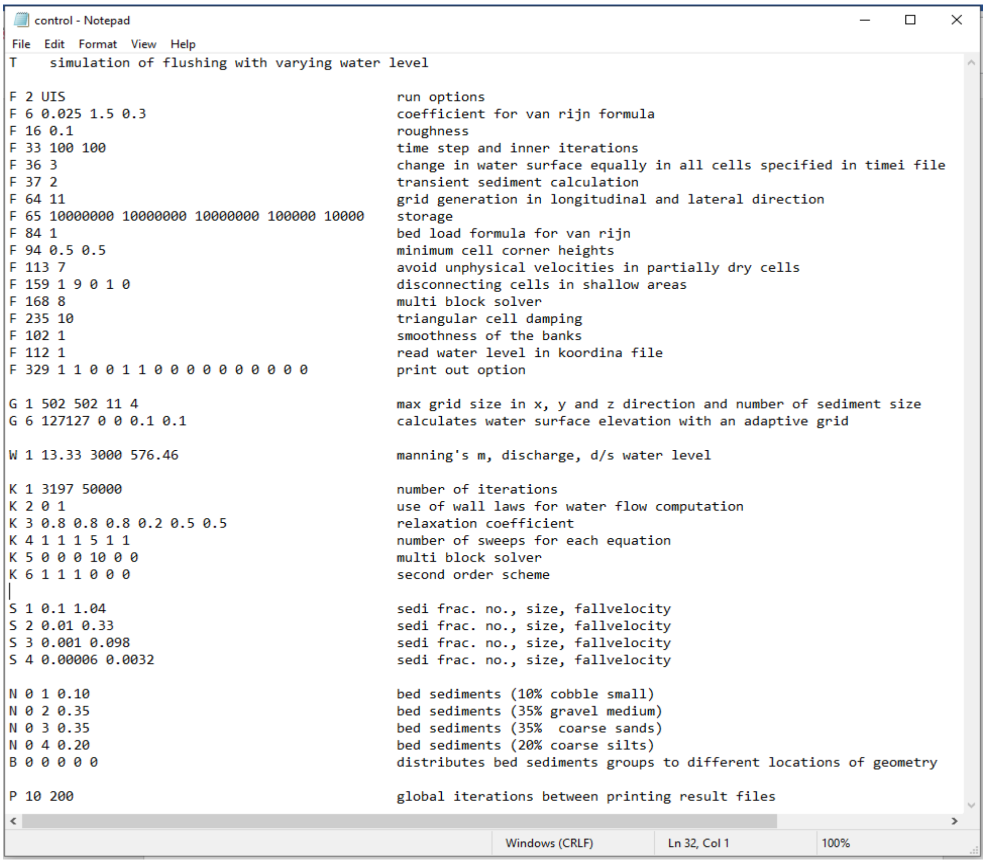

```
T    simulation of flushing with varying water level

F 2 UIS                                         run options
F 6 0.025 1.5 0.3                               coefficient for van rijn formula
F 16 0.1                                        roughness
F 33 100 100                                    time step and inner iterations
F 36 3                                          change in water surface equally in all cells specified in timei file
F 37 2                                          transient sediment calculation
F 64 11                                         grid generation in longitudinal and lateral direction
F 65 10000000 10000000 10000000 100000 10000    storage
F 84 1                                          bed load formula for van rijn
F 94 0.5 0.5                                    minimum cell corner heights
F 113 7                                         avoid unphysical velocities in partially dry cells
F 159 1 9 0 1 0                                 disconnecting cells in shallow areas
F 168 8                                         multi block solver
F 235 10                                        triangular cell damping
F 102 1                                         smoothness of the banks
F 112 1                                         read water level in koordina file
F 329 1 1 0 0 1 1 0 0 0 0 0 0 0 0 0 0           print out option

G 1 502 502 11 4                                max grid size in x, y and z direction and number of sediment size
G 6 127127 0 0 0.1 0.1                          calculates water surface elevation with an adaptive grid

W 1 13.33 3000 576.46                           manning's m, discharge, d/s water level

K 1 3197 50000                                  number of iterations
K 2 0 1                                         use of wall laws for water flow computation
K 3 0.8 0.8 0.8 0.2 0.5 0.5                     relaxation coefficient
K 4 1 1 1 5 1 1                                 number of sweeps for each equation
K 5 0 0 0 10 0 0                                multi block solver
K 6 1 1 1 0 0 0                                 second order scheme

S 1 0.1 1.04                                    sedi frac. no., size, fallvelocity
S 2 0.01 0.33                                   sedi frac. no., size, fallvelocity
S 3 0.001 0.098                                 sedi frac. no., size, fallvelocity
S 4 0.00006 0.0032                              sedi frac. no., size, fallvelocity

N 0 1 0.10                                      bed sediments (10% cobble small)
N 0 2 0.35                                      bed sediments (35% gravel medium)
N 0 3 0.35                                      bed sediments (35%  coarse sands)
N 0 4 0.20                                      bed sediments (20% coarse silts)
B 0 0 0 0 0                                     distributes bed sediments groups to different locations of geometry

P 10 200                                        global iterations between printing result files
```

Figure D. 3 Control file for simulation with varying water level

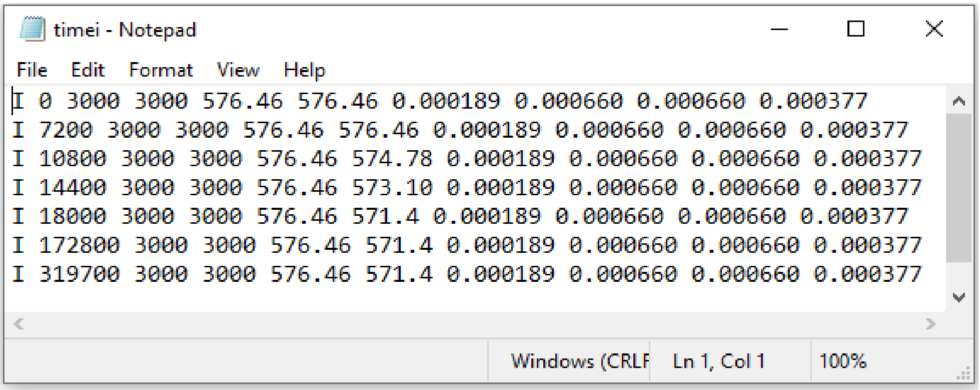

```
I 0 3000 3000 576.46 576.46 0.000189 0.000660 0.000660 0.000377
I 7200 3000 3000 576.46 576.46 0.000189 0.000660 0.000660 0.000377
I 10800 3000 3000 576.46 574.78 0.000189 0.000660 0.000660 0.000377
I 14400 3000 3000 576.46 573.10 0.000189 0.000660 0.000660 0.000377
I 18000 3000 3000 576.46 571.4 0.000189 0.000660 0.000660 0.000377
I 172800 3000 3000 576.46 571.4 0.000189 0.000660 0.000660 0.000377
I 319700 3000 3000 576.46 571.4 0.000189 0.000660 0.000660 0.000377
```

Figure D. 4 Timei file for simulation with varying water level

It is assumed that it takes 3 hours for the gates to open completely. For the first two hours, the water level is at the existing operational level. Now the gates are opened slowly and the water level decreases by 1.68 meters each hour up to 3 hours. When the gates are fully opened, the water level reaches 571.4 masl.

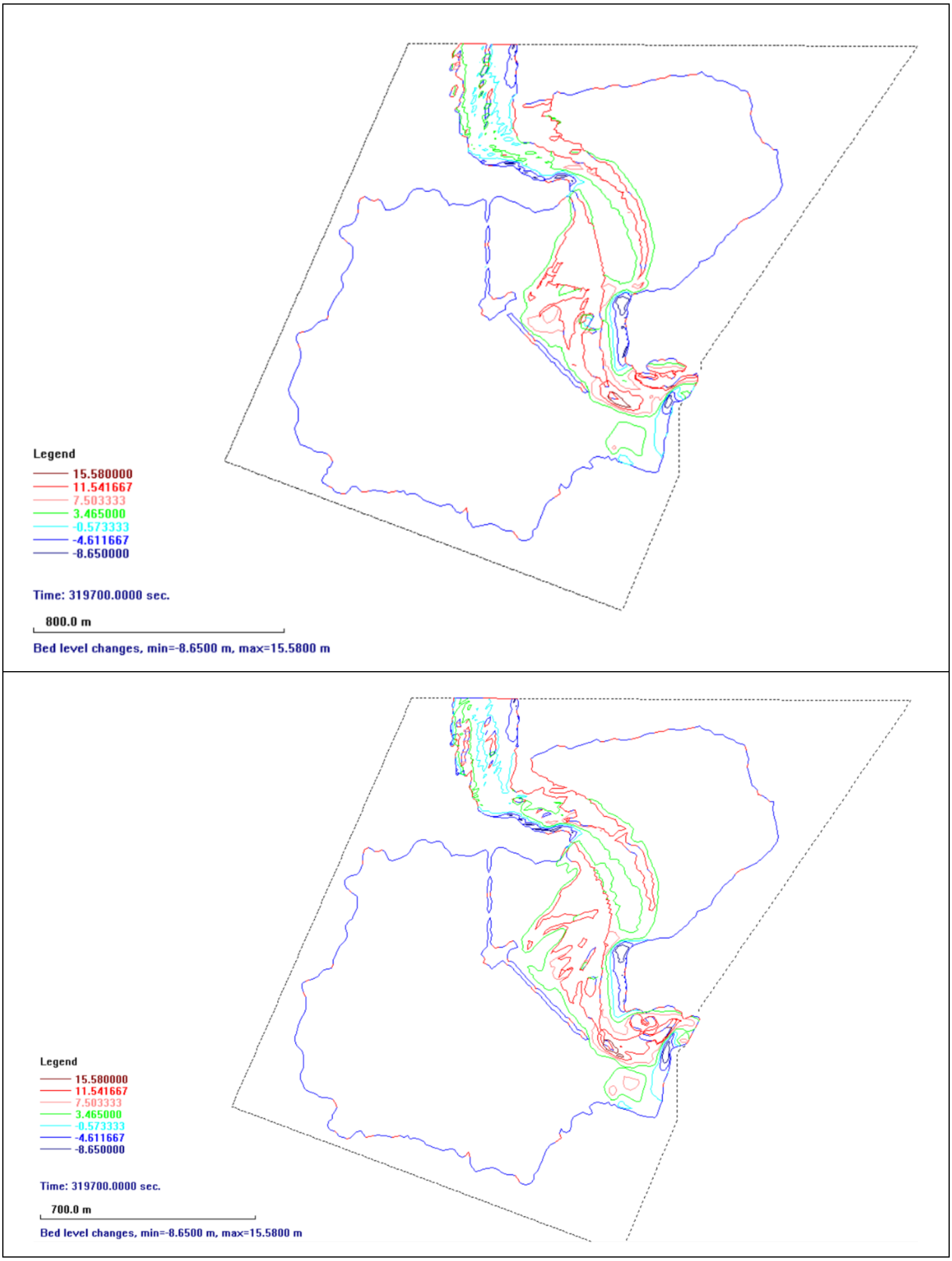

Figure D. 5 Bed changes not considering (top) and considering (bottom) varying water level

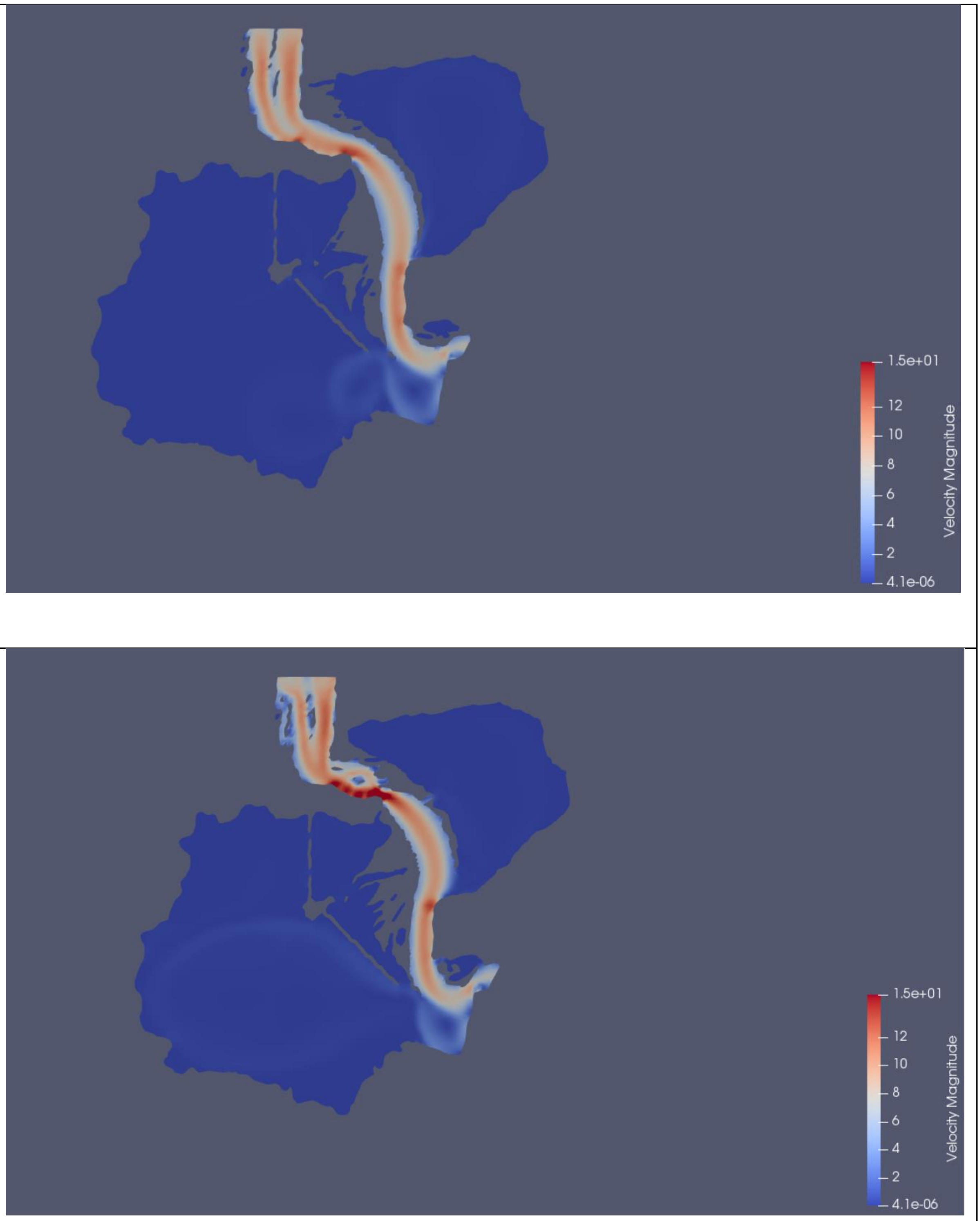

Figure D. 6 Horizontal velocity not considering (top) and considering (bottom) varying water level